# NATIONAL ACADEMIES OF SCIENCE AND ENGINEERING

## NATIONAL RESEARCH COUNCIL

### of the

### UNITED STATES OF AMERICA

### UNITED STATES NATIONAL COMMITTEE

### International Union of Radio Science



## National Radio Science Meeting

## 5-8 January 1988

Sponsored by USNC/URSI
in cooperation with
Institute of Electrical and Electronics Engineers

University of Colorado
Boulder, Colorado
U.S.A.

National Radio Science Meeting
5-8 January 1988
Condensed Technical Program

<u>MONDAY, 4 JANUARY</u>

<u>2000-2400</u>

USNC-URSI Meeting                                              Broker Inn

<u>TUESDAY, 5 JANUARY</u>

<u>0855-1200</u>
| | | |
|---|---|---|
| A-1 | Time Domain Measurements | CR1-40 |
| B-1 | Numerical Methods | CR2-28 |
| D-1 | Numerical Simulation of Solid State Devices | CR1-42 |
| G-1 | Ionospheric Modeling | CR2-26 |
| H/G/B-1 | Ionospheric Scintillation Theory | CR1-9 |
| J-1 | Radio Scattering From Icy Bodies | CR0-30 |

<u>1115-1200</u>
| | | |
|---|---|---|
| J-2 | Radar Astronomy of the Inner Solar System | CR0-30 |

<u>1355-1700</u>
| | | |
|---|---|---|
| A-2 | Microwave and Millimeter Wave Measurements | CR1-42 |
| B-2 | Scattering - I | CR2-28 |
| B-3 | Antennas | CR2-6 |
| D-2 | High Frequency Techniques | CR1-40 |
| F/B-1 | Random Media Theory/Measurements | CR1-46 |
| G-2 | Ionospheric Propagation | CR2-26 |
| J-2 | Radar Astronomy of the Inner Solar System (continued from Tuesday morning) | CR0-30 |

<u>1700-1800</u>
| | |
|---|---|
| Commission A Business Meeting | CR1-42 |
| Commission D Business Meeting | CR1-40 |
| Commission G Business Meeting | CR2-26 |
| Commission J Business Meeting | CR0-30 |

<u>WEDNESDAY, 6 JANUARY</u>

<u>0830-1200</u>
Plenary Session                                           Duane G0-30

<u>1355-1700</u>
| | | |
|---|---|---|
| A-3 | Antenna and EM Fields Measurement | CR1-42 |
| B-4 | PDE-Based Methods for EM Problems in Open Regions | CR1-40 |
| B-5 | Guiding Structures | CR2-6 |
| C-1 | Signal Processing Theory | CR0-36 |
| E-1 | High Power Electromagnetics I. HEMP/EMP / II. Lightning | CR1-46 |
| F-1 | Satellite Remote Sensing A. Special Session on SSM/I / B. Satellites and Sea Floor | CR2-28 |
| G-3 | Ionospheric Modification | CR2-26 |
| H-1 | Waves in Space Plasmas | CR1-9 |
| J-3 | Image Processing in Astronomy | CR0-30 |

<u>1535-1700</u>
| | | |
|---|---|---|
| G/H-1 | Ionospheric-Induced Errors in Ranging/Doppler Systems | CR1-9 |

United States National Committee

INTERNATIONAL UNION OF RADIO SCIENCE

PROGRAM AND ABSTRACTS


National Radio Science Meeting
5-8 January 1988


Sponsored by USNC/URSI in cooperation
with IEEE groups and societies:

Antennas and Propagation
Circuits and Systems
Communications
Electromagnetic Compatibility
Geoscience Electronics
Information Theory
Instrumentation and Measurement
Microwave Theory and Techniques
Nuclear and Plasma Sciences
Quantum Electronics and Applications

Officers of URSI resident in
   the United States:
   (including Honorary
   Presidents)

   Honorary President                Prof. Henry G. Booker*

Chairmen and Vice Chairmen of
   Commissions of URSI
   resident in the United
   States:

   Chairman of Commission B         Prof. Thomas B.A. Senior
   Chairman of Commission F         Dr. Robert K. Crane

Foreign Secretary of the U.S.
   National Academy of
   Sciences                         Dr. William E. Gordon

Chairman, National Research
   Council, Commission on
   Physical Sciences,
   Mathematics, and Resources       Dr. Norman Hackerman

Chairman, National Research
   Council, Board on Physics
   and Astronomy                    Prof. Norman F. Ramsey

Honorary Members                    Dr. Harold H. Beverage
                                    Dr. Ernst Weber

NRC Staff Director                  Mr. Donald C. Shapero

NRC Program Officer                 Dr. Robert L. Riemer

NRC Administrative Specialist       Ms. Helene E. Patterson

   * Member of USNC/URSI Executive Committee

# DESCRIPTION OF THE
## INTERNATIONAL UNION OF RADIO SCIENCE

The International Union of Radio Science is one of 18 world scientific unions organized under the International Council of Scientific Unions (ICSU). It is commonly designated as URSI (from its French name, Union Radio Scientifique Internationale). Its aims are (1) to promote the scientific study of radio communications, (2) to aid and organize radio research requiring cooperation on an international scale and to encourage the discussion and publication of the results, (3) to facilitate agreement upon common methods of measurement and the standardization of measuring instruments, and (4) to stimulate and to coordinate studies of the scientific aspects of telecommunications using electromagnetic waves, guided and unguided. The International Union itself is an organizational framework to aid in promoting these objectives. The actual technical work is largely done by the National Committee in the various countries.

The officers of the International Union are:

| | |
|---|---|
| President: | Prof. A.L. Cullen (U.K.) |
| Past President: | Dr. A.P. Mitra (India) |
| Vice Presidents: | Dr. Ing. H.J. Albrecht (F.R.G.) |
| | R.L. Dowden (New Zealand) |
| | E.D. Jull (Canada) |
| | Prof. V. Zima (Czechoslovakia) |
| Secretary-General | J. Van Bladel (Belgium) |
| Honorary Presidents: | G. Beynon (U.K.) |
| | H.G. Booker (U.S.A.) |
| | W. Dieminger (West Germany) |
| | I. Koga (Japan) |
| | J.A. Ratcliffe (U.K.) |

The Secretary-General's office and the headquarters of the organization are located at Avenue Albert Lancaster, 32, B-1180 Brussels, Belgium. The Union is supported by contributions (dues) from 38 member countries. Additional funds for symposia and other scientific activities of the Union are provided by ICSU from contributions received for this purpose from UNESCO.

The International Union, as of the XXth General Assembly held in Washington, DC in August 1981, has nine bodies called Commissions for centralizing studies in the principal technical fields.

Every three years the International Union holds a
meeting called the General Assembly. The next is the
XXIIIrd, to be held in 1990. The Secretariat prepares and
distributes the Proceedings of the General Assemblies. The
International Union arranges international symposia on
specific subjects pertaining to the work of one or several
Commissions and also cooperates with other Unions in
international symposia on subjects of joint interest.

Radio is unique among the fields of scientific work in
having a specific adaptability to large-scale international
research programs, since many of the phenomena that must be
studied are worldwide in extent and yet are in a measure
subject to control by experimenters. Exploration of space
and the extension of scientific observations to the space
environment are dependent on radio for their research. One
branch, radio astronomy, involves cosmic phenomena. URSI
thus has a distinct field of usefulness in furnishing a
meeting ground for the numerous workers in the manifold
aspects of radio research; its meetings and committee
activities furnish valuable means of promoting research
through exchange of ideas.

Steering Committee:

S.W. Maley, Chairman (303) 492-7004
D.C. Chang
D.S. Cook
P.L. Jensen
M.G. Kindgren

Technical Program Committee:

| | |
|---|---|
| D.C. Chang, Chairman | M. Kanda |
| K. Davies | S.W. Maley |
| R.S. Elliott | E.K. Miller |
| J.R. Fisher | C.M. Rush |
| M.D. Grossi | E.K. Smith |
| J.R. Herman | E. Soderberg |
| T. Itoh | C.T. Swift |
| | A.D. Wyner |

Session A-1    0855-Tues.    CR1-40
TIME DOMAIN MEASUREMENTS
Chairman: William L. Gans, Electromagnetic Fields Division, National
Bureau of Standards, Boulder, CO 80303


A1-1      PULSE MEASUREMENTS IN THE PICOSECOND DOMAIN
0900      J.R. Andrews
          Picosecond Pulse Labs, Inc.
          Boulder, Colorado    80306

This  is  a  tutorial  lecture  emphasizing  the
extremely  broadband  nature  (DC-GHz)  of  picosecond
pulse  measurements  and  the  many  places  in  which
significant    errors    can    occur.    The    following
subject    areas    are    covered:    oscilloscopes,
calibration  standards,  coaxial  cables,  connectors
and probes.

A1-2
0920

TWO    LAYER    DIELECTRIC    MICROSTRIPLINE
STRUCTURE:    SiO2   ON   Si   AND   GaAs   ON   Si
MODELING AND MEASUREMENT

R.A. Lawton
Boulder Research Associates
Boulder, Colorado    80303

The    two-layer    dielectric    microstripline
structure is a structure that has found use in a
number of applications.   Two examples are in pulse
waveform  filtering  to  generate  a  pulse  waveform
standard  and  in  the  use  of  high  quality  silicon
substrates in the manufacture of gallium arsenide
devices.

This  paper  will  describe  the  concept  of
reference  waveform  standards  using  the  two-layer
dielectric  microstripline  structure  (R.A.  Lawton,
N.S.  Nahman  and  J.M.  Bigelow,  IEEE  Trans.  I&M,
IM-33,  No.  3,  201-205,  1984)  and  the  further
modeling  that  has  been  recently  completed.
Scattering  parameters  are  computed  from  the
distributed element circuit model and compared with
measured  values  over  the  frequency  range  from  90
MHz  to  18  GHz  for  a  microstripline  made  from  a
wafer  with  silicon  dioxide  on  silicon.   The
sensitivity of the phase of S21 and the magnitude
of   the   characteristic   impedance   to   various
parameters is also discussed.

The  application  of  these  techniques  to  the
gallium  arsenide  on  silicon  system  will  be
described  and  illustrative  calculations  will  be
given.

Note:   This  work  was  performed  while  Lawton  was
with the National Bureau of Standards.

A1-3      PICOSECOND SILICON PHOTOCONDUCTIVE SWITCH
0940      BASED TIME-DOMAIN METROLOGY
          W.R. Eisenstadt, Assistant Professor
          Department of Electrical Engineering
          University of Florida
          Gainesville, Fl. 32611

The silicon photoconductive switch has been established as a picosecond time-domain measurement tool over the past five years.  The photoconductive switch permits characterization of on-substrate integrated circuit signals with bandwidths above 75-GHz (W.R. Eisenstadt et al., Picosecond Electronics and Optoelectronics, Springer-Verlag, **21**, 66-69).

An overview of the experimental methodology used to perform picosecond photoconductor based time-domain measurements is presented.  This overview discusses; 1) fabrication of photoconductors on the silicon substrate, 2) ion-implantation of photo-conductors to produce picosecond switches, 3) pulsed laser system for on-substrate photo-optic measurements, 4) cross-correlation measurements that characterize photoconductors, and 5) IC test structure measurements in a photoconductor based sampling system. Examples of current photoconductive switch research are reviewed.

The photomicrograph below displays the top-side of an IC test structure used to develop picosecond silicon photoconductive switches.  The white areas are microstrip transmission lines and the black gaps between the lines are photoconductive switches.
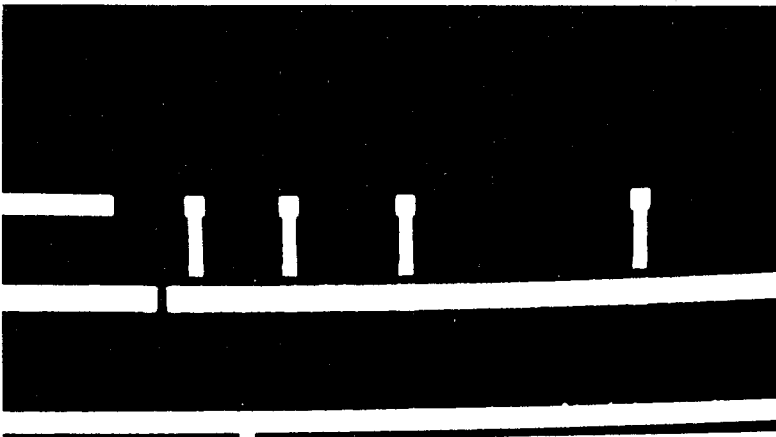
A1-4
1020
OPTIMIZATION AND APPLICATION OF ULTRA-HIGH-SPEED OPTOELECTRONIC TIME DOMAIN MEASUREMENTS
N.G. Paulter, Staff Member
Los Alamos National Laboratory
Los Alamos, NM   87544

Very high-frequency electronic devices and circuits have introduced the requirement of measurement capabilities that extend into the hundreds of GHz range. Optoelectronic and electrooptic techniques are under investigation to perform these measurements. The technique presented here is an optoelectronic one, based on photoexcitation and the subsequent relaxation of carriers in semiconductor photoconductive devices. (N.G. Paulter and R.B. Hammond, Proc. of the Critical Review of Technology 795, SPIE, Bay Point, FL, Mar. 1987.)

The optimization of the optoelectronic measurement test structure and applications of the measurement are given. The test structure optimization includes consideration of semiconductor substrate (SOI, SOS, GaAs), implant schedule, and transmission line structure (coplanar waveguide, coplanar strips, and microstrip). Modification of the chosen transmission line structure to enhance response magnitude without speed degradation and to minimize device area requirement without affecting temporal resolution are discussed. Novel applications of this measurement technique are presented.

The sketch below is of an arrangement used to characterize high-speed electronic devices. The PCEs (photoconductive circuit elements) are the active regions of a semiconductor.
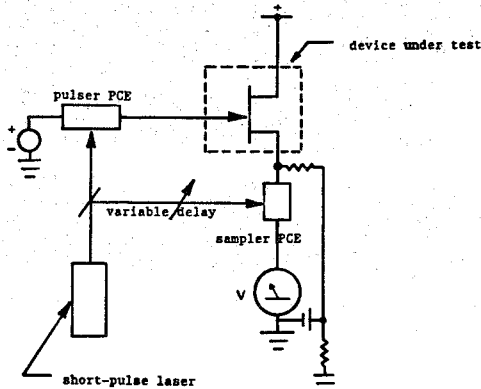
A1-5         ELECTRO-OPTIC SAMPLING AND THE
1040         CHARACTERIZATION OF ULTRAFAST ELECTRONIC
             DEVICES

G. A. Mourou and J. F. Whitaker
Ultrafast Science Center, Laboratory for Laser Energetics
University of Rochester
250 East River Road
Rochester, NY  14623

With the extreme interest in subpicosecond phenomena and the operation of electronic devices in the single-picosecond regime has arisen the need for new measurement techniques.  Beginning with the invention of the electro-optic sampling system at the University of Rochester, a revolution in the characterization of extremely short electrical events was triggered.  The study of the propagation of signals with bandwidths exceeding one terahertz has been carried out for normal and superconducting transmission lines, and devices such as MESFETS, permeable base transistors, and resonant tunneling diodes have also been investigated.

The implementation of the electro-optic sampling technique involves the marriage of the fields of optics and electronics.  An 80-fs pulse from a mode-locked dye laser provides an excitation beam which is used with a semiconductor to generate very short electrical transients.  A probe beam split off from the same laser pulse, is used to sample the change in index of refraction induced by the electrical waveform in an electro-optic crystal.

In this manner, parameters such as the switching speed of a MIT Lincoln Laboratory resonant tunneling diode have been measured.  This device, containing a single, double-barrier quantum well and displaying a prominent negative differential resistance characteristic, switches from a high to low current level in 2 ps (see Figure).
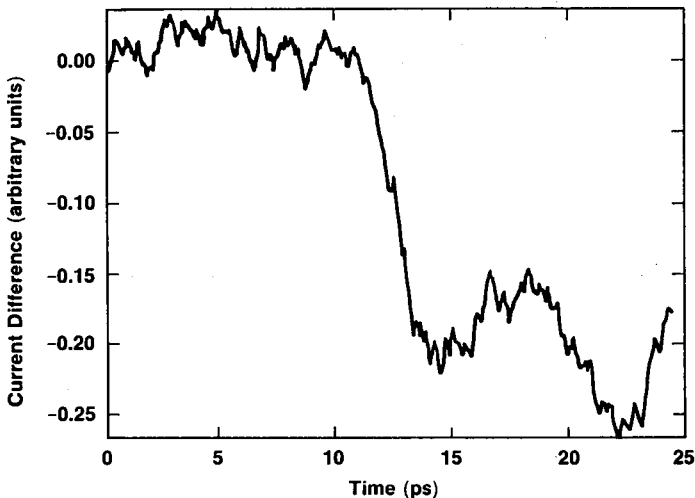


switching time of resonant tunneling diode

5

A1-6
1100

ULTRA-WIDE BANDWIDTH INSTRUMENT FOR TIME
DOMAIN MEASUREMENTS BASED ON JOSEPHSON
JUNCTIONS
E.R. Hanson, G.K.G. Hohenwarter,
S.R. Whiteley and S.M. Faris
HYPRES, Inc.
500 Executive Boulevard
Elmsford, NY    10523

The promises of the ultra-high performance
properties of superconductivity and Josephson
junction technologies have been known for quite
some time. This presentation describes the
integration of the first system to demonstrate
those properties, as a 5 ps, 50 microvolt
sensitivity sampling oscilloscope and time domain
reflectometer instrument. In order to accomplish
this, several technological hurdles had to be
overcome including perfecting a manufacturing
process for building Josephson junction IC chips,
develop an innovative cooling technique, deal with
interfaces and interconnections with bandwidths in
excess of 70 GHz and develop the room temperature
hardware and software necessary to make the
instruments convenient, easy to use, and easy to
learn, in addition to making available functions
and features users have come to expect from
sophisticated digital instruments. The
presentation will cover the following topics:
* circuit design for both a fast rise time
   sampling oscilloscope and a time domain
   reflectometer;
* circuit fabrication and operation;
* operation of the unique cooling system;
* various aspects of system integration;
* circuit interconnections and packaging;
* unique problems associated with Josephson
   junction systems;
* examples of the technology's capabilities
   demonstrating the superior switching speed
   and sensitivity of superconducting
   integrated circuits as well as other unique
   features.

A1-7
1120

# AN APPROACH TO REAL-TIME ESTIMATION OF THE
# DERIVATIVE OF DAMPED-EXPONENTIAL TIME-DOMAIN WAVEFORMS

W. Ross Stone
IRT Corporation
1446 Vista Claridad
La Jolla, CA 92037

Waveforms which are decaying exponential functions of time are often encountered in electromagnetic measurements. In some applications, the desired information is contained in the derivative of the data (which, of course, is also of exponential form), and it is desired to predict the value(s) of the function and its derivative in real time (as data is being collected). To be practical, a solution to this problem must remain robust in the presence of noise, and over the substantial dynamic ranges often encountered with such signals. Furthermore, in the applications considered in this paper, although the basic functional form of the waveform is known to be a decaying exponential, the decay constant is unknown and/or time varying. Least squares estimators (including polynomial and orthogonal function fitting) can tend to provide an overly "smooth" solution to such problems, with resultant errors in long-time estimation. Kalman-Bucy filters are often better suited to such estimation problems. However, they usually are formulated for problems in which the underlying model is known, or the unknown component can be "lumped" with the noise in the measurements.

This paper considers another approach to the problem, using recursive real-time Fourier analysis. A derivative theorem is used to recursively compute future-time estimates of the desired solution. The behavior of this approach as a function of measurement noise, decay rate, dynamic range, and length of time into the future for the estimate is examined, both analytically and numerically. Circumstances under which this approach should display substantially robust behavior in the presence of common noise distributions, and the reasons why, are explained. Examples using measured data are also presented.

B1-1
0900

**THE USE OF SUBSECTIONAL UNIFORM DISTRIBUTIONS
IN THE GALERKIN-MOMENT METHOD SOLUTION
OF ELECTROMAGNETICS PROBLEMS**
Bradley L. Brim  and  David C. Chang
Department of Electrical and Computer Engr.
University of Colorado
Boulder, CO  80309

When implementing a Galerkin Moment Method solution
it may be advantageous to choose a subsectional
expansion with very simple distributions.  Ignoring
delta functions (ie: point expansion/matching),
uniform distributions are the most simple choice
possible.  However, the solution of integro-
differential equations places certain constraints on
the expansion/testing functions.  For example, in an
EFIE (electric field integral equation) formulation
the existence of a second order differential operator
implies that currents must be continuous in the
direction they flow, but may be discontinuous normal
to the direction of their flow.  This means that
"rooftop" expansions are the most simple
distributions that may be used, which yield an
expansion for current that is piecewise-linear in the
direction of its flow and piecewise-constant in
directions normal to its flow.

We will present three methods by which one may use
constant distributions for both current and charge in
Galerkin solutions for electromagnetics.  Firstly,
two EFIE formulations will be considered in which
approximate rather than exact relationships are
enforced to relate charges and currents.  The first
of these is based on an integrated form of charge
conservation and yields charge cells that are not
shifted with respect to current cells.  The second is
based on the spreading of concentrated charges and
yields shifted charge cells.  The exact variational
nature of these two formulations is lost, but
adequate numerical performance is maintained.  Next,
a true MPIE (mixed potential integral equation)
formulation will be presented in which charges and
currents are each treated as unknown trial
expansions.  The variational nature of this
formulation is maintained throughout.  These methods
will be compared based on their physical
interpretations, boundary conditions, numerical
results, and numerical efficiency for a few select
sample problems involving flat dipoles and microstrip
structures.  Recommendations will be made as to the
use of these methods.

8

B1-2      GUIDELINES FOR MODELING WITH THE ELECTRIC FIELD INTEGRAL
0920      EQUATION TRIANGULAR SURFACE PATCH CODE

W. A. Johnson*
Pulsed Power Theory Division
Sandia National Laboratories
Albuquerque, New Mexico  87185

R. M. Sharpe and D. R. Wilton
Department of Electrical Engineering
University of Houston
Houston, Texas  77004

Previous  progress  in  the development of the Electric Field
Integral  Equation  Triangular  Surface  Patch  Code has been
reported (W. A. Johnson, "Current Progress in the Development
of  and  Modeling with the EFIF Surface Patch Code," IEEE-APS
Meeting, Vancouver, British Columbia, June 1985).  Since this
time,  new  capabilities  have  been  developed  and modeling
experience  has  been  gained.   In  particular,  the present
version  of  this  code  has  the  following capabilities: an
arbitrary  number  of  triangles  may be attached to an edge;
multiple  disjoint  bodies  may  be  modeled;  non-orientable
surfaces may be modeled; symmetry planes may be accounted for
by placing perfect electric or perfect magnetic conductors in
the x=0, y=0, and z=0 planes; the Thevenin circuit parameters
for  a  pair of terminals defined at an edge may be computed;
lumped  and  surface  impedance  loading  may  be added to an
otherwise  perfectly  conducting  body;  excitation  by plane
waves,  voltage  sources  or  both  may  be  used;  far field
patterns  and radar cross sections may be computed; and field
calculations  at  general  observation  points may be carried
out.   Modeling  guidelines  aimed  at the intelligent use of
these   capabilities,   understanding   the  limitations,  and
avoiding  pitfalls  will  be  discussed.   Several  realistic
problems  that  have  been  solved  with  this  code  will be
presented.

B1-3    NUMERICAL SOLUTION OF THE INTERIOR BOUNDARY
0940    VALUE PROBLEM OVER ROTATIONALLY SYMMETRIC
        INHOMOGENEOUS DOMAINS USING FINITE
        INTEGRATION TECHNIQUE

J. Lebaric, Campus Box 119, Rose-Hulman
Institute of Technology, 5500 Wabash Av.,
Terre Haute, IN 47803
D. Kajfez, Electrical Engineering Dept.,
University of Mississippi,
University, MS 38677

Numerical solution of the interior EM boundary
value problem has been obtained using the Finite
Integration Technique (FIT) (T. Weiland, URSI Int.
Symp. on EM Theory, 537-542, Budapest 1986.). The
technique involves simultaneous volume and field
discretization by the virtue of "dual grids" and
allows for a systematic discretization of the curl
and divergence equations of Maxwell, the result
being an equivalent standard algebraic eigenvalue
problem involving large but sparse matrices.
Computer implementation of FIT, program package
FITPAK capable of solving for the mode resonant
frequencies, field distributions and Q-factors, has
been applied to cylindrical cavities with arbitrary
distributions of dielectric media. Comparisons of
measured and numerical results confirm the abscence
of non-physical ("spurious") modes in the numerical
solution.
Electric field lines for the $TM_{01}$ mode in a
dielectric-rod-tuned tubular dielectric resonator
resting on alumina substrate are shown in the
figure below, to illustrate FITPAK versatility.
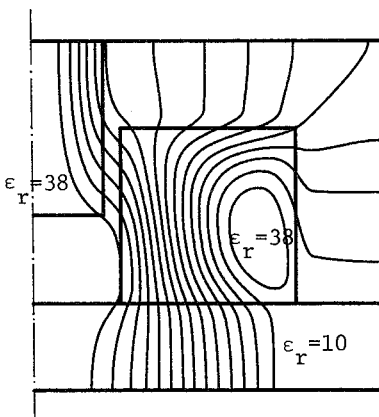
B1-4    ALTERNATIVE FORMS OF THE MIXED-POTENTIAL
1020    ELECTRIC FIELD INTEGRAL EQUATION
        IN LAYERED MEDIA

K.A. Michalski and D. Zheng
Department of Electrical Engineering
Texas A&M University
College Station, TX 77843

The most general and efficient numerical procedures developed to date for solving the problems of radiaton and scattering by objects of arbitrary shape in free space are based on the so-called mixed-potential form of the electric field integral equation (EFIE) [Glisson and Wilton, *IEEE Trans. Antennas Propagat.*, AP-28, 593-603, 1980; Rao *et al.*, *ibid.*, AP-30, 409-418, 1982; Schaubert *et al.*, *ibid.*, AP-32, 77-85, 1984]. There has been a considerable interest in extending these procedures to the case of objects in layered media [Mosig and Gardiol, *Advances in Electronics and Electron Physics*, 59, 139-237, 1980; Johnson, *Radio Sci.*, 18, 1273-1281, 1983; Michalski, *Arch. Elektr. Übertrag.*, AEÜ-39, 317-322, 1985; Wilton and Singh, *AP-S Int. Symp.*, 229-272, 1985; Michalski and Zheng, *ICAP 87*, 507-511, 1987].

In this paper, three alternative forms of the mixed-potential EFIE in plane-stratified dielectric media are developed and their properties are discussed. It is shown that for objects that penetrate one or more interfaces, one of these forms enjoys a clear advantage over the others. The authors have applied this equation in conjunction with the triangular-patch code [Rao *et al.*, *op. cit.*] to compute the current distribution on a conductive surface of arbitrary shape penetrating the interface between contiguous half-spaces. Preliminary numerical results are presented.

B1-5
1040

# APPLICATION OF MAPPING FUNCTIONS FOR NUMERICAL SOLUTION OF SCATTERING FROM POLYGONS

L. Shafai and H. Moheb
Department of Electrical Engineering
University of Manitoba
Winnipeg, Manitoba, Canada  R3T 2N2

In numerical solution of scattering from conducting objects integral equations are commonly used to formulate the problem for the surface current distributions. These current distributions are then determined by utilizing the moment methods to reduce the integral equations to a matrix equation. The process involves a segmentation of the scattering surface into a finite number of sub-surfaces, over which the induced currents are represented by appropriate basis functions. For three-dimensionl objects the segmentation is over the entire object and results in matrices of large dimensions. Consequently, the solution becomes limited to objects small in terms of the wavelength. The matrix dimension can be reduced by utilizing the symmetry of the geometry, or, when the induced currents can be expanded in terms of orthogonal sets such as Fourier series. The latter have been used in problems involving bodies of revolution to reduce the overall matrix to a number of small matrices of the azimuthal modes.

In the present study the method is extended to objects with polygonal cross-sections. A mapping function is used to express the induced currents in terms of an angular variable in the transformed domain. The process reduces the two-dimensional integral equations to a set of one-dimensional ones along the generating line of the object, similar to the case of bodies of revolution. The method is then used to study the scattering from a few geometries such as cubes, prisms, and plates. The method is general and can be used for any geometry, provided a mapping function is already available or can be determined.

B1-6       COMPUTATIONAL METHODS IN THE DIAKOPTIC
1100       ANALYSIS OF A CYLINDRICAL ANTENNA
           Chalmers M. Butler, William A. Walker, Robert G. Kaires
           Department of Electrical and Computer Engineering
           Clemson University, Clemson, SC 29634-0915
           and
           Felix Schwering
           U. S. Army CENCOM
           Fort Monmouth, NJ 07703

The modified diakoptic theory can be used to analyze cylindrical antennas to a high degree of accuracy. The basic point of view which one adopts in developing this theory is quite different from that of the method of moments but in several ways the computations involved in implementing the two solution methods are similar. Moreover, as is well known to be true of the method of moments, there are alternate procedures which one may employ in a modified diakoptic analysis of a given antenna problem. Using the cylindrical antenna as an example, the authors describe fundamentally different ways to carry out the analysis necessary to determine the current on the antenna by the diakoptic theory. An interesting feature of these alternate methods is that, in a single computation, one represents the antenna current in two distinct linear combinations of different basis functions. Also of interest is the fact that, in an iterative procedure used to achieve convergence of the current in the diakoptic analysis, the method of moments is employed in intermediate steps. Results obtained by means of the alternate procedures alluded to above are presented and are compared to one another and to data obtained via the method of moments. Convergence of the methods is discussed too.

# ON REDUCING THE NUMBER OF FREQUENCY SAMPLES NEEDED TO RECONSTRUCT AN ELECTROMAGNETIC TRANSFER FUNCTION *

G. J. Burke, Lawrence Livermore National Laboratory
Livermore, CA 94550

E. K. Miller, Rockwell Science Center, Thousand Oaks, CA 91360

S. Chakrabarti and K. R. Demarest, U. of Kansas, Lawrence, KS 66045

A frequently encountered problem in electromagnetics is that of determining the response of an object over a frequency band. This transfer function is typically obtained by many successive evaluations of a numerical solution. In a method of moments solution for a large model this repetition can consume excessive computer time. One way of reducing the number of evaluations is by introducing *a priori* knowledge of the expected frequency behavior in the form of a pole series. Another approach is to compute frequency dervatives which can be evaluated recursively in significantly less time than for the initial solution. The derivatives can then be used in an expansion about the frequency or for interpolation between frequency points. Both of these approaches are discussed here.

Derivatives of the current can be obtained from a method of moments solution at any frequency $f_0$ by taking derivatives of the matrix equation at $f = f_0$ and solving recursively as

$$ZI = V \qquad I = Z^{-1}V$$
$$Z'I + ZI' = V' \qquad I' = Z^{-1}(V' - Z'I)$$
$$Z''I + 2Z'I' + ZI'' = V'' \qquad I'' = Z^{-1}(V'' - Z''I - 2Z'I')$$
$$\cdots \qquad\qquad \cdots$$
$$\cdots \qquad I^{(n)} = Z^{-1}\left[V^{(n)} - \sum_{r=1}^{n} C_{n,r} Z^{(n)} I^{(n-r)}\right]$$

where $C_{n,r}$ is the binomial coefficient. The derivative matrices can be evaluated without too much additional effort if they are done simultaneously so that terms can be shared. Also, each successive derivative requires on the order of $N^2$ operations as opposed to the $N^3$ operations for the initial matrix solution. The derivatives can be used in a Taylor series expansion about a frequency or for interpolation between frequencies. Rational approximations derived from the derivatives are more efficient for representing the resonances of the response, however. Use of a pole series can similarly reduce the overall time for evaluating a transfer function by limiting the number of frequency samples needed. Results of both of these approaches are compared.

NUMERICAL SIMULATION OF SOLID STATE DEVICES
Chairman: T. Itoh, The Univ. of Texas, Dept. of Electrical and Computer
Engineering, Austin, TX 78712


D1-1       ENSEMBLE MONTE CARLO MODELING OF HEMTS
0900       D. K. Ferry
           Center for Solid State Electronics Research
           Arizona State University
           Tempe, AZ 85287-6206

     The  high-electron-mobility transistor (HEMT) provides a
cross between the Si MOSFET and the GaAs MESFET, in that  the
carriers  are confined to a quantized channel, with an inver-
sion density controlled by the metal gate, but the device  is
normally  a depletion mode metal-gate transistor.  The use of
Ensemble Monte Carlo techniques to model this  device  allows
one  to  avoid simplifying assumptions in the transport model
and to concentrate on the details of the scattering processes
themselves.

     Transport in such devices is complicated by the  transi-
tions  between  two- and three-dimensional characteristics of
the electrons  themselves (U.  Ravaioli  and  D.  K.  Ferry,
Superlattices    and    Microstructures   2,    377-380,   1986).
Quantization in the channel is another detail  that  must  be
considered.   In this talk, these facets of the modeling will
be discussed and several approaches used  by  various  groups
outlined.

D1-2       MONTE CARLO SIMULATIONS OF HIGH ENERGY ELECTRON
0920       TRANSPORT IN SEMICONDUCTORS

K. Hess and U. Ravaioli
Coordinated Science Laboratory and
Department of Electrical and Computer Engineering
University of Illinois
1101 W. Springfield Ave.
Urbana, IL 61801

Recent developments of research on high energy transport in semiconductors are reviewed concentrating on results of Monte Carlo simulations. It is shown that large scale computation has resulted in considerable advances in the understanding of such diverse topics as impact ionization, high energy injection and ballistic transport as well as overshoot and nonlocal effects in field effect transistors.

This review concentrates on electron energy distributions above certain energy thresholds such as the impact ionization threshold and electron transport over barriers including the emission of electrons out of the semiconductor (cold cathodes). In the course of these discussions we also will present results related to new forms of devices such as hot electron transistors (HET's) and high mobility transistors (HEMT's).

D1-3  **SIMULATION OF BALLISTIC DEVICES ON A**
0940  **SUPERCOMPUTER**

Michael Shur[+] and Jingming Xu[++]
+Department of Electrical Engineering
University of Minnesota,Minneapolis, MN 55455
++Department of Electrical Engineering
University of Toronto, Toronto, Canada

We present the results of the simulation of ballistic hot electron transistors using Monte Carlo method. This simulation is based on the study of the transport of a large number of electrons in the base of hot electron transistors (i.e. in the region between the emitter and collector barrier). This study shows that the angular distribution of the electrons arriving to the collector barrier is more focused. This caused by the acceleration of electrons in the built-in electric field in the base region as well as by the fact that the electrons injected into the base under large angles are more likely to be scattered, hence more likely to loose energy and contribute to the base current. Hence, the distribution function of electrons arriving to the collector barrier is more suited for the effective launching of ballistic electrons. This leads to a concept of utilizing a doped and graded layer following a conventional emitter to accelerate and shape the electron beam for an efficient injection into the next stages. As an example of the concept, we proposed Double Base Hot Electron Transistors (DBHETs) where the first ( doped and/or graded ) base region acts as an "electron gun" accelerating electrons and as a "lens" providing a better focused ballistic electron beam that is injected into the second base where an input signal is applied. (No input signal is applied to the first base.) Using the Monte Carlo method, we calculate the energy and angular distributions of electrons at the collector and the barrier sandwiched in between the first and second bases. We also calculate the mean transit time, as a function of energy, across the base. The results of the calculation demonstrate potential advantages of Double base devices.

We also discuss applications of the Monte Carlo method to the studies of the electron transport in compensated material. These studies show that sharply increased impurity scattering in compensated compound semiconductors changes the conditions of intervalley transitions and affects the Ridley-Watins-Hilsum-Gunn effect causing (under certain conditions) the appearance of two maxima of the velocity vs. electric field curve.

D1-4    ADVANCED DEVICE THEORY & CONCEPTS
1020    H. L. Grubin
        Scientific Research Associates, Inc.
        Glastonbury, CT 06033

The issues of submicron high speed and high frequency semiconductor devices have focused on problems such as velocity overshoot and more recently, the breakdown of the Fermi golden rule, quantum phase-based transport and tunneling.  Also high speed devices have concentrated mainly on the electronic component of transport. The questions that continually arise with respect to these devices focus on the question of the feasibility of extracting, experimentally, the relevant high speed parameters.  The issues of hole as well as electron transport, high speed limitations and the role of experiment in extracting fundamental concepts will be addressed.

D1-5      OPTIMIZATION OF THE P SUBSTRATE DOPING FOR
1040      THE N CHANNEL GaAs SUBMICRONIC-GATE
          MESFET'S
          S. El-Ghazaly, T. Itoh and G. Salmer[*]
          Department of Electrical and Computer Engineering,
          The University of Texas at Austin,
          Austin, Texas 78712, USA.

Microwave coplanar FET's are thin film devices since their active layers are just few tenths of a micron. The performance of these MESFET's is highly affected by the properties of the substrates as well as the properties of the active layer. Growing the active layer directly on the substrate results in a poor quality transistor due to the crystallographic defects and the diffusion of impurities to the active layer. To avoid these problems, an epitaxially grown undoped buffer layer is introduced between the active layer and the semi-insulating substrate. Considerable number of free carriers are injected into this buffer layer while they travel under the gate. This carrier injection produces a higher saturation current, a lower transconductance ($g_m$) and a higher drain output conductance ($g_d$) ( G. Salmer *et al*. Proc. Int. Symp. GaAs and Related Compounds, 1984). To improve the MESFET performance, the authors proposed the use of a P substrate, or P buffer layer to increase the transconductance and reduce the drain output conductance ( S. El-Ghazaly *et al*. XXIInd  General Assembly of the Int. Union of Radio Science, 1987).

The P substrate problem is investigated using a two dimensional numerical model which solves Poisson's equ., continuity equ. and energy conservation equ. The mobility and the electron temperature are functions of the average electron energy. This model is capable of correctly simulating the submicronic gate MESFET taking into account the non-stationary effects such as velocity overshoot ( S. El-Ghazaly *et al*. Proc. 13th European Solid State Devices Research Conf., 1983). Several MESFET structures of gate lengths equal to 0.5 $\mu$m were simulated. These structures include symmetrical MESFET's, which has no substrate effects, MESFET's on buffer layers and MESFET's on P substrates.

It was observed that MESFET's on P substrates demonstrate a considerably high transconductance compared to MESFET's on buffer layers. Due to the increase of the electrons confinement to the active layer, the gate-to-source capacitance is also high. However, MESFET's on P substrates demonstrate a higher current-gain cutoff frequency compared to the corresponding MESFET's on buffer layers. The doping of the P layer has a great influence on the MESFET parameters. The results of the optimized doping to obtain the best MESFET performance will be presented as well.

* Centre Hyperfrequences et Semiconducteurs,
  Universite des Sciences et Techniques de Lille,
  59655 Villeneuve d'Ascq Cedex, France.

D1-6
1100

SIMULATION AND MODELING OF PHYSICAL PHENOMENA IN
MICROELECTRONIC DEVICES: G. Iafrate, Electronics Technology and
Devices Lab, Ft. Monmouth, NJ 07703-5302

D1-7
1120

PANEL DISCUSSION ON DEVICE MODELING AND SIMULATION

G1-1    **MODELLING IONOSPHERIC DENSITY STRUCTURES**
0900    R. W. Schunk and J. J. Sojka
Center for Atmospheric and Space Sciences
Utah State University
Logan, Utah 84322-4405, U.S.A.

Large-scale density structures are a common feature in the high-latitude ionosphere. They have been observed in the dayside cusp, polar cap, and nocturnal auroral region over a range of altitudes, including the $E$-region, $F$-region and topside ionosphere. Relative to background densities, the perturbations associated with large-scale density structures vary from about 10% to a factor of 100. These structures can be created by a variety of mechanisms, including particle precipitation in the dayside cusp, in sun-aligned polar cap arcs, and in the nocturnal auroral oval; by structured electric fields which lead to structured enhanced loss rates; and by large-scale plasma convection which acts to separate and distort ionospheric density features. The origins, lifetimes and transport characteristics of large-scale density structures were studied with the aid of a three-dimensional, time-dependent ionospheric model. The study considered blob creation due to particle precipitation, the effect that structured electric fields have on the ionosphere, and the lifetimes and transport characteristics of density structures for different seasonal, solar cycle, and interplanetary magnetic field (IMF) conditions. The main conclusions drawn from the study are: (1) The observed precipitation energy fluxes are sufficient for blob creation if the plasma is exposed to the precipitation for 5–10 minutes; (2) Within 10–20 minutes after blob creation by precipitation, the $F$-layer recovers its shape, and hence, the source characteristics cannot be determined from the profile shape after this time period; (3) Structured electric fields produce structured electron densities, ion temperatures, and ion composition; (4) The lifetime of an $F$-region density structure depends on several factors, including the initial location where it was formed, the magnitude of the perturbation, season, solar cycle and IMF; and (5) Depending on the IMF, horizontal plasma convection can cause an initial structure to break up into multiple structures of various sizes, remain as a single distorted structure, or become stretched into elongated segments. These and other aspects of large-scale plasma density structures will be described.

G1-2
0940

URSI ACTIVITIES TO FOSTER IMPROVED IONOSPHERIC
   MODELS
Charles M. Rush
National Telecommunications and Information
   Administration
Institute for Telecommunication Sciences
Boulder, CO 80303

The International Radio Science Union has taken an active role in the development of improved ionospheric models that can aid in predicting the performance of telecommunication systems that rely on the ionosphere. The development of the International Reference Ionosphere (IRI) has been jointly sponsored by URSI and COSPAR for a number of years. In August 1986 an URSI-sponsored workshop brought together model builders and model users in an attempt to foster communication and appreciation of the needs of each for the other. This workshop identified a number of areas where further work is required in order to bring the results of ionospheric modeling into telecommunications applications. Commission G decided at the Tel Aviv General Assembly to form a new Working Group to look at the general topic of ionospheric models. This Working Group is currently defining its terms of reference and studies it will undertake.

In this paper we will review the status of these URSI activities and point out those areas where further URSI work is likely to be directed. Also, discussion will be given to studies that are needed to be addressed so that ionospheric model developments readily find their way into improvements in telecommunication system prediction and performance assessment.

G1-3
1000

# Mapping of $f_0F_2$

By
Kenneth Davies
NOAA/ERL/SEL, Boulder, CO 80303

## ABSTRACT

Working Group 5 of URSI has recently developed a new numerical map for a global representation of $f_0F_2$. The new maps are based on the Fox-McNamara (Australian) data base which includes both observed data and theoretical data obtained from a physical model of the ionosphere. Each map is described by 988 coefficients, which is consistent with those used by the CCIR. The new maps provide an improved description over ocean areas.

G1-4
1040

THE IONOSPHERIC RESPONSE TO A LARGE GEOMAGNETIC
STORM:  COMPARISON OF CALCULATED AND OBSERVED
VALUES
D. N. Anderson
Air Force Geophysics Laboratory
Hanscom AFB, MA  01731-5000
M. Mendillo and K. Davies

The large geomagnetic storm on Feb. 8, 1986 produced
dramatic increases in both TEC and NMAX values at a number
of observing stations across the continental United States.
Ionosonde data from Boulder indicated an order of magnitude
increase in NMAX from $2 \times 10^5$ el/cm$^3$ to $1.8 \times 10^6$ el/cm$^3$
between 1400 and 1600 LT while at PT. Arguello, California
the density increased from $4 \times 10^5$ to $3 \times 10^6$ el/cm$^3$.  To
better understand the mechanisms which brought about these
dramatic increases, we calculate electron density
distributions as a function of latitude and local time by
solving the time-dependent plasma continuity equation
including the effects of production, loss and transport of
ionization.  The separate and combined effects of both
meridional neutral wind and zonal and meridional E x B
drifts are studied to determine which transport mechanisms
are responsible for the observed changes in NMAX, HMAX and
TEC.  The sudden increase in NMAX followed by a sharp
decrease on the afternoon of the first day is a classic
ionospheric-response signature to geomagnetic storms in the
American sector.  We discuss the implication of our
findings to other longitude sectors.

G1-5   The MUF(3000) as an F-region Variability Parameter
1100

Adolf K. Paul
Naval Ocean Systems Center
Ocean and Atmospheric Science Division
Code 544
San Diego,California 92152-5000

Acoustic  gravity waves  continuously  modify  the F-region  with a
variable  degree of intensity. The resulting deformations  are visible
as oscillatory  variations of the virtual heights at fixed frequencies
and to a lesser extent  as variations of the maximum electron density.
The virtual height oscillations  are usually delayed in phase at lower
frequencies (heights)  compared  with  heigher  frequencies (heights).
The results  are height  dependant tilts  which can have  a variety of
significant  consequences  ranging  from errors  in the computation of
electron density profiles  to large uncertainties in direction finding
attempts.
     The MUF(3000)  is a standard parameter  and is  either directly  or
indirectly scaled for every ionogram. The height-frequency coordinates
where the MUF is determined  correspond  to a point  very close to the
middle of the lower half  of the F-region profile and temporal changes
of the MUF usually  reflect  a combination  of changes  in the virtual
heights  and electron density in the vicinity of this point. For those
reasons it appears  that the temporal variations of the MUF could be a
direct indicator  for the reliability  of ionospheric quantities. This
can be verified by comparison  of various F-region parameters with the
time derivative of the MUF(3000).

G1-6
1120

EVALUATION OF A LONG WAVELENGTH PROPAGATION MODEL
USING VLF DATA COLLECTED ABOARD A SHIP

Jerry A. Ferguson
Rita P. Brown
Ocean and Atmospheric Sciences Division (Code 544)
Naval Ocean Systems Center
San Diego, CA  92152-5000

VLF and LF signal strength data were collected aboard the MST Callaghan over the period between March 1985 and November 1985 while the ship made repeated crossing of the North Atlantic.  the crossings were generally between ports on the east coast of the United States and Bremerhaven, West Germany. One crossing was from the east coast of the United States to Alexandria, Egypt.  Good data were obtained from the US Navy transmitters at Annapolis, MD (21.4 KHz) and Cutler, ME (24.0 KHz) and from the British stations at Rugby (16.0 KHz) and Anthorne (19.0 KHz).  These data provide the basis for statistical evaluation of signal strength variations and of the calculations of the long wavelength propagation capability (LWPC) being developed at the Naval Ocean Systems Center.

Results indicate a complete lack of solar zenith angle (seasonal) dependence on these paths.  The calculations using the model of the daytime ionosphere in the LWPC shows excellent agreement with these measurements.

G1-7
1140

## SSL RANGE ESTIMATION USING DIFFERENT IONOSPHERIC MODELS

Leo F McNamara
Andrew Antennas
Technology Park 5095
AUSTRALIA

Observations of the elevation angle and bearing of signals from distant HF transmitters, made with the single station location system SKYLOC, have been used to investigate the range accuracy obtainable with different models of the vertical distribution of electron density. Several N(h) profile shapes have been considered, all anchored at layer peaks defined by fairly standard procedures:-

1.  A single 3-parabola profile for each hop

2.  A variable 3-parabola profile which varies along the circuit

3.  A variable Dudeney profile (JATP 40, 195, 1978)

4.  A variable 3-layer Chapman profile

5.  A variable International Reference Ionosphere profile (UAG-83)

Models (1) and (2) were converted into a set of quasi-parabolic profiles, for rapid no-field range estimation. Raytracing for models (3), (4) and (5) was three-dimensional, including the earth's magnetic field. The E layer was essentially the same for all profiles.

The five models have been scored according to how close their calculated ranges came to the correct range for F2 propagation. No significant differences were found for models (1) to (4), but model (4) usually gave the longest ranges and thus scored highest when all methods underestimated the range. The IRI profile fared badly, failing to support the observed propagation on many occasions, and scoring poorly on the other occasions.

Range estimates for F1 propagation present a confusing picture, indicating a generally unsatisfactory modelling of this region.

H/G/B1-1   REVIEW OF PATH INTEGRAL TECHNIQUES AND
0900       SOLUTIONS OF THE FOURTH MOMENT OF WAVES
           PROPAGATING IN RANDOM MEDIA

R. G. Frehlich

Cooperative Institute for Research in the Environmental Sciences

University of Colorado

Boulder, CO  80309

Series solutions for the fourth moment of waves propagating through random media using path integral techniques are reviewed. The solution for the random phase screen is presented using Green's function techniques. Narrow angular scattering is assumed. The analogous result for extended random media is then derived using the path integral representation of the Green's function and the Markov approximation. The application of these results to extended incoherent sources is reviewed. The analogous result for space-time fourth moments of "frozen" random media is presented.

H/G/B1-2  SCINTILLATION AND SCATTERING IN
0920      INHOMOGENEOUS  MEDIA

Y. L. Li and C. H. Liu, Dept. of Electrical and Computer
Engineering, University of Illinois, Urbana,IL 61801

This paper presents a method for studying scintillation and scattering of
waves due to random irregularities embedded in a three-dimensional linearly
inhomogeneous medium.  In particular, the effects of the scattered fields on
field distribution in the shadow zone will be investigated.  The analysis is
based on Green's function for such a medium derived from the path integral
approach and expressed exactly by a onefold integral.  The scattered waves
which include the effects of  random irregularities are computed using the
Born approximation.  The total field distribution in the shadow zone can be
obtained by summing the incident wave and the contribution from the
scattered waves.  The method is quite general since source position and
irregularity shapes are allowed to vary widely.  A program for computing
the field wherever the source and irregularities are distributed and the
numerical techniques used to improve the program efficiency will be
discussed.  A technique used to generate random scatterers with prescribed
spectral behavior will be presented.  Numerical results for the various
position of source and irregularities will be shown.   These results
demonstrate that, depending on the position of irregularities, the field
distribution in the shadow zone can be drastically modified by scattered
fields.

H/G/B1-3
0940
INTENSITY    CORRELATION    FUNCTION    FOR    WAVES    OF
DIFFERENT    FREQUENCIES    PROPAGATING    THROUGH    A
RANDOM MEDIUM

A. Bhattacharyya[1] and K. C. Yeh
Department of Electrical and Computer Engineering
University of Illinois
Urbana, IL 61801

The fourth moment equation for waves of two different frequencies propagating through a two-dimensional extended random medium with a wavenumber-dependent refractive index is solved numerically. The numerical scheme is based on a split-step algorithm which approximates the solution by replacing the extended medium by a series of phase screens interspersed with diffraction layers. The phase screens give rise to different phase perturbations for the two waves. In addition to this, diffraction in the region between two phase screens also depends on the wave frequency. Therefore, in the calculation of intensity cross-correlation function for waves of different frequencies, propagation within the irregularity slab becomes increasingly important as the thickness of the slab is increased, unlike the case of monochromatic waves, where the intensity auto-correlation function for an extended medium is very well approximated by that for a single centrally located phase screen which produces the same mean square fluctuation of phase (H. G. Booker et al., J. atmos. terr. Phys., 47, 381-399, 1985).

Under multiple scattering conditions and with the assumption of "frozen flow", the intensity cross-spectrum shows increasingly steep decrease at high spatial frequencies as the ratio of the two wave frequencies deviates farther from unity. This feature is present for irregularities with either a Gaussian or a power-law power spectrum. The intensity cross-spectrum has the same behavior at high spatial frequencies when the refractive index of the medium is independent of wave frequency (S. J. Miller, Proc. R. Soc. Lond., A410, 229-249, 1987). However, at the low frequency end, the nature of the intensity cross-spectrum is determined by the wavenumber dependence of the refractive index fluctuations.

The effect of increasing the strength of the irregularities on the normalized correlation function of intensity fluctuations on waves of different frequencies is also investigated. In the weak scintillation limit, the decorrelation is independent of the strength of the irregularities. As the refractive index fluctuations increase in strength, at first only the lower frequency wave undergoes multiple scattering and this leads to rapid decorrelation of the intensities of the two waves, but when both waves undergo multiple scattering, there is little further loss of correlation.

The two-frequency space-time intensity correlation function is obtained for the "non frozen" situation where the irregularities have random velocity fluctuations with standard deviation $\sigma_v$ superimposed on a uniform drift. The effects produced by the velocity fluctuations are similar to those in the monochromatic case (A. W. Wernik et al., Radio Sci., 18, 743-764, 1983; S. J. Franke and C. H. Liu, AGARD Conference Preprint, No. 419, 15-1, 1987). The peak value of the cross-correlation function for a non-zero spatial separation decreases as $\sigma_v$ increases and the peak itself moves towards a smaller time lag and has a positive skewness. However, velocity fluctuations become increasingly ineffective in causing decorrelation as the ratio of the two frequencies deviates farther from unity.

---

[1] On leave from the Indian Institute of Geomagnetism, Bombay, India.

H/G/B1-4    SPECTRAL DOMAIN METHODS FOR RADIOWAVE
1020        PROPAGATION IN CONTINUOUS RANDOMLY
            IRREGULAR MEDIA

Charles L. Rino
Mission Research Corporation
2300 Garden Road, Suite 2
Monterey, California 93940

The parabolic wave equation has been used extensively for propagation in continuous randomly irregular media. It assumes (1) small local perturbations (the Markov approximation), (2) narrow-angle scatter, and (3) negligible backscatter. More recently, the cumulative forward scatter single backscatter approximation has been used to improve backscatter computations. In this paper we describe a spectral-domain method for computing the first- and second-order moments of the wavefield that fully accommodates backscatter and makes minimal restrictions on angular extent. The forward and backward scattered wavefields are characterized by an exact spectral-domain formulation of the scalar Helmoltz equation. The interaction of the wavefields with the medium is characterized by incremental forward and backward scattering functions. Approximate forms are computed in terms of the spectral density function of the relative permittivity fluctuations. Solutions are obtained for incident plane and spherical waves, which yield the well-known results derived from the parabolic wave equation when the backscatter terms are neglected. The general results give new insights into backscatter enhancements by showing that they depend on the correlation between scattered waves in the strict forward and backward directions.

Computations are performed to illustrate the effects of backscatter on VHF transionospheric radiowaves.

# THE MUTUAL COHERENCE FUNCTION IN REFRACTING MEDIA

L. J. Nickisch
Mission Research Corporation
2300 Garden Road, Suite 2
Monterey, California 93940

It has been recently shown (R. J. Hill, J.Acoust.Soc.Am, 77, 1742-1753, 1985) that a parabolic-type wave equation holds in refracting media provided that a particular coordinate system is used, the so called orthogonal trajectory coordinates. These coordinates are defined by path length along a deterministic ray and the surface of constant phase of the deterministic field at that path length. A stochastic equation for the two frequency mutual coherence function can be obtained from the parabolic wave equation. We show that this equation can be approximately solved by integration over the deterministic ray path corresponding to the mean refractive index.

The solution requires knowledge of the metric tensor for the surface of constant phase as well as information about deviated ray paths. We show that this information is given by integrating a set of differential equations describing deviated ray paths, obtained by varying the Hamilton equations for three-dimensional rays with respect to the independent variables.

H/G/B1-6   ANALYSIS AND INTERPRETATION OF
1100       WIDEBAND SATELLITE DATA

Dennis L. Knepp
Mission Research Corporation
2300 Garden Road, Suite 2
Monterey, California 93940

Fifty satellite passes with the most severe scintillation data measured during the course of the DNA Wideband Satellite Experiment in the late 1970s are re-examined in order to test the two-component description of the in-situ electron density irregularity spectrum. Analytic results for the two-position, single-frequency mutual coherence function and the signal decorrelation time inferred from the two-component irregularity spectrum model are compared to measurements. A comparison of measurement and theory for the single-position, two-frequency mutual coherence function is presented using data from seven coherently related UHF tones. The theoretical ramifications of the two-component model will also be discussed.

Specific parameters including the signal decorrelation time, the decorrelation distance and the channel bandwidth are determined from the data. Through specific analysis procedures that apply coherent signal processing techniques to the Wideband measurements, it is shown that these parameters quantitatively determine many aspects of the performance of a radar that might operate through a disturbed propagation channel.

H/G/B1-7
1120

# NUMERICAL FULL-WAVE SOLUTIONS TO THE MAXWELL EQUATIONS
# IN CONTINUOUSLY RANDOM MEDIA

L. J. Nickisch
Mission Research Corporation
2300 Garden Road
Monterey, CA 93940

Patricia Calvert
Naval Research Laboratory
4555 Overlook Ave.   Code 8344
Washington, DC 20375

Full-wave solutions to the Maxwell equations have been implemented numerically using the time domain finite difference (TDFD) method [Yee, K. S., "Numerical Solution of Initial Boundary Value Problems Involving Maxwell's Equations in Isotropic Media,"IEEE Transactions on Antennas and Propagation, Vol. AP-14, No. 3 (1966)], but the physical extent of the regions one could consider were limited by computer speed and storage requirements. With the advent of specialized parallel processing machines such as the Connection Machine, it is now possible to perform such calculations much more efficiently. The Connection Machine in particular is designed to efficiently perform nearest neighbor calculations over a full array simultaneously, reducing the time required to obtain TDFD solutions to Maxwell's equations by several orders of magnitude. Because of the power of these computational resources the applicability of this method has now broadened to include areas such as wave propagation.

Current methods used to predict the behavior of waves travelling through the ionosphere use certain simplifying assumptions to the Maxwell equations. The first approximation generally made is to ignore the polarization coupling terms in the wave equation, reducing the equations to scalar Helmholtz form. This equation is typically further reduced to the parabolic wave equation, a transport-type, small angle scatter equation. Thus backscatter is ignored. The TDFD method requires no such simplifications, but is capable of solving the full vector problem with tensor dielectric. The method is based on the Maxwell curl equations, which are first order differential equations in time. Finite difference approximations are applied to the differential operators and the equations solved in small time steps. The evolution of an incident pulse on the dielctric structure of interest can thus be followed, and since the full content of the Maxwell equations is included in the calculation, all effects are properly accounted for (e.g., polarization coupling, backscatter, Faraday rotation, etc.), limited only by the accuracy inherent in the grid resolution and boundary effects.

J1-1                    RADAR STUDIES OF COMETS
0900                    J. K. Harmon
                       Arecibo Observatory
                       P.O. Box 995
                       Arecibo, PR 00613

Five comets have been detected with Earth-based radar:
Encke, Grigg-Skjellerup, IRAS-Araki-Alcock (IAA), Sugano-
Saigusa-Fujikawa (SSF), and Halley. In each case, with the
probable exception of Halley, the dominant echo has come from
the nucleus. Since all of the observations have been of the
simple CW type, it has not been possible to determine simul-
taneously both the size and reflectivity of a comet nucleus
from radar data alone. However, comparison of the radar re-
sults for IAA and Halley with other data suggests that the
nuclei of these objects have relatively porous surfaces. The
two closest-approaching objects (IAA, SSF) gave strong echoes
from which it was possible to measure the shape and polariza-
tion of the nucleus Doppler spectrum. These echoes were simi-
lar in appearance to those obtained from many asteroids and
were consistent with nucleus surfaces which are very rough on
scales of a meter or larger. About 25% of the radar cross
section of IAA was contained in a broadband component whose
Doppler spectrum and polarization were consistent with scat-
tering from cm-size grains in the inner coma. The most recent
comet radar detection was that of Halley in November 1985.
The broad Doppler spectrum and unusually high radar cross
section (30 $km^2$) of the Halley echo are inconsistent with a
nucleus echo given what we now know about the nucleus from
the spacecraft encounters. Thus we conclude that the Halley
echo most likely came from large grains such as those associ-
ated with Comet IAA. The high radar cross section could then
be explained by the fact that Halley was a much more active
comet than IAA.

The major goals of future radar work are 1) to resolve
the nucleus of a comet with ranging-type observations, and
2) to observe additional bright active comets such as Halley,
if possible at small heliocentric distances when nucleus ac-
tivity is highest. Future comet observations at Arecibo will
rely on new-comet apparitions, as the prospects for observ-
ing known periodic comets are poor for the next few years.
Proposed upgrades to the Arecibo telescope and radar system
could significantly improve both the frequency and scientific
value of comet radar detections.

J1-2
0920
RADAR PROPERTIES OF THE ICY GALILEAN SATELLITES
S. J. Ostro
183-501, Jet Propulsion Laboratory
California Institute of Technology
Pasadena, CA   91109

Radar echoes from Europa, Ganymede, and Callisto are extremely strong and have bizarre polarization properties. At $\lambda 13$ cm, these objects' average radar reflectivities dwarf values reported so far for other radar-detected planetary targets, including the Moon, the inner planets, a few comets, and several dozen asteroids. The satellites' radar albedoes increase logarithmically from Callisto to Ganymede to Europa, whose radar reflectivity is similar to that of a metal sphere. The satellites' average, total-power, angular scattering law is $\sigma_0(\theta) \sim (\cos\theta)^{1.5}$.

When the radar transmission is circularly polarized, most targets return echoes with the incident handedness reversed, but for the icy satellites the handedness is, quite remarkably, preserved. The circular polarization ratio, $\mu_c$, of echo power in the same sense of circular polarization as transmitted (the SC sense) to that in the orthogonal (OC) sense, averages 1.2, 1.6, and 1.6 for Europa, Ganymede, and Callisto, compared to about 0.1 for the Moon and < 0.4 for most other targets. The linear polarization ratio, $\mu_L$, of OL to SL power, is ~0.5 for all three satellites, or nearly 20 times the lunar value.

The available data indicate that the unusual radar signatures vanish for wavelengths much smaller than a centimeter or as large as one meter. Significant albedo and/or polarization features are common in the echo spectra and, in a few cases, the source of a radar scattering anomaly can be identified tentatively in Voyager images. (For a complete description of the radar dataset, see my review in *Satellites of Jupiter*, D. Morrison, ed., Univ. of Arizona Press, 1982, pp. 213-236.)
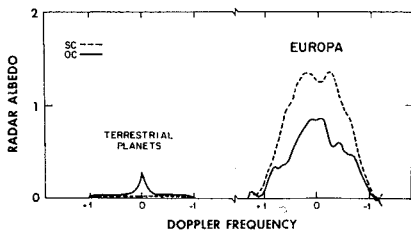


Typical $\lambda 13$-cm echo spectra for the terrestrial planets and Europa. Radar albedo is radar cross section divided by the target's projected area. The abscissa has units of half the echo bandwidth.

J1-3        INTERNAL REFRACTION AS A POSSIBLE CAUSE
0940        OF THE PECULIAR SCATTERING FROM THE
            GALILEAN SATELLITES.

T. Hagfors
National Astronomy and Ionosphere Center
Space Sciences Building
Cornell University
Ithaca, NY 14853

The radio wave scattering from the icy Galilean satellites is peculiar in that the cross section is larger than that of a metal sphere, yet the distribution of scattered power over the disk is relatively uniform, and lacking the quasispecular highlight characteristic of other bodies. Furthermore, the sense of circular polarization of most of the returned power is oppositely polarized to that of other solar system targets.

Several theoretical models have been deviced to explain this behavior involving hemispherical craters, randomly oriented surface cracks and voids, buried craters and refracting "lenses" of various types.  The talk discusses details of the refracting lens model, elaborating on the original idea (T. Hagfors, Gold, T. and M. Ierkic, Nature, 315,637-640, 1985).  It is shown that the model is capable of explaining the observed scattering properties.  The physical mechanisms which can give rise to the structures postulated are discussed, as well as experiments which may be required to determine whether the postulated scattering mechanism is the correct one.

J1-4
1020

THE RADAR-GLORY THEORY OF ECHOES FROM THE ICY
GALILEAN MOONS OF JUPITER

Von R. Eshleman
Stanford University
Stanford, CA 94305

The well-known electromagnetic phenomenon of total internal reflections (TIR) at a dielectric interface may be central to an explanation for the puzzling characteristics of radar echoes from Europa, Ganymede, and Callisto, giant ice-clad moons of Jupiter. A model in which TIR occurs in a geometry that favors the backscatter direction has the inherent properties needed to explain the exceptional strengths, surprising lack of specularity, and anomalous polarizations of the icy-moon echoes. Optical glory involves TIR in a spherical geometry (cloud water droplets) that favors backscatter (hence its appearance in the anti-solar direction). However, a roughly hemispherical geometry appears more appropriate for the icy-moon setting where cratering and flooding are known to occur. Hemispheres can be much superior to spheres as glory sources since they provide a break-out (and break-in) mechanism for the otherwise trapped TIR modes. To obtain radar glory from TIR in a hemispherical source, the hemisphere must have a higher refractive index than its curved surroundings. This leads to a proposed model of buried craters to explain the radar observations of the icy moons of Jupiter. The negative discontinuity in refractive index at the flood-crater interface could be due either to an overburden of higher density than the original surface material or to the formation of a thin low-density film on the old surface prior to flooding, due to ice sublimation or frost formation. More complete understanding of he icy-moon echoes, which are fundamentally different than the returns from rocky planets and Earth's moon, is important in basic studies of the icy bodies of the outer solar system and for planning radar mapping surveys of their surfaces.

J1-5    GALILEAN SATELLITES, GEOLOGY: E.M. Shoemaker, Branch of
1040    Astrogeologic Studies, U.S. Geological Survey, Flagstaff, AZ 86001

J2-6    OBSERVATIONS OF SATURN'S RINGS: D.O. Muhleman, California Institute
1100    of Technology, Pasadena, CA 91125

J2-1      PROPOSED UPGRADE OF THE ARECIBO TELESCOPE: D.B. Campbell, Arecibo
1120      Observatory, Arecibo, PR 00612

# GOLDSTONE SOLAR SYSTEM RADAR UPGRADE

J2-2
1140
N. A. Renzetti
Jet Propulsion Laboratory
4800 Oak Grove Drive
Pasadena, CA  91109

An extensive upgrade of the Jet Propulsion Labora-tory's Goldstone Solar System Radar (GSSR) is planned for a 1993 operational date. The GSSR shares equipment and facilities with the Deep Space Network (DSN) and increase in performance will be accomplished by modifying the system components used uniquely by the GSSR, and by using the improvements planned for the overall DSN.

The major hardware upgrade will be to increase the GSSR X-band transmitter power output from 360kw at the feedhorn to 1 mw cw. This 4.4 db improvement coupled with a 2 db increased antenna performance will more than quadruple the effective radiated power from the GSSR X-band transmitter. Additional performance benefit will be realized with the upgrade of the exciter to provide sufficient drive for four Klystrons and to incorporate a phase correction loop necessary for the 1 mw combining. Using a new phase correction loop, the exciter design is expected to provide approximately 40 db in phase noise improvement over the current system.

The second major upgrade is to the DSN's Digital Data Acquisition hardware and software. Major modifications will accommodate complex, multi-channel dual circular polarization data acquisition. This will allow the GSSR to be used in gathering a much more extensive data base than is currently possible. In addition, the DAS bandwidth per channel will be increased to accommodate the enhanced resolution and wider spectral coverage which is being required in carrying out more detailed planetary radar measurements.

In addition to these major upgrades, improvements to the monitor and control system will be carried out. In particular, a new modularized distributed control system is being designed around Hewlett Packard's Vectra computer, an industrial equivalent of an IBM PC-AT. The plan is to have the various equipments, needed to support the 1 mw radar, connected with the control console via an IEEE-488 bus and fiber optic links. ADA will be the programming language and artificial intelligence techniques are currently being evaluated for transmitter maintenance augmen-tation. A prototype rule-based expert system is currently undergoing evaluation.

Session A-2    1355-Tues.    CR1-42
MICROWAVE AND MILLIMETER WAVE MEASUREMENTS
Chairman: David F. Wait, Electromagnetic Fields Division, National
Bureau of Standards, Boulder, CO 80303

A2-1
1400

# A FIRST-ORDER FIELD CORRECTION TO THE CHARACTERISTIC ADMITTANCE OF A COAXIAL LINE

W.C.Daywitt   Electromagnetic Fields Division
National Bureau of Standards
Boulder, Colorado 80303  USA

Since coaxial lines have been in heavy use for years it is an odd fact that a complete set of field equations correct to first order in the skin depth cannot be found it the literature, although Stratton does give a piece of this field in his book on electromagnetic theory (*Electromagnetic Theory*. New York: McGraw-Hill, p.552, 1941). In the process of correcting this situation for another application (W.C.Daywitt, *Metrologia* 24, 1987) the effect of the the first order field terms on the characteristic admittance and the distributed line parameters was calculated. The results are reported in this talk.

The coaxial line is treated as perfectly concentric with an infinitely thick outer conductor, and when the characteristic admittance $(2\pi a H_a / \int_a^b E_r \, dr)$ is calculated from the resulting field equations, the following expression for the admittance is obtained:

$$Y_0 = \hat{Y}_0 \left( 1 + \frac{\delta Y_0}{Y_0} + a\mathcal{E}_a - \frac{\int_a^b \mathcal{E}_r \, dr}{ln(b/a)} \right)$$

where $\hat{Y}_0$ is the characteristic admittance for a lossless line, $\delta Y_0/Y_0$ is the usual term accounting for finite conductivity, and the last two terms are the first order field corrections. The electric field corrections $\mathcal{E}_a$ and $\mathcal{E}_r$ are obtained from the equation

$$\mathcal{E}_r = \frac{rh^2}{2} \left( ln\frac{b}{r} + \frac{1}{2} - \frac{ln(b/a)}{1+b/a} \right)$$

where $h^2$ is the usual correction to the principal wave propagation constant.

The last two terms in $Y_0$ cause a 6.4% decrease in the distributed line resistance, while their effects on the other distributed line parameters are found to be negligible.

In addition to the results just presented, the investigation led to a first order correction $\Delta\gamma_m$ in the propagation constant for the symmetric $TM_{0m}$ modes. For a positive harmonic time variation, this correction is

$$\Delta\gamma_m = \frac{jkz_s}{ab\gamma_m} \left[ \frac{aJ_0(k_m a)N_0(k_m a) + bJ_0(k_m b)N_0(k_m b)}{J_0(k_m a)N_0(k_m a) - J_0(k_m b)N_0(k_m b)} \right]$$

where $J_0$ and $N_0$ are first and second kind Bessel functions, $k$ is the free space wavenumber, and $z_s$ is the normalized surface impedance of the conductors.

A2-2      INDUSTRY NOISE PARAMETER MEASUREMENTS
1420      W. C. Mueller, Sr. Applications Engineer, MSG
          Avantek Inc. 3175 Bowers Avenue
          Santa Clara, Ca 95054-3292

The following is a technique suitable for use between 2 and 18 GHz for determining the four noise parameters $F_{min}$, $|\Gamma_{opt}|$, $\angle\ \Gamma_{opt}$, $R_n$ using standard production test equipment.

Measurement Technique (single sideband technique):
      Ensure:ENR is set correctly (include correction for isolator if used); oscillator is stable to within ±1 MHz; choice of IF combined with rejection of filter provide at least 40 dB rejection. Connect (Noise Source) to (Second Stage). Set gain reading to 0.0 dB. Record $F_2$ in dB. Now connect (Input Tuner), (DUT), and (Output Tuner) as shown. Set tuners to 50Ω position. Record $F_{50}$, $G_{50}$ in dB. Adjust (Input Tuner) for lowest noise, (Output Tuner) for highest gain. Record $F_{meas}$, $G_{meas}$, settings of tuners (slug and slide positions). Take tuners to a vector Network Analyzer, reproduce the tuning settings, record full s parameters for both (Input Tuner) and (Output Tuner).

Calculations:
  $F_{min}$: $F_{min}$ in dB = $10\ \log_{10}\ [F_{meas(lin)}-(F_{2(lin)}-1)/G_{meas(lin)}]$
                 $-\ 10\ \log_{10}\ [|s_{21}|^2\ /\ (1-|s_{22}|^2)]$
      where  $x_{lin} = 10^{x/10}$ and $x = 10\ \log_{10}\ (x_{lin})$
  $\Gamma_{opt}$ , (Noise Source) s par. are measured both with the noise diode on and with it off. An average $s_{11}$ is taken. A model is made of the test fixture (50Ω line + capacitive fringing). These are combined with the measured s par of (Input Tuner) to yield $\Gamma_{opt}$.
  $R_n$ : $R_n = 12.5\Omega(10^{F_{50}/10} - 10^{F_{min}/10})(1+|\Gamma_{opt}|^{-2} + 2\cos(\angle\Gamma_{opt})/|\Gamma_{opt}|$
  Note:$G_A$ = $G_{meas}$ + loss(Input Tuner) + loss(Output Tuner); tuner loss = $10\ \log_{10}[|s_{21}|^2\ /\ (1-|s_{22}|^2)]$;  $G_A$ calculation provides noise parameter verification: check against predicted s par. gain at $\Gamma_{opt}$.

Concerns: s par of tuners (repeatability of settings and connections, significant figures, correcting for non-50Ω); temperature corrections; fixture model; diode $s_{11}$; $R_n$ determination when $\Gamma_{opt}$ is near 50Ω.
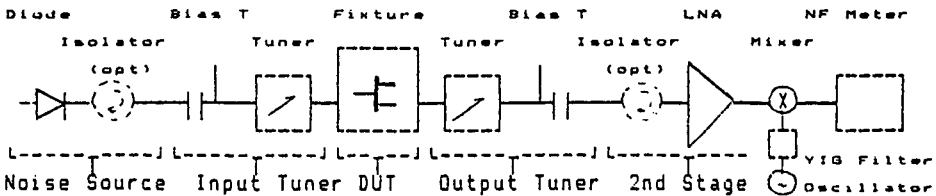


NOISE PARAMETER MEASUREMENT SETUP

A2-3
1440

# MULTIVARIATE STATISTICAL CONTROL OF THE NBS AUTOMATED RADIOMETER

Dr. D. S. Friday, Electromagnetic Fields Division
National Bureau of Standards
Boulder, Colorado 80303

Each of the new NBS automated radiometers is designed to operate over a particular band of frequencies. A set of special check-standards will be maintained for each radiometer for the purpose of monitoring the stability of its measurements over time. In a band, checks will be made at several frequencies and it is desirable to have a single indicator of system stability for the entire band. The fluctuations in these measurements are a random process and it is important to efficiently detect real changes in the system while ignoring normal variation. Statistical methodology is proposed whereby the check-standard noise sources can be measured at several frequencies each time a radiometer is tested, and a single control chart is used to monitor the system performance. If the single chart exhibits an anomaly and suggests a more detailed investigation, then individual frequency charts can be studied.

The multiple frequency charts are based on a principal component transformation. Each data vector represents the measurements at the various frequencies on a specific check-standard at a particular point in time. The transformation is derived from prior measurements done over the history of the device. That is, all such vectors for which the radiometer was stable during past checks. The current observation vector is then compared statistically to the past data. The maximum eigenvalue and its distribution is then used for monitoring the entire frequency band. It has the appealing interpretation that this eigenvalue contains the most information, in a linear sense, on the joint variation at all the frequencies. Other relevant statistical control methodology for the radiometers is also discussed.

A2-4     MEASURING CONNECTOR INSTABILITIES
1500     WITH HIGHLY REFLECTING LOADS

John R. Juroshek
National Radio Science Meeting
National Bureau of Standards
U.S. Department of Commerce
Boulder, CO 80302

Instabilities   and   inconsistencies   in   rf
coaxial connectors are one of the basic mechanisms
that   are   currently   limiting   the   accuracy   of
coaxial   impedance   measurements   at  the   National
Bureau of Standards.   Impedance changes that occur
at the rf connector joint, during disconnection or
reconnection, are often of the order of 1 part in
$10^3$   or   greater.     This   fact   coupled   with   the
customers demands for better accuracy in impedance
measurements has led to a significant effort to
both improve the quality of the rf connectors and
to measure and model its parameters.   This talk
describes the results of some of that effort.

The   talk   describes   how   the   sensitivity   of
measuring connector parameters can be increased by
using   high   VSWR   and   swept   frequency   measurement
techniques.     Subjecting   the   connector   to   a   high
VSWR   and   swept   frequency   means   that   at   some
frequencies the joint will be at a current maximum
while at other frequencies it will be at a current
null.     The   experimenter   is   therefore   able   to
identify the resistive, capacitive, and inductive
components   of   the   joint   as   well   as   any   changes
that   occur   in   these   components.     Experiments   on
some devices with 14-mm connectors are described.
It   is   shown   that   the   change   in   reflection
coeficient,   $\Gamma$,   for   a   device   with   connector
instabilities can be up to 4 times greater for the
high VSWR environment as compared to the matched
or VSWR=1 environment.

A2-5
1520

# INTERCOMPARISON OF NBS NOISE STANDARDS

David F. Wait and George Counas
Electromagnetic Fields Division
National Bureau of Standards
Boulder CO  80303  USA

The National Bureau of Standards has constructed a
primary noise standard (1 - 12.4 GHz) which operates at
liquid nitrogen temperatures that overlaps the frequency
coverage of two prior NBS primary noise standards; namely the
WR284 (2 - 4 GHz) waveguide primary standard which operates
at 419 C, and the WR90 (8 - 12 GHz) waveguide primary
standard which operates at 1000 C.  This has provided an
opportunity to compare two independently developed primary
noise standards.

The new coaxial noise standard was used to measure the
noise temperature of two WR284 working noise standards at
3.0 GHz and 3.95 GHz (originally calibrated using the NBS
WR284 primary noise standard); and four WR90 working
standards at 8.2 GHz, 9.0 GHz, and 11.2 GHz (originally
calibrated using the NBS WR90 noise standard).  The agreement
between the old and the new calibrations was within $\pm$ 0.35%
for all frequencies.

The typical estimated errors in a calibration
measurement, old or new, are similar.  Sources of error and
approximate estimated contribution to the measurement
uncertainty of a working standard are; (a) uncertainty in the
output of the standards ($\pm$0.5%), (b) uncertainty in measured
power ratios ($\pm$0.5%), (c) mismatch uncertainty ($\pm$0.2% for
calibrations of waveguide standards using the old manual
comparison radiometers, negligeable with the coaxial standard
using the new automated noise comparison radiometer), (d)
radiometer nonlinearity ($\pm$0.01%), (e) switch asymmetry in the
new automated comparison radiometer ($\pm$0.2%), (f) connector
non-repeatability ($\pm$0.8% for the coaxial connectors at the
higher frequency, negligeable for the waveguide flange
connectors), (g) i.f. offset error ($\pm$0.2%), and (h) random
error ($\pm$0.3%).

Interestingly, the difference between the old and the
new calibrations is less than the estimated uncertainty
caused by either the old or the new primary standard alone.
It is on the order of the random uncertainties in the
measurement procedures.  It is about one third of the
connector loss for the coaxial standard operating at the
upper frequencies.  In other words, the agreement is better
than one might expect.  Comments on the significance of the
close agreement in the intercomparison of NBS primary noise
standards will be discussed in this paper.

A2-6   **TEST SYSTEM FOR WR-22 BAND NOISE SOURCES**
1540   P. E. Nolan, Staff Engineer
       Lockheed Missiles and Space Co.
       Primary Standards Laboratory
       Orgn. 48-75, Bldg. 195A
       P. O. Box 3504
       Sunnyvale,CA 94088

This facility has recently developed a test system that can accurately determine excess noise ratio for both solid-state and gas-discharge type sources in WR-22 Band at 33 to 50 GHz. Estimated accuracy is +-0.15 dB. Key component in the system is a commercial hot-cold load combination that was adapted for this application. Several aspects of the hot and cold references will be considered.

The ability to make accurate measurements is dependent on various factors associated with the mixer and local oscillator used to down-convert millimeter-wave signals to the IF range. Three methods of reducing the mismatch error caused by mixer input impedance are covered. Characteristics of the local oscillator can also adversely affect measurement results so that consideration should be given to the selection.

The measurements are preferably made in some type of room that is free of interfering sources. Effects on the measurements caused by radiation from an instrument controller and leakage from an RF bridge are discussed.

Verification of system performance was accomplished as part of a measurement assurance program involving other defense contractors and two equipment suppliers.

A2-7
1600

HIGH FREQUENCY TEST METHODS FOR GaAs MMICs: T.H. Miers, D. Williams, V. Hirsch, and M. Brunsman, Ball Aerospace Systems Division, P.O. Box 1062, Boulder, Colorado 80306

Testing strategy and methodology is extremely important for successful realization of GaAs MMICs (Monolithic Microwave Integrated Circuits). Since this is so closely coupled and is invaluable to the design activity and data base generation, it is important that standardized testing with automatic reduction and rapid feedback be integrated with the entire MMIC activity. Accurate and reliable standards and deembedding techniques are required for the data to be useful from a design standpoint. Standard methods and test structures are needed to track and characterize process and material behavior. Well known and accurate testing and deembedding techniques are necessary for device and circuit performance evaluation.

Standard Process Control Monitor (PCM) structures compatible with in-process wafer level microwave/millimeter wave parameter evaluation are extremely valuable. These structures must allow testing without the use of through substrate via holes. Therefore coplanar waveguide transmission media is a natural for this application. GaAs devices embedded in coplanar waveguide (CPW) transmission media are useful test structures to determine the high frequency effects of material and process variables upon device behavior. Correlations between material/process parameters and device performance are not well known and these structures are designed for in-process automated testing for generating such a data base. Device modeling and circuit performance predictions are also possible from analysis of CPW FETs or components. This also gives circuit designers a wealth of information for statistical design purposes. Large amounts of high frequency statistical data can be generated from these in-process wafer level test devices.

Wafer level probe and testing techniques for measurement of GaAs devices and circuits at frequencies up to 26.5 Ghz will be presented. Additionally, measurement and deembedding techniques for in-fixture evaluation of GaAS devices and MMIC's for noise parameters up to 26.5 Ghz and S parameters up to 50 Ghz will also be presented.

A2-8        MILLIMETER WAVE NOISE CALIBRATION AND
1620        MEASUREMENTS
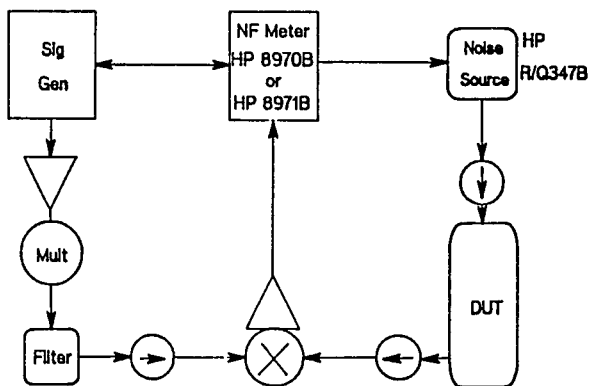            Peter Tong
            Stanford Park Division
            Hewlett Packard
            1501 Page Mill Rd., 5M
            Palo Alto, CA 94304

This paper is separated into 2 parts.  The first part is
on the theory, methods and accuracies of the calibration
of millimeter wave noise sources.  The second part
describes accurate and automated noise figure
measurements at millimeter wave frequencies.

The introduction of two new millimeter wave noise sources,
one at 26.5-40 GHz and the other at 33-50 GHz, relies on
accurate noise calibration.  The computer controlled
calibration procedure is based on room temperature and
liquid nitrogen loads.  It will be described and its
accuracy will be elaborated.

The noise sources allow accurate noise measurements.  The
methods discussed include a simple method which
eliminates noise figure contributions of the measurement
system and a second method which eliminates errore due to
impedance mismatches and the effect of the measurement
system noise.  This paper also contains techniques and
examples of double sideband(DSB) and single sideband(SSB)
measurements of passive and active devices.

The figure below shows a typical DSB measurement system
with maximum DSB system noise figure of 7.5dB across the
whole waveguide band.

## Double Side Band Measurement System:

B2-1      SCATTERING FROM PARTIAL SURFACES OF REVOLUTION

1400      M. P. Hurst and L. N. Medgyesi-Mitschang
          McDonnell Douglas Research Laboratories
          P.O. Box 516
          St. Louis, MO 63166

Electromagnetic problems dealing with bodies of revolution
(BORs) have been the subject of extensive investigations using
a variety of classical, analytical, and more recently,
numerical methods.  When the Galerkin technique is used with a
harmonic circumferential expansion along $\phi$, there is modal
decoupling in the integral operators.  (J. R. Mautz and R. F.
Harrington, AEU **32**, 159-164, 1978; P. L. Huddleston et al. **AP-
34**, 510-520, 1986.)  This coupling is true for conducting as
well as for penetrable surfaces or bodies.  This highly
desirable mathematical property is lost if the problem lacks
rotational symmetry.

This paper examines classes of partial surfaces of
revolution in the presence of perfectly electrically or
magnetically conducting (p.e.c. or p.m.c.) image planes where
modal decoupling is preserved by a judicious choice of
circumferential basis functions.  As an application of the
general formulation, a class of surfaces is examined in the
context of reflectors in a compact range.  The effect of edges
on the near-field behavior of these reflectors is discussed.

B2-2    SCATTERING BY A COMPOSITE AND ANISOTROPIC
1420    CIRCULAR CYLINDRICAL STRUCTURE:   EXACT SOLUTION

H. Massoudi, N.J. Damaskos
Damaskos, Inc., P.O. Box 469,
Concordville, PA   19331
and
P.L.E. Uslenghi
Department of Electrical Engineering and Computer
Science
University of Illinois, Chicago, IL   60680

Exact analytical solution for the two-dimentional
problem of electromagnetic (EM) scattering by a composite
and anisotropic circular cylindrical structure is presented
in this paper.  The scatterer consists of a metallic
cylinder coated by a lossy anisotropic layer and by an
impedance sheet.  In the anisotropic layer both permit-
tivity and permeability tensors, when referred to principal
axes $(\rho, \varphi, z)$, are biaxial and diagonal.  The impedance
sheet is also anisotropic and is characterized by a surface
admittance tensor $\overline{\overline{\eta}}$.  The primary EM sources are either an
arbitrarily polarized plane wave, normally incident on the
cylinder, or line sources parallel to the axis of the
cylinder.

Closed form expressions are derived for the EM fields in
the biaxial layer, induced currents on the conducting core
and on the impedance sheet, and also the scattered fields
in the exterior region.  The axial components of the EM
fields are expressed in terms of Fourier Series whose terms
are products of radial eigenfunctions and azimutal harmonic
functions.  It is shown that, in the anisotropic region,
the radial eigenfunctions satisfy the Bessel differential
equation with complex orders.

Curves showing the bistatic scattering cross-section as
a function of the scattering angle, for a variety of com-
posite anisotropic geometries, are presented.  In addition,
the extension of this analysis to EM scattering by a multi-
layered anisotropic cylinder, for oblique incident, is
discussed.

B2-3     ELECTROMAGNETIC SCATTERING FROM
1440     NONLINEAR ANISOTROPIC CYLINDERS

M.A. Hasan
Systems Engineering, RCA/ESD
Moorestown, N.J.   08057

P.L.E. Uslenghi
Dept. of Electrical Engineering and Computer Science
University of Illinois at Chicago
Chicago, IL   60680

The solution of the electromagnetic scattering of
obliquely incident plane waves from homogeneous, nonlinear
anisotropic cylindrical structures is obtained.  The medium
of the scatterer is characterized by Volterra-type integrals
for the electric and magnetic flux density vectors.  For the
particular case of a nondispersive dielectric medium, the
displacement vector $\underline{D}$ reduces to a Taylor series expansion
near zero.

The nonlinear problem is solved using both the iteration
method and the perturbation method, and the results are com-
pared.

The effect of nonlinearities on the field properties
both inside and outside the scatterer, together with the
effect on the radar cross section are investigated.  A
numerically efficient computer code is developed and tested
on a variety of scattering media for solid and hollow cylin-
drical bodies.

It is concluded that the two methods give nearly
identical results for small nonlinearities, or if the char-
acteristic dimension of the scatterer is small compared to
the wavelength.  However, the results obtained using the
iteration method diverge from the linear results, with
distortion, faster than those obtained by the perturbation
method.

# A UNIFORM GTD TYPE ANALYSIS OF ELECTROMAGNETIC PLANE WAVE SCATTERING BY A FULLY ILLUMINATED PERFECTLY CONDUCTING SEMI-INFINITE CONE

Keith D. Trott
RADC/EECT
Target Characterization Branch
Applied Electromagnetics Division
Hanscom AFB, MA 01731, USA

Prabhakar H. Pathak
The Ohio State University
ElectroScience Laboratory
1320 Kinnear Rd
Columbus, OH 43212, USA

Fredric A. Molinet
Societe Mothesim
Centre de la Boursidiere
92357 Le Plessis-Robinson, France

A uniform high frequency asymptotic solution, based upon the physical optics (PO) approximation, is obtained in the format of the uniform geometrical theory of diffraction (UTD) to describe the fields diffracted by the tip of a semi-infinite perfectly conducting cone when it is fully illuminated by an electromagnetic plane wave. The PO approximation is based upon the use of the geometrical optics (GO) currents on the cone. The solution is expressed in terms of an integral, over finite limits, which can be numerically integrated without difficulty. Previous solutions based upon PO are valid only on the deep shadow side of the reflection shadow boundary (RSB) and become singular at the RSB; however, the present solution is uniform in the sense that it remains bounded and continuous within the transition region adjacent to the RSB. Outside the transition region, the various terms in the integral form of the solution can be interpreted in terms of the geometrical theory of diffraction (GTD) as being associated with the incident, surface reflected, and tip diffracted ray fields. The results from the uniform asymptotic PO solution compare well with previously published results for narrow angle semi-infinite cones (L.B. Felsen, IRE Trans. Antennas and Propagat., AP-5, 121-129, 1957). In addition, the results compare well with measurements and an independent moment method (MM) solution for scattering by a finite flat-backed cone. For the finite cone, several higher order wave interactions are found to be significant; one such interaction is between the tip and the base of the cone. It appears that until now, there were no expressions in the open literature to calculate this tip-base wave interaction even though it was suspected to be important (W.D. Burnside, L. Peters, Radio Sci, Vol 7, No.10, 943-948, 1972). The present work provides the expressions necessary to calculate this interaction and also to confirm its relative importance.

B2-5    ON THE INVERSE SCATTERING BY A PARABOLIC REFLECTOR
1540    ANTENNA
A.Z.Elsherbeni, Electrical Engineering Department,
University of Mississippi, University, MS 38677
Z.Y.Chen, The Institute of Electronics Academia
Sinica, Beijing, China
M.Hamid, Electrical Engineering Department,
University of Manitoba, Winnipeg, Canada   R3T 2N2
(On leave at the University of Central Florida,
Orlando, Florida 32816)

Approximate relations for retrieving the aperture diameter
and focal distance of a parabolic reflector antenna are de-
rived from out of band inverse scattering procedure.  A de-
tection system consisting of four probes is proposed which
could be fixed in position or mounted on a moving platform
(e.g. ship or aircraft).  The first probe (sending probe) is
responsible for transmitting the test plane wave signal,
whereas the second probe (sensing probe) is used to correct
the orientation of the incident plane wave on the reflector
in order to maintain normal incidence by maximizing the back
scattered signal at a specific wavelength.  At frequencies
much lower than the operating frequency of the reflector
feed, the main re-radiation lobe from the reflector due to
the test plane wave signal, is found to be broad, therefore
the remaining two receiving probes should be highly di-
rective.  An incident plane wave with a low frequency rela-
tive to the operating frequency of the feed horn is employed.
Numerical results are presented to illustrate the method and
to show that while it does not require any time domain or
phase measurements, highly accurate scattering data are
necessary, especially if the observation angles of the re-
ceiving probes are close to each other.  The method is yet to
be extended to arbitrary polarization, wave type and di-
rection of incidence as well as to other types of antennas.
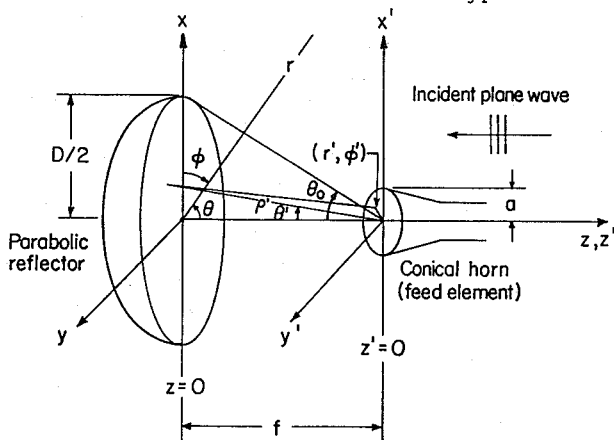
B2-6    **Response of a Souce in a Composite Medium**
1600    W.C. Chew
        Department of Electrical and Computer Engineering
        University of Illinois
        Urbana, IL 61801

We will discuss the solution to the problem of the radiation of a source on top of a composite half space where the inhomogeneity is varying in two dimensions, and the field is varying in three dimensions. This represents a two-and-one-half dimensions problem.

To solve this problem, we divide the inhomegeneity into layers, whose whose electromagnetic parameters are varying in one dimension. The eigenmodes in each layer is found by a one dimensional finite element method. Then boundary conditions at the interface between the layers are matched. From the boundary conditions, we define transmission and reflection operators at each interface. With the available of these reflection and transmission operators, we can gain a physical feel for the scattering process at each interface. Because of this, we can write down the propagation of waves through many layers of the medium easily, and also the solution of a source in such a medium.

We will illustrate the applications of this solution in geophysical sensing and integrated optics.

$$\epsilon_1(z), \mu_1(z)$$
$$\epsilon_2(z), \mu_2(z)$$
$$\epsilon_3(z), \mu_3(z)$$
$$\epsilon_{n-1}(z), \mu_{n-1}(z)$$
$$\epsilon_n(z), \mu_n(z)$$

$SOURCE$
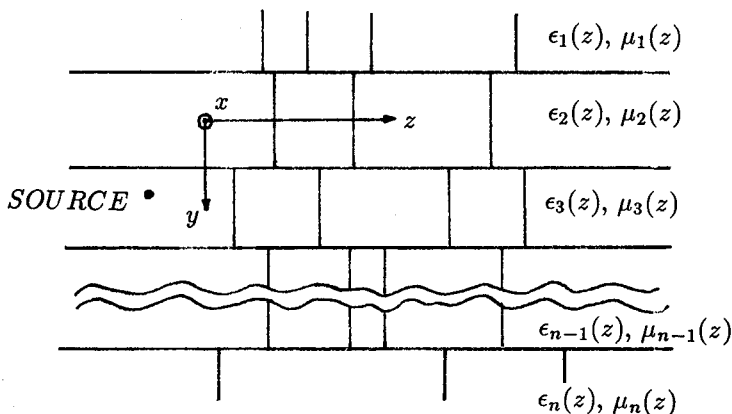
B2-7
1620

## CURRENT INDUCED ON AN INFINITELY LONG CONDUCTING CYLINDER RESIDING ON A GROUND PLANE DUE TO AN INCIDENT PLANE WAVE

T.C.K.Rao,Electrical Engineering Department,University of Lowell
Lowell,MA 01854.
R.Barakat,Division of Applied Sciences,Harvard University
Cambridge,MA 02138.

        An exact solution for the problem of plane wave scattering by
an infinitely long conducting cylinder that is situated on the
surface of a perfectly conducting ground plane is presented.The
total field consists of contributions from the incident field,the
reflected field and the scattered fields from the cylinder and the
image cylinder.By employing the addition theorem for the cylindrical
waves,a set of two coupled infinite system of equations for the even
and odd expansion coefficients is obtained.These coefficients are
numerically evaluated by a matrix inversion procedure.The induced
current is calculated from the coefficients for the case of an
obliquely incident plane wave of the TM type.The magnitude of the
current is plotted as a function of the angle of incidence and the
electrical radius of the cylinder as shown in the Figure.
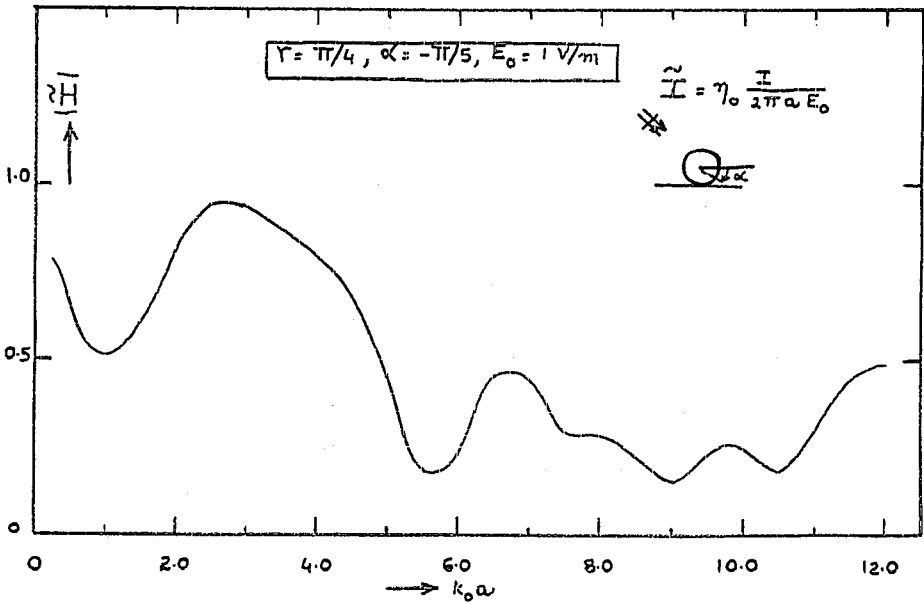
B2-8    EM SCATTERING BY BURIED OBJECTS OF LOW CONTRAST
1640    David A. Hill
        Electromagnetic Fields Division
        National Bureau of Standards
        Boulder, Colorado 80303

The plane-wave, scattering-matrix formulation provides a convenient means for combining antenna, scattering, and interface effects that arise in detection of buried objects [D.A. Hill and K.H. Cavcey, IEEE Trans., GE-25, 422-431, 1987]  However, it requires the full plane-wave scattering matrix [D.M. Kerns, Plane-Wave Scattering-Matrix Theory of Antennas and Antenna-Antenna Interactions, National Bureau of Standards Monograph 162, 1981] for the buried object for all incident and scattered plane waves.  For scatterers of arbitrary shape where numerical methods are generally required to determine the scattering characteristics, this requires a large amount of computation.

In this paper we use the Born approximation to obtain an approximate expression for the scattering matrix of the buried object in terms of an integral over the volume of the object.  For simple shapes (such as a sphere, a circular cylinder, or a rectangular box), the volume integral can be evaluated analytically to obtain a closed-form expression for the scattering matrix.  The Born approximation requires small contrast between the electrical properties of the buried object and the earth.  This requirement is restrictive, but the low-contrast case is important because it represents a difficult detection situation.

We present numerical results for scattering by buried spheres, cylinders, and boxes for plane-wave incidence.  Far field results are obtained by asymptotic methods, and near field results are obtained from two-dimensional fast Fourier transform (2D FFT).  The advantages of 2D FFT are speed and simplicity, and Sommerfeld integrals are avoided.  Only a portion of the scattering matrix is used for plane-wave incidence, but the total scattering matrix will be useful when the buried scatterer is illuminated by a realistic near-field source.

B3-1
1400

# COUPLED LINE MODEL FOR MULTIRESONATOR WIDEBAND MICROSTRIP ANTENNAS

K.C. Gupta and Brian Bandhauer
Dept. of Electrical and Computer Engineering
University of Colorado
Boulder, CO   80309-0425

Various multi-patch configurations of rectangular shaped microstrip antennas have demonstrated [Kumar and Gupta, IEEE-APS International Antenna Propagat. Symp., Houston, 1983] considerably larger bandwidth than that obtained from single patch configurations commonly used.   Out of the various configurations proposed, a multipatch arrangement with the patches coupled along the non-radiating edges [Kumar and Gupta, IEEE Trans. AP-33, 1985] is attractive as its size can be made very compact by reducing the widths of the individual patches.   When the widths of these patches become small, the capacitive coupling alone (as considered in the previous work) is not sufficient to provide an accurate analysis.

This paper proposes a coupled line model for multiple patch microstrip antenna configurations wherein the adjacent patches are gap-coupled along the non-radiating edges.   The case of a two-patch configuration is considered in detail.   A four-port network model for a coupled microstirp section is taken as the basic building block of the equivalent network model.   When the two patches are of unequal length, the extra length of one of the patches is accounted for by an additional capacitance at the corresponding end of the coupled line section.

Detailed computed results for two-patch antennas based on the proposed model will be presented.   Current experiments performed to verify the proposed model will be reported.

B3-2      AN INVESTIGATION OF THE IMPEDANCE
1420      OF REACTIVELY LOADED MICROSTRIP ANTENNAS
          Stuart A. Long and Ajaz Ali Khan
          Department of Electrical Engineering
          University of Houston
          Houston, Texas 77004

In the past, printed-circuit or microstrip antennas have proven to be quite versatile and have been used in a wide variety of applications. Their main advantages include structural simplicity, ease of construction, ruggedness, conformability, low profile, and low cost. In some applications, however, it would be quite desirable to be able to exert some control over the impedance of the element without affecting the pattern or the resonant frequency. This feature would be most valuable for use in a scanned phased array to alter the active array impedance of the elements to compensate to some degree for scan blindness. This investigation has shown that such an element can be designed through the use of suitably placed reactive loads.

Using previous theoretical work (W.F.Richards and Y.T.Lo, Electromagnetics, 3, 371-385, 1983), it is seen that the input impedance can be varied with a single short-circuit load without altering the resonant frequency. This impedance can be varied for a fixed feed location by the movement of the nodal line of the loaded resonant mode as the position of a short-circuit load is varied. The results indicate that a single short circuit placed on the proper locus can provide the required modification. Movement of the short circuit along this path can then be used to adjust the resonant resistance over a wide range of values. Unfortunately this rather simple structure tends to produce levels of cross polarization that can be undesirable in some applications. The use of a pair of symmetrically located loads can be used instead to eliminate this cross polarized component and, as an added advantage, allows even further flexibility in impedance control.

The proper loci for load positions have been calculated and plotted, and several configurations have been fabricated and tested. In each case good agreement was found between theory and experiment.
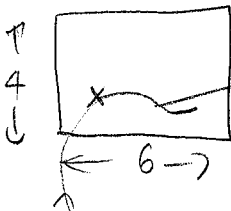


locus of points of shorting pin position for resonance; the closer pin is to feed, the lower impedance Z is.

feed (1,1)
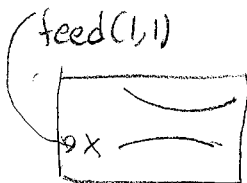
Symmetrical pins (one on each curve) are used to reduce XPOL introduced by above configuration...

B3-3
1440

## ANALYSIS OF COMPOUND SLOTS

Sembiam R. Rengarajan
Department of Electrical and Computer Engr.
California State University, Northridge
Northridge, CA  91330

This paper presents a mathematical model to analyze broad wall compound slots, having an offset from the center line and a tilt angle with respect to the longitudinal axis of rectangular waveguides. Figure shows the geometry of the problem. The slot is imbedded in an infinite planar conductor. The electric field in the slot is expanded in terms of entire domain sinusoidal functions in the longitudinal direction with a constant transverse distribution. The internal fields are in terms of Stevenson's Green's functions and the external terms are those of half space. Wall thickness is rigorously accounted for by considering a waveguide between inner and outer apertures.

*400,000 / terms!*

Compound slots are used in antenna array applications as radiating elements or coupling slots between main line and branch line guides. Their analysis has been complicated by the mathematical and computational work involved and hence antenna designs are presently relying on experimentally measured data. Numerical results presented in this work have considerable practical application.
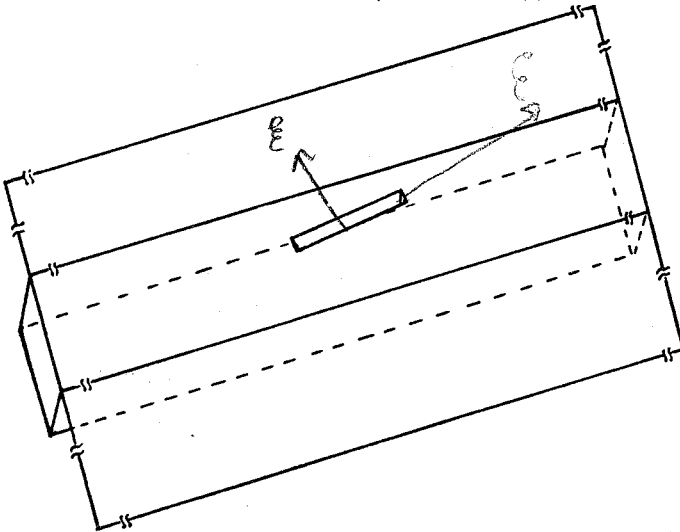


*Can ignore $E_p$*
*Match only $H_{long}$*

*Compound ≡ offset and inclined*

*Elliott says this is very important result since experimental approaches are very lengthy*

B3-4   PLANAR ARRAY EXCITATIONS TO PRODUCE FLAT-
1500   TOPPED BEAMS

R.S. Elliott and Y.U. Kim
Department of Electrical Engineering
University of California
Los Angeles, CA 90024

The advent of satellites has spawned the growth of an-
tennas whose patterns can cover a portion of the earth's
surface (e.g., the U.S.) more or less uniformly.  Conven-
tionally, this is done with a cluster of horns feeding a
parabolic dish, with the pencil beams due to the individual
horns forming an overlapping two-dimensional mosaic on the
targeted area.  Disadvantages of this approach are a ripple
in the coverage of about 3 dB, no control over the side lobes,
and a modest aperture efficiency.

Potentially, a properly excited planar array can over-
come all of these shortcomings.  This paper addresses the
question of pattern synthesis for such arrays.  A modifica-
tion of Orchard's technique (H.J. Orchard, et al, IEEE,
Part H, 132, 63-68, 1985) is used to generate a pattern with
a flat-topped beam, controlled ripple, and controlled side
lobes, due to an equispaced linear array.  The requisite ex-
citation is used as the collapsed distribution for the planar
array.  With the aid of a Baklanov transformation one can then
deduce the two-dimensional excitation.  An example will illus-
trate the procedure.

Overlap of pencil beams (from feeds in a reflector)
gives about 3 dB ripple

Can reduce planar array array factor to that
of the form of a linear array for one pattern cut,

To extend to other φ-cuts considers rect. array
2N×2N. let w = cos u · cos v  (Baklanov)
gives a one variable polynomial (w).

Yahya cautioned that multiple beam design
is different from contoured beam design which
Elliott is attacking.

B3-5    ANALYSIS OF A CYLINDRICAL ANTENNA INSIDE
1520    A HOLLOW, INFINITELY LONG, CONDUCTING
        CYLINDER – WITH EXPERIMENTAL VERIFICATION
        Anthony Q. Martin and Chalmers M. Butler
        Department of Electrical and Computer Engineering
        Clemson University, Clemson, SC 29634-0915

A solution technique is presented for the current induced on a cylindrical antenna residing coaxially within a hollow, infinitely long, conducting cylinder of circular cross section. The analysis begins with an integral equation formulated in terms of the magnetic vector potential Green's function for an axially-directed dipole inside the cylindrical tube. This Green's function consists of an infinite series of Sommerfeld-type integrals whose integrands comprise combinations of Bessel functions. With circularly symmetric excitation and when the antenna and cylinder axes coincide, the series simplifies to a single term (a Sommerfeld integral). When the antenna is not too long electrically, the integral equation can be solved by standard numerical methods. These methods employ either real-axis integration or integration along an alternate contour when the integrand possesses real-axis singularities.

The accuracy of the integral equation solution is verified through comparisons with measured data. Measurements are performed below the cutoff frequency of the (empty) cylindrical tube, allowing substitution of the infinite-length tube by one of finite length. Measured and computed data are presented for the current and charge induced on the inner wall of the conducting cylinder. Data for the driving point-admittance of thin-wire and sleeve-fed antennas are presented. Preliminary results reveal that the integral equation solutions are very accurate.

B3-6   COMPUTATION OF THE FIELD DUE TO A
1540   CYLINDRICAL ANTENNA INSIDE A CONDUCTING
       CYLINDRICAL TUBE

Anthony Q. Martin and Chalmers M. Butler
Department of Electrical and Computer Engineering
Clemson University, Clemson, SC 29634-0915

For a cylindrical antenna residing coaxially within a hollow, infinitely long, conducting cylinder, we present a comparison of techniques for computing interior fields. The field components are expressible in terms of a direct contribution due to the antenna and a reflected contribution due to the cylinder. While the reflected contribution is computed from a Sommerfeld-type integral, the direct contribution can be expressed either as a Sommerfeld integral or as an integral over the antenna current. The disadvantages of numerically evaluating the former is that the integrand is oscillatory and that the convergence can be slow. Also, the presence of a factor containing Bessel functions makes difficult the application of techniques to address the oscillations. The disadvantage of numerically evaluating the latter integral is that the integrand can be unbounded or highly peaked at various locations within the range of integration. The findings of an investigation of the relative merits of the two computational methods are presented. The results of these computations are supported by measured data.

B3-7    IMPLEMENTATION OF A HYBRID METHOD FOR
1600    COMBINING FULL WAVE AND QUASI-STATIC
        METHODS IN ANTENNA PROBLEMS    *Bob*
        P. D. Mannikko and R. G. Olsen
   Electrical and Computer Engineering Department
          Washington State University
              Pullman, WA 99164-2752

Recently, a hybrid method for the analysis of
electromagnetic problems involving electrically
small but geometrically complex sub-regions was
presented (R. G. Olsen and G. L. Hower, "On the
Use of Quasi-Static Techniques in Electrically Small
Regions of Electromagnetic Problems", 1987 National
Radio Science Meeting Digest, p 127) . The method
provides a detailed electrical description of the
electromagnetic fields in the complex sub-region.
This information is useful for analyzing the
breakdown properties of antenna loads and is not
available from codes which treat these sub-regions
as lumped elements. The analysis involves the
simultaneous solution of integral equations for both
the quasi-static and full wave regions while
accounting for the mutual coupling between the
different regions.

The method has since been numerically
implemented using moment method techniques for
axially symmetric wire antennas with "capacitive
like", electrically small loads which may consist of
conductors and dielectrics. Results are given for
several geometries including capacitor loaded and
top hat loaded antenna configurations. Wherever
possible, input impedance and current distributions
are compared with results from existing wire antenna
codes.

*Can correct MININEC using an effective length
of h+a (monopole over perfect ground plane).*

B3-8    **EFFECTS OF RANDOM ERRORS ON REFLECTOR**
1620    **SURFACE COMPENSATION USING ARRAY FEEDS**

Y. Rahmat-Samii
Jet Propulsion Laboratory
California Institute of Technology
Pasadena , CA   91109

To overcome the deteriorating effects of thermally (or gravitationally) slowly varying reflector surface distortions, arrays in the focal plane of reflectors can be used. The complex excitation coefficients of the array are typically obtained using a focal plane conjugate field match concept. This is achieved by utilizing a vector diffraction analysis approach which results in the determination of the complex excitation coefficients by requiring both the gain and sidelobe control and by incorporating the knowledge of the surface distortion.

Once the complex excitation coefficients are determined they are then used to set the attenuators and phase shifters for each element. The reflector is subsequently illuminated by the array with the adjusted excitation coefficients to result in the improved performance. In practice, however, the array excitation coefficients may not be set exactly and there will be random and systematic errors in setting the attenuators and phase shifters.

In this paper, the effects of random errors on the reflector performance are studied by using numerical simulations in generating random errors for both the amplitude and phase excitation coefficients of the array. It is shown that for specified thermal distortions of an offset reflector antenna how much random errors can be tolerated. Results of many simulations will be presented for different antenna configurations, array geometries and random error specifications. The results of this investigation will be useful in defining practical error bounds for the application of the surface compensation techniques and in performing meaningful measurements.

D2-1                    ADVANCES IN QUASI-OPTICAL
1400          MILLIMETER-WAVE INTEGRATED CIRCUITS

Tatsuo Itoh
Dept. of Electrical and Computer Engineering
The University of Texas
Austin, TX 78712

Traditionally, microwave and millineter-wave components have consisted of distinctly separate components such as antennas, mixers, diplexers, amplifiers and oscillators. Recently, these compnents are built in an increasing degree in a planar form in preference to a waveguide format. Many of these planar components constructed in hybrid or monolithic forms are more cost effective and more flexible in design than their waveguide counterparts. However, the RF front ends such as the mixers and transmitters are usually connected to external antennas. As the frequency of operation is increased, the loss caused by transmission medium between  the antenna and the front end increases significantly. An alternative approach is to fabricate an antenna directly integrated onto the planar substrate. In this scheme, it is possible to create a mixer and an antenna integrated into a single element. These mixers are called the quasi-optical mixers. The output port of the antenna and the RF input port of the mixer are indistinguishable and usually not accessible.

In addition to the quasi-optical mixers, there is an emerging technology to create planar quasi-optical structures that perform othere "active' functions such as frequency-multiplying, control and amplification. Technology for quasi-optical planar components is still not matured and a number of trials and new concepts are experimented. This talk summarizes some of the recent development in this area of research. The technology summarized here is not only useful at higher frequencies but also is believed to be available for low cost component development.

D2-2
1440

# NOVEL INTEGRATION OF A COPLANAR WAVEGUIDE FED MICROSTRIP ANTENNA WITH AMPLIFIER[*]

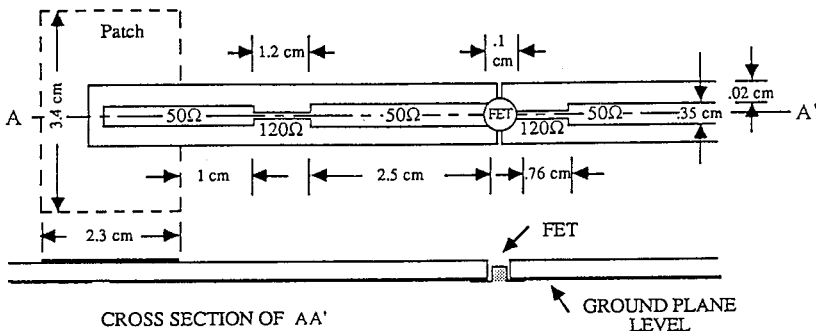P. Aoyagi, J. Brenneman, S.L. Chuang and Y.T. Lo
Department of Electrical and Computer Engineering
University of Illinois at Urbana-Champaign
Urbana, IL 61801

Microwave integrated circuits using coplanar waveguides with microstrip antennas are investigated experimentally. We consider a hybrid integration of microwave amplifiers, and matching networks using coplanar structures and coplanar-fed microstrip antennas. In particular, the possiblity of integrating microwave amplifiers (realized entirely with coplanar line) electromagnetically with microstrip antennas is demonstrated. This novel configuration should prove useful for MMIC phased array integration.

As a preliminary test of the integration between a microstrip antennas and coplanar line structures, a 4.0 GHz single element microstrip antenna array was interfaced via proximity feed to a microwave amplifier realized on coplanar line. The diagram below shows a successful integration scheme with the amplifier. Our results show that the amplifier adds approximately 13 dB gain in the radiation pattern over that without the amplifier.



CROSS SECTION OF AA'

D2-3
1500

## INTEGRATED OPTICAL DEVICES*

S. L. Chuang
Department of Electrical and Computer Engineering
University of Illinois at Urbana-Champaign
1406 W. Green Street
Urbana, IL 61801-2991

Integrated optical devices and their applications to microwave modulation will be discussed. These include semiconductor lasers, optical directional couplers, quantum-well electro-optical modulators and superlattice photodetectors.

Based on an improved coupled-mode theory derived from a generalized Lorentz reciprocity theorem (S. L. Chuang, J. Lightwave Technal., LT-5, 5-15 and 174-183, 1987), optical directional couplers and optical filters have been investigated theoretically and the results agree very well with those for the experiment.

New designs of electro-optical modulators using intersubband optical transitions in quantum-well structures have been proposed. The optical absorption properties of a quantum-well structure are controlled by an external bias field. The optical power output is thus modulated by the applied electric field. Our theoretical prediction (D. Ahn and S. L. Chuang, Phys. Rev. B, 35, 4149-51, 1987) was recently confirmed by experiment (K. Bajema et al, Phys. Rev. B, 36, 1300, 1987).

A novel design of superlattice photodetectors has also been proposed (S. L. Chuang and K. Hess, J. Appl. Phys. 59, 2885-94, 1986). Some recent experiments also confirm our early prediction of the physical mechanisms of the device.

A general overview of these integrated optical devices especially novel devices using quantum-well structures and their microwave modulation will be presented. Possible future research in this area will be discussed.

F/B1-1      AN ASYMPTOTIC FORM OF THE FLAT SURFACE IMPULSE
1340        RESPONSE FOR LARGE OFF-NADIR POINTING ANGLES
            Gary S. Brown
            Bradley  Department  of  Electrical  Engineering
            Virginia   Polytechnic   Institute   and   State
              University
            Blacksburg, Virginia  24061

     The  flat  surface  impulse  response  is  an  important
ingredient  in  describing  how  a  short  pulse  radar  altimeter
responds,  in  the  mean,  to  a  rough  surface. It  includes  all
effects  except  those  due  to  the  radar  pulse  shape,  tracking
loop  jitter,  and  the  range  spread  of  the  surface  roughness.
One  of  the  most  important  included  characteristics  is  the
pointing  angle  of  the  radar  antenna  relative  to  nadir.    In  a
previous  paper  [G.S.  Brown,  IEEE Trans. Antennas & Propag.,
AP-25,  67-74,  1977]  an  analytic  expression  for  the  flat
surface  impulse  response  involving  an  infinite  series  of
Bessel  functions  was  derived  to  describe  the  effects  of  a
nonzero  pointing  angle.  This  series  reduces  to  essentially
one  term  when  the  pointing  angle  is  less  than  one  antenna
beamwidth.  However,  when  the  pointing  angle  becomes  large.
such  as  the  case  with  a  multiple  beam  altimeter,  a  very
large  number  of  terms  in  the  full  Bessel  function  series
must  be  retained.  Although  this  can  be  done  via  downward
recurrence,  it  is  time  consuming  process.  In  this  paper,  the
integral  giving  rise  to  this  series  is  reexamined  and  the
large  angle  problem  is  identified  and  explained. By  expand-
ing  this  integral  about  a  point  of  maximum  contribution,  we
are  able  to  derive  a  much  more  compact  (closed  form)  result.
We  compare  this  result  with  conventional  radar  formulas
based  on  an  illuminated  area  established  by  the  antenna
beamwidth  and  the  slant  range  cell  size  due  to  the  radar
pulsewidth. We  emphasize  the  approximations  that  must  be
satisfied  in  order  for  this  approximation  to  give  essential-
ly  the  same  result  as  the  Bessel  series.

F/B1-2
1400

BACKSCATTER ENHANCEMENT FROM SPARSELY DISTRIBUTED
LARGE PARTICLES WITH ROUGH SURFACES
Ezekiel Bahar and Mary Ann Fitzwater
Electrical Engineering Department
University of Nebraska-Lincoln
Lincoln, NE   68588-0511

The incoherent diffuse specific intensities (modified
Stokes parameters) backscattered from a parallel layer con-
sisting of sparse random distributuions of finitely conducting
particles with smooth and rough surfaces are evaluated.   The
normally and obliquely incident excitations at infrared and
optical frequencies are vertically or horizontally polarized.
The particle surface roughness, which is characterized by its
joint probability density function, is assumed to be suffi-
ciently rough in order to significantly effect the diffuse
specific intensities.   Thus, the full wave approach is used
to determine the phase matrix as well as the extinction
coefficient that appears in the equation of radiative trans-
fer.   The enhanced backscattered intensities that depend
upon the particle surface roughness are compared with the
enhanced backscatter that is associated with Mie scattering
from smooth spherical particles.   The enhanced backscattered
diffuse specific intensities are evaluated for different
particles sizes, complex permittivities, roughness parameters
and excitations.   The effects of varying the optical thick-
ness of the layer are also considered.   Since the enhanced
backscatter phenomenon reported here is primarily due to the
particle surface roughness it appears in both the first
order and the multiple scatter solutions of the radiative
transfer equations.

F/B1-3    PROPAGATION OVER IRREGULAR INHOMOGENEOUS TERRAIN*
1420      R. M. Bevensee
          Lawrence Livermore National Laboratory
          Livermore, California  94550

Recently an article entitled "Propagation Over an Inhomogeneous Irregular Surface," (Z. Wu, T. S. M. Maclean, D. J. Bagwell, and M. J. Mehler) was submitted to Radio Science.  In it the authors show how to compute the surface field launched by a vertical current source with one Volterra integral equation derived from the Compensation Theorem.  Furthermore, they compute the total ground wave (space wave and surface wave) in a manner which allows for cliff-type surface discontinuities. The assumptions, including the usual neglect of backscatter, appear not to be serious.  Computations of field over homogeneous surfaces with cliff-type discontinuities show very good agreement with measurements over long distances from the discontinuities.

We will compare this work with the Compensation-Theorem formulation of the writer, which presently treats $TM_\rho$ surface wave propagation over irregular inhomogeneous terrain and requires the solution of three Volterra integral equations to obtain the surface field at a distant point.  In particular, we will consider the possibility of modifying this formulation to describe the total ground wave (space wave and surface wave) and also cliff-type discontinuities.

We will also describe the modified formulation for $TE_\rho$ surface wave propagation due to a horizontal current source.

F/B1-4
1440

## SOME NEW RESULTS IN RANDOM-MEDIUM BACKSCAT-
## TERING

David A.de Wolf
Bradley Dept.of Electrical Engineering
Virginia Polytechnic Inst. and State U.
Blacksburg, VA 24060

Inspired by the phase-screen approach of C.L.Rino
(J. of Wave-Mat. Int., 1, 181-204, 1986), we have
re-examined the problem of wave propagation and
scattering in a random medium with weak extended
fluctuations of refractive index. As in Rino's
work, we include backscatter effects by working
with the scalar wave equation rather than its para-
bolic approximation. We employ Bremmer's forward-
and backward-wave operator formalism to recast the
wave equation into two pseudo one-dimensional equa-
tions, and then solve for first and second moments
(average field and mutual coherence).

The results for the mutual coherence are of partic-
ular interest. Four first-order differential equa-
tions are obtained for the four squared flux quan-
tities that can be formed from the forwards and
backwards fields. These are solved for zero and for
nonzero transverse separation of observation
points, and in the former case they incorporate
energy conservation and reduce to the usual result
when backscatter is ignored. The connection with
backscatter enhancement is discussed. The interpre-
tation appears to differ from previous results.

F/B1-5      A SPATIAL FILTERING TECHNIQUE FOR REMOVING PHASE
1500       ERRORS IN AUTOMATED BISTATIC SCATTERING MEASUREMENTS
           Marc G. Cote
           Rome Air Development Center
           Applied Electromagnetics Division
           Target Characterization Branch
           Hanscom AFB, MA 01731

     A spatial filtering scheme for removing phase errors in
electromagnetic scattering  data is examined experimentally
and theoretically.  Measuring the coherent narrowband plane-
wave scattering pattern of an object (target) as a continuous
function of bistatic angle is problematic because the direct
coupling between the transmit and receive antennas may dominate
the total field.  This problem can be alleviated in many cases
by using a background subtraction technique.  The technique re-
quires measuring the amplitude and phase of the total elec-
tric field with and without the target.  Subtracting the back-
ground field, i.e. the field without the target, from the
total field with the target leaves the scattered field of the
target, provided multiple interactions between the target and
its surrounding are negligible.  Gross uncertainties in the
resultant data can arise from small errors in the phase of the
background data if the target scattered field is small rel-
ative to the background.  We will show that, for a -10 dB
target-to-background ratio, a 0.5 degree phase error produces
a 10% uncertainty in the amplitude of the electric field
scattered by the target.  This uncertainty shows up as high
frequency variations in the target scattering pattern.  To re-
move this uncertainty we filter the data applying the natural
$k(a + \lambda)$  spatial frequency band limit common to ordinary
radiating objects (L. J. Chu, J. Appl. Phys., vol. 19, pp.
1163-1175, Dec. 1948).  This bandlimited filtering scheme
allows us to make accurate automated bistatic scattering
measurements of targets with regions of low scattering.
Scattering measurements with and without filtering will be com-
pared to theoretically predicted scattering for a number of
targets.

F/B1-6    MEASURED SIGNAL DEGRADATION EFFECTS BY ROADSIDE
1540      TREES AT UHF AND L-BAND FOR MOBILE SATELLITE SYSTEMS

Julius Goldhirsh
The Johns Hopkins University/Applied Physics Labora-
tory, Johns Hopkins Road, Laurel, Maryland 20707
Wolfhard J. Vogel
The University of Texas at Austin,
10100 Burnet Road, Austin, Texas 78758

During June 1987, the Applied Physics Laboratory of the
Johns Hopkins University and the Electrical Engineering Re-
search Laboratory of the University of Texas at Austin per-
formed a fifth in a series of propagation measurements re-
lated to planned Mobile Satellite Systems (MSS). The previ-
ous four experiments involved transmitter platforms repre-
sented by remotely piloted aircraft (static measurements) and
helicopters (static and dynamic measurements), and the re-
ceiver and data acquisition systems were located on a van op-
erated by the University of Texas [W.J. Vogel and J. Goldhirsh,
IEEE Trans. Antennas and Prop., AP-34, 1460-1464, 1986;
J. Goldhirsh and W.J. Vogel, IEEE Trans. Antennas and Prop.,
AP-35, 598-596, 1987]. Fundamental aims of these previous
helicopter measurements were to assess the cumulative fade
distributions at UHF for a geometry in which the van was in
motion and roadside trees contributed shadowing effects.
They were made in Central Maryland only at UHF (870 MHz) and
during the October 1985 and March 1986 periods. The former
periods represented a time in which the deciduous trees con-
tained small moisture contents as the leaves were in the pro-
cess of falling (approximately 80% of full blossom) in
October and the trees were bare in March.

The June 1987 measurements, which are the subject of
this paper, were also implemented in Central Maryland and rep-
licated the geometries and road configurations of the previous
two helicopter-van tests. The major differences were: (1)
Both UHF (870 MHz) and L-Band (1.5 GHz) were simultaneously
transmitted, and (2) deciduous trees were in full blossom
having larger moisture contents than during previous tests.
Measurements at the L-band frequency were a result of the re-
cent FCC ruling that this band (in the vicinity of 1.5 GHz)
be used for the planned MSS system. In this paper, cumulative
fade distributions at L-band and UHF are described for typi-
cal roads and for various fixed elevation angles and distances
between the van and the helicopter. These distributions are
compared to previous roadside fade results made in the absence
of leaves and the effects of foliage are described. Enhanced
attenuations at L-band relative to the UHF measurements are
also characterized.

F/B1-7     UHF FADING IN FACTORIES
1600       Theodore S. Rappaport and Clare D. McGillem
           Engineering Research Center for Intelligent Manufacturing Systems
           School of Electrical Engineering
           Purdue University
           West Lafayette, IN 47907

There has been much interest recently in characterizing UHF propagation in and around houses and office buildings (S.E. Alexander, Elec. Letters, 19;20,860,1983; D.C. Cox, R.R. Murray, A.W. Norris, BSTJ,62;9,2695-2717,1983 and BSTJ,63;6, 921-954,1984; D.M.J. Devasirvatham, IEEE Trans. A.&P., AP–34;11,1300-1308,1986; R.J.C. Bultitude, IEEE Comm. Mag.,25,6,5-12,1987). Rappaport and McGillem have recently reported propagation measurements at 1300 MHz in factories (T.S. Rappaport, C.D. McGillem,Elec. Letters,23;19,1015-1017,1987).

In this paper, we detail the measurement apparatus and the experiments performed to characterize narrow band fading within five large and fully opeational factories. It is believed that such propagation measurements have not been available previously in the literature. The propagation experiments are designed to determine path loss, shadowing, small scale spatial fading, and temporal fading of the factory radio channel. It is found that most line of sight (LOS) paths exhibit gain over free space path loss whereas obstructed (OBS) paths have power fall off as distance to the 2.8 power. Local area fading is found to be primarily Rayleigh, although Rician and Log-normal distirbutions fit some of the data well. Temporal fading appears to be Rician with K=10 dB.
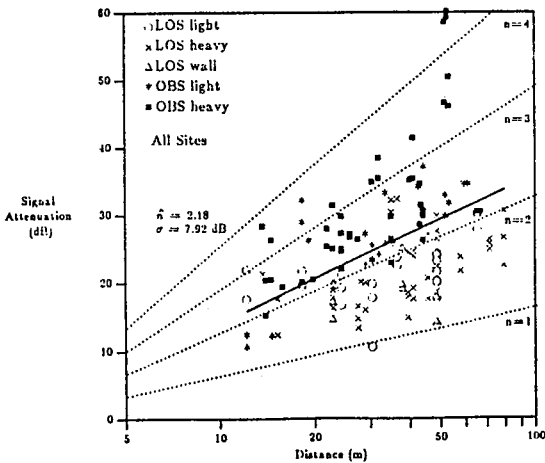


Large scale path loss at all sites.

SECOND MOMENT ESTIMATES FROM A
METEOROLOGICAL RADAR

Janet S. Gibson
Michael J. Carpenter
National Oceanic and Atmospheric Adminstration/ERL
Wave Propagation Laboratory
Boulder, CO 80303
and
National Center for Atmospheric Research
Boulder, CO 80307

## ABSTRACT

Spectral moment estimation is of importance to radar meteorologists for several reasons. Zero moment estimates measure average power received by the radar. This can be related to total liquid water content within the pulse volume by an assumed drop size distribution. First moments are estimates of Doppler mean velocity and thus can give the meteorologist information on particle speed, and direction from which wind is inferred. Second moment estimates lead to information on turbulent dissipation rates and wind shear.

This paper describes and compares the results of two signal processing techniques used to compute spectral moments in a meteorological pulsed Doppler radar system operated by the Wave Propagation Laboratory, Environment Research Laboratories, NOAA, in Boulder, Colorado.

Signal transmission, data acquisition, real time processing of the returned echo from the analog-to-digital converter through a pulse pair processor, and the current post spectral analysis techniques used are reviewed briefly. Post spectral analysis techniques included are a pulse pair algorithm and a discrete fast Fourier transform method. These two methods are used to estimate mean Doppler velocity, average power received, power spectral density, and spectral width. The results of processing simulated by the two methods are compared for various ranges of spectral widths and various signal to noise ratios. The resulting biases are explored.

F/B1-9      CALCULATION BY NUMERICAL INTEGRATION OF
1640        DIFFRACTION ATTENUATION AT VHF AND UHF

J. H. Whitteker
Communications Research Centre
3071 Carling Avenue
P.O. Box 11490, Station H
Ottawa, Canada
K2H 8S2

The Communications Research Centre has a computer program (J.H. Whitteker, IEEE Int. Conf. Communications, 44-48, 1983) that predicts propagation attenuation at VHF and UHF over terrestrial paths, using a topographic data base. For the calculation of diffraction attenuation, the terrain is modelled as a small number of circular hills to which known solutions are applied. While the results are usually good, they are sometimes inaccurate because the terrain has been over-simplified, and because the theory available for more than one obstruction has limited validity.

A new method of calculation has been worked out which applies approximate diffraction theory (Fresnel approximation) to a terrain model that retains most of the complexity of the real terrain. (A preliminary version was reported on at this conference two years ago.) The terrain is modelled along the propagation path simply by connecting the given terrain points with straight lines. The earth may be imperfectly reflecting, and may also be assigned a roughness. The classical solutions of the diffraction problem are not used. Instead, a new solution is found for each path profile starting from elementary principles, making the calculation a kind of numerical simulation. The method is to find the radiowave field as a function of height above each terrain point by integrating over the field above the preceding terrain point, using Huygens' principle for both direct and reflected waves.

The method of calculation has been tested against rigorous diffraction theory (residue series) in the special case of a smooth spherical earth, on paths up to 100 km, with agreement to 2 dB. It has also been tested for up to 40 collinear equally spaced knife edges (no reflection) and the results agree with a result by Lee (J. Math. Physics, 19, 1414-1422, 1978) and Vogler (Radio Sci. 17,1541-1546, 1982) to well within 2 dB. Verification of reciprocity has been also made for simple asymmetrical paths, with agreement to a few decibels. Finally, comparisons have been made with measurements on real paths, with mixed results. The accuracy seems to be limited by uncertainties in the terrain.

Since the field must be found at many points, the algorithm requires much more computer time that the one mentioned in the first paragraph. However, efforts to eliminate unnecessary steps in the calculation are expected to result in a program with acceptable speed.

G2-1        MODELING OF HIGHLY IRREGULAR PROPAGATION PATHS
1400        AT VLF AND LF
            F. Perry Snyder
            Ocean and Atmospheric Sciences Division (Code 544)
            Naval Ocean Systems Center
            San Diego, CA   92152-5000

Global longwave propagation is often modeled using a
waveguide model formulation wherein a naturally or artifi-
cially produced irregular earth-ionosphere waveguide is
accommodated by modeling the propagation path as discrete
homogeneous segments of some appropriate definition.  The mode
summation is found by matching the mode fields across the dis-
continuities between the various consecutive slabs - a
procedure commonly called mode conversion.  Reported computa-
tional procedures usually employ one of two possible mode
conversion formulations.  Although both formulations use full
wave modal solutions, one matches electromagnetic field com-
ponents (numerically obtained) throughout the entire height
range of the guide, resulting in an orthogonal set of modal
height gain functions.  The other matches electromagnetic
field components (analytically defined) only throughout the
height region below ionospheric elevations, resulting in an
"almost orthogonal" set of modal height gain functions.  The
use of numerically obtained field components provides an exact
formulation but is very computer run-time intensive.  The
analytic forms, although resulting in an approximate formula-
tion, are very fast on the computer.

Apparently quite accurate under most conditions, the
bounds of the validity of the approximate mode conversion for-
mulation has never been clearly shown.  Also, the approximate
formulation has been recently found to exhibit numerical in-
stabilities, resulting in sharp discontinuities in the
computer field strength.  These instabilities appear most fre-
quently associated with the higher frequencies into the LF
band and with naturally or artificially stressed ionospheres.

The validity bounds as well as the occurrence of in-
stabilities in the approximate formulation has been
investigated and the results are reported.  A controlling fac-
tor is found to be the departure of the analytic forms for the
height gains from the numerically obtained full-wave forms
near ionospheric evaluations.  Some potential procedures to
circumvent the failure of the approximate procedure while
maintaining good computer efficiencies is discussed.  Longwave
propagation modeling based on a mixed application of the two
mode conversion forms is also described.

G2-2    ALFAN2: A SECOND EXPERIMENT TO MEASURE
1420    TE & TM RADIO NOISE IN THE EARTH-
IONOSPHERE WAVEGUIDE

A.C. Fraser-Smith[1], J.P. Turtle[2], P.R. McGill[1], and
R.A. Helliwell[1]

[1]Space, Telecommunications and Radioscience Laboratory
Stanford University
Stanford, CA 94305
[2]Radio Propagation Branch
Rome Air Development Center
Hanscom Air Force Base, MA 01731

Last year at this meeting we reported some of the results of a first experiment to measure TE and TM noise in the earth-ionosphere waveguide. Called ALFAN (for Airborne Low Frequency Atmospheric Noise), the experiment involved the flight of a specially-designed instrumentation package on a free-floating balloon. The flight took place on August 4, 1986, in New Mexico: the balloon was launched soon after dawn from a location near Roswell, it flew at an altitude of 18–21 km for roughly five hours, and the flight was terminated near White Sands.

The ALFAN measurement system consists of three identical low frequency receivers and an octahedron-shaped loop antenna arrangement consisting of two orthogonal vertical loops and one horizontal loop suspended below the instrumentation package. In level flight the two vertical loops respond to time variations of the horizontal magnetic field and the horizontal loop responds to variations of the vertical magnetic field. Thus, for low frequencies, measurements can be made simultaneously on electromagnetic waves propagating in the Transverse Magnetic (TM) and Transverse Electric (TE) modes.

The TE-to-TM noise ratios at 42.5 kHz that were obtained during the ALFAN flight were appreciably larger (by approximately 10 dB) than those reported during earlier theoretical and experimental studies. To confirm these ratios and to obtain new information about the ratios during the night, a second ALFAN experiment, designated ALFAN2, was conducted on May 16, 1987, once again in New Mexico. The instrumentation package and antennas for the second experiment were essentially the same as for the first, with some improvements; the balloon was launched at Holloman AFB near White Sands at 0336 LT and the flight was terminated around 0859 LT near Deming. Once again the instrumentation package was recovered without damage.

During the daylight portion of the ALFAN2 flight, the measured TE-to-TM noise ratios at 42.5 kHz were comparable to those obtained during the ALFAN flight, thus confirming the earlier result. During the nightime portion of the flight the measured ratios were even higher, with the measured TE noise levels being roughly the same or even greater than the TM noise levels. There was an interesting large decrease (by roughly 20 dB) in the strength of the TE signal from an LF station (55.5 kHz) in the San Francisco area during the transition from night to day.

G2-3      AN HISTORICAL REVIEW OF MINIMUF - A MUF PREDICTION
1440      ALGORITHM
          D.B. Sailors
          Ocean and Atmospheric Sciences Division
          Naval Ocean Systems Center
          San Diego, CA  92152-5000

The development of MINIMUF is reviewed beginning with
MINIMUF-1.0 concluding with the current version under develop-
ment MINIMUF-7.0.  MINIMUF was developed for predicting the
MUF on small mobile propagation forecast terminals.  The
parameter foF2 is modeled as a response of a dynamic system
"driven" by a function of cos $\chi$ (the cosine of the instan-
taneous solar zenith angle) and based on the analogy to a
signal-lag linear system (e.g., an RC circuit).

The versions differ mainly in how the solutions to the
differential equation for cos $\chi$ were implemented.  The foF2 in
Version 1.0 was given by a linear relationship between
cos $\chi_{eff}$ and sunspot number; its M-factor had only a range
dependence.  Version 2.0 introduced a sunspot number depend-
ency in the foF2 and a latitude dependence at the equator in
the M-factor.  In version 3.0 the form of the fit of cos $\chi$ to
foF2 was non-linear and correction factors were added to the
M-factor for high-latitude paths.  In MINIMUF-3.5, the M-
factor was changed to make it applicable beyond 8000 km.  In
these versions a fit was made to 36 path-months of data
measured on three paths.

Subsequent modifications to MINIMUF were made to repre-
sent phenomena not previously considered.  In MINIMUF-4.0
there was an attempt to include the E-layer in the determina-
tion of the MUF.  MINIMUF-5.0 was developed for ray-tracing
applications where $h_m F2$ and foF2 are needed.  MINIMUF-85
(Version 6.0) included sunspot dependence in both the foF2 and
M-factor calculations, seasonal and time dependence in the M-
factor, and a special polar model for high-latitude paths.

A more accurate MINIMUF algorithm for use in a sounder
updating is being developed.  Both improved foF2 and M-factor
models are being developed.  The basis for the foF2 model is a
data base of foF2 data measured at 175 sites.  For the mid-
latitudes supplementary data produced using model data from
Rush et al. (Radio Science, 19, 1083-1097, 1984; Radio
Science, 18, 95-107, 1983) is being used in ocean areas to
fill gaps.  For low-latitudes a semi-empirical model due to
Anderson et al. (Radio Science, 22, 292-306, 1987) is being
used to fill in gaps.   The MINIMUF parameters for the diur-
nal variation of foF2 will be determined as a function of
sunspot number, season and geographic location.  The M-factor
model is based on a calculation proposed by Sailors et. al.
(Naval Ocean Systems Center TR 1121, July 1986) which uses the
distance factor M(D)F2 developed by Lockwood (IEE Proc., 130,
pt. F, no. 4, June 1983).

G2-4    THE VERTICAL IONOGRAMS AND DISPERSIVE BANDWIDTH
1500    FOR AN OBLIQUE PATH

K. C. Yeh, Department of Electrical and Computer
Engineering, University of Illinois, Urbana, IL
61801
Haim Soicher, Center for $C^3$ Systems, US Army
Communications-Electronics Command, Fort Monmouth,
NJ 07703

The propagation geometry and dispersiveness of the
ionospheric medium will both give rise to dispersion of an
electromagnetic pulse. In this connection, a useful measure
of the propagation channel is the dispersive bandwidth.
There are many ways to define dispersive bandwidth, but they
all lead to very similar results. For several model
ionospheres, the dispersive bandwidth has been computed.
These curves will be shown. A simple analytical relation
has been obtained that enables us to compute the dispersive
bandwidth for a given oblique path, frequency and vertical
ionogram. This relation is used to compute the dispersive
bandwidths for a typical day by using real ionograms.

G2-5
1540

## IONOSPHERIC LIMITATIONS TO THE ACCURACY
## OF SSL RANGE ESTIMATION

Leo F McNamara
Andrew Antennas
Technology Park 5095
AUSTRALIA

The single station location (SSL) technique for the determination of the position of an HF transmitter overcomes several of the difficulties inherent in the use of a traditional bearing-only DF network, such as the transmitter being audible at only one station of the network. The SSL technique combines observations of the elevation angle and bearing of signals from the transmitter with procedures for raytracing through a model of the ionosphere, to produce an estimate of the position of the transmitter.

The SSL technique also has its limitations, mostly imposed by the ionosphere and by our inability to model it successfully on all occasions. This paper will describe some of these limitations, and discuss procedures for their elimination, or at least for their minimization.

The diagram illustrates one of the more interesting cases encountered during a trial of the Andrew SSL system SKYLOC. The transmitter was at North West Cape, 2783km from the SSL site, and on a bearing of 294.6 degrees. However ray-retracing placed the transmitter in the middle of the extremely inhospitable Great Victoria Desert. This case will be discussed in some detail.



ACCUMULATED ELEVATION ANGLE HISTOGRAM



ACCUMULATED AZIMUTH ANGLE HISTOGRAM
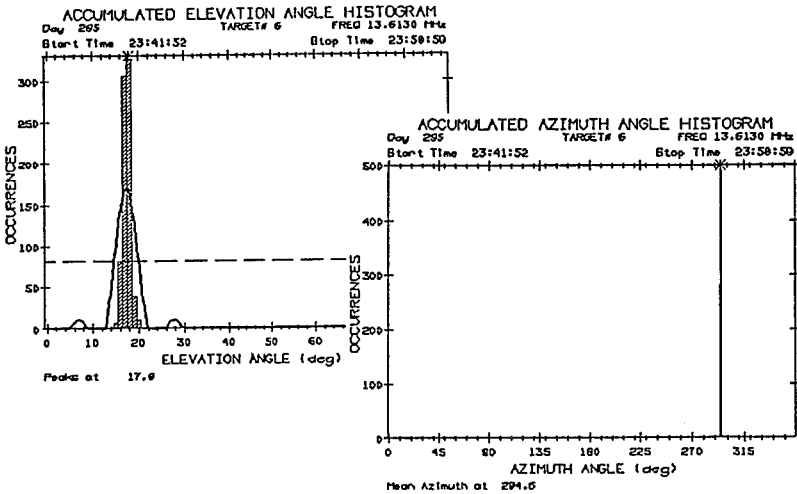
G2-6   PERFORMANCE OF METEOR BURST COMMUNICATION SYSTEMS
1600      IN THE PRESENCE OF ENHANCED D-LAYER IONIZATION

Thaddeus Kaliszewski

The MITRE Corporation
Burlington Road
Bedford, Massachusetts 01730

Meteor Burst Communication (MBC) is supported by radio
waves scattered by ionized trails that are formed by small
particles upon their entry into the earth's atmosphere.  The
ionization of the meteor trails varies depending on the
energy of the entering particles and on their angle of entry.
Typically, the ionization is high enough to support communi-
cations at very high frequencies (VHF).

A normal, undisturbed D-layer is rather innocuous at VHF,
even though the layer is interposed between most of the
trails and the ground terminals.  The D-layer screening be-
comes a concern when its ionization is enhanced by the influx
of ionizing particles or radiation.  The origins of such en-
hancement can be either natural or man-made.

The D-layer screening has the effect of reducing the
radio visibility of the meteor trails.  More importantly, it
reduces also the performance of the meteor burst communica-
tion systems.  The two indices of performance, the throughput
and the packet delay, are greatly affected by the increase in
absorption of the layer.  In certain extreme cases, the
absorption can be high enough to cause a total blackout.

In the present paper, the effect of D-layer screening is
modeled in the context of a reference meteor burst communica-
tions circuit.  Performance indices are computed as a func-
tion of both frequency and absorption.  A critical absorp-
tion, at which a total blackout occurs, is also identified
for the particular circuit under consideration.

G2-7    DETERMINATION OF UPPER ATMOSPHERIC TIDES
1620    FROM RANDOMLY SPACED METEOR ECHOES

C. A. Whitmore
S. K. Avery
Department of Electrical and Computer Engineering
University of Colorado, Boulder
Campus Box 425
Boulder, CO 80309

## ABSTRACT

Radar echoes from ionized meteor trails have proven useful in estimating tidal components in upper atmosphere winds. Previous signal processing methods have used the pulse pair processor to determine the mean velocity of the neutral wind from the echo doppler shifts. From these velocity points (which are randomly spaced in time) and an a priori estimate of the tidal components, amplitudes and phases of the tides are then estimated. A new technique, however, does not assume a priori knowledge of the frequency components, but instead interpolates the randomly spaced data into a uniformly spaced representation, and then performs standard spectrum analysis to determine more accurate tides.

A minimum-energy, reduced rank interpolator has been derived. This interpolator has been tested through simulations, with the results comparing favorably with well-known estimators acting on evenly-spaced data. A new study on this topic involves deriving an analytic relationship between the resulting mean squared error of the interpolator and several factors: the average sampling density of the random sampler, the noise variance in each sample, and the bandwidth of the desired signal. In my talk I will discuss this interpolator and its performance characteristics.

J2-3       MARS: RECENT RADAR RESULTS
1400       T. W. Thompson and L. Roth
           Jet Propulsion Laboratory
           California Institute of Technology
           Pasadena, CA  91109

We report on three topics; radar altimetry of the Martian cratered highlands from 1971-1973 observations, Mars reflectivities from the 1986 observation, and possibilities for Mars observation for the next few oppositions.  The radar altimetry of crater highlands is a new reduction of old data, while the Mars reflectivities and dielectric constants are preliminary results from the new 1986 data.  Finally, the consequences of Mars and earth orbital configuration on earth-based radar observations of Mars through the next two decades will be discussed.

Topography in the $-14^{\circ}$ to $-22^{\circ}$ latitude strip of the martian cratered highlands was measured by the Goldstone Solar System Radar during the 1971/1973 perihelic oppositions.  Overall, the landscape is flat.  Most of the local relief is provided by the structural elements of large impact craters.  Low or non-existent exterior relief, rather than overall shallowness, is the distinguishing characteristic of large martian craters.

Radar echoes from the planet Mars were obtained on 26 S-band (wavelength = 12.5 cm) and 2 X-band (wavelength = 3.5 cm) tracks using the Goldstone Radar in 1986.  These observations took advantage of the favorable 1986 opposition since the earth-Mars distance in July was 0.40 AU, the smallest earth-Mars distance since the 1971 and 1973 oppositions.  The observations were conducted via the cw-spectra techniques like those of Harmon et al. (1982 and 1985).  A continuous tone was transmitted at Mars and the radar echo was sampled to obtain a Doppler-spread spectrum.  Each received cycle was separated into polarized (opposite sense circular, OC) and depolarized (same sense circular, SC) periods.  Also, a minute or two of noise was recorded in each transmit-receive cycle.

Coverage on Mars started at $-8^{\circ}$ in June, travelled north toward the equator to $-3^{\circ}$ during August, and then migrated south to $-14^{\circ}$ for the last run in October.  These are new areas for earth-based radars.  Longitudes $180^{\circ}$ to $90^{\circ}$ have low polarized (OC) reflectivities, high depolarized (SC) reflectivities and inferred bulk dielectric constants of 3.0-4.0.  These values in general agree with those observed by Harmon et al. (1985) for areas north of the equator.  In contrast, longitudes $75^{\circ}$ to $0^{\circ}$, the Valles Marineris, have high polarized (OC) reflectivities, low depolarized reflectivities and inferred bulk dielectric constants near 5.0.  Longitudes $360^{\circ}$ to $180^{\circ}$ have intermediate values with inferred bulk dielectric constants of 3.5-4.5.

RECENT OBSERVATIONS AND IDENTIFICATION OF FEATURES ON THE MOON
AND VENUS: D.B. Cambell, Arecibo Observatory, Arecibo, PR 00612

J2-5        VENUS:  REGIONS OF HIGH SURFACE PERMITTIVITY
1440        G. H. Pettengill,  Center for Space Research, Rm 37-241
            Massachusetts Institute of Technology
            Cambridge, MA  02139

Regions on the surface of Venus, generally located at high altitude, have been determined to possess high values of dielectric permittivity. Values as high as 39 (in the Maxwell Montes area) have been inferred from both radar scattering and radio emission observations at wavelengths between 5 and 20 cm.  In the absence of liquid water, the most likely explanation for this behavior. appears to be a "loading" of surface rock with small, electrically conducting inclusions.

Laboratory measurements of artificially produced material (J. M. Kelly *et al*, J. Appl. Phys., **24**, 258-262, 1953), as well as of natural pyrite-containing minerals (S. D. Nozette, Ph.D. Thesis, M.I.T. Dept. of Earth, Atmosphere and Planetary Sci., Nov. 1982) show that a volume fraction of about 13% conducting inclusions embedded in a host rock having an intrinsic permittivity of 5 will yield an effective bulk dielectric permittivity of 39.

J2-6
1520
# A VENUS TOPOGRAPHY MODEL
P.G. Ford
Center for Space Research, 37-491
MIT, Cambridge, MA 02139
and
E. Eliason
U.S. Geological Survey
2255 Gemini Drive,
Flagstaff, AZ 86001

Sources of systematic error contributing to the Pioneer Venus topography model (Pettengill *et al.* J. Geophys. Res. 85, 8261–8270, 1980) have been studied. The chief factors are spacecraft timing uncertainties and inaccuracies in orbit determination. These errors have been estimated, and the planetary radius values corrected, by two methods: a) adjusting the Keplerian elements of the orbit, and b) imposing a "smoothness" constraint on local variations in planetary radius.

The resulting topographic model and error estimates agree well with available earth-based measurements, and will provide the basis for the automatic mapping system under development for the Magellan project.

J2-7     RADAR STUDIES OF ASTEROIDS
1540     S. J. Ostro
         183-501, Jet Propulsion Laboratory
         California Institute of Technology
         Pasadena, CA  91109

Echoes from 30 mainbelt asteroids (MBA's) and 17 near-Earth asteroids (NEA's) have provided a wealth of unique information about these objects' sizes, shapes, spin vectors, and such surface characteristics as decimeter-scale morphology, topographic relief, regolith porosity, and metal concentration.  On average, small NEA's are much rougher at decimeter scales than MBA's, comets, or the terrestrial planets.  Some of the largest MBA's (e.g., 1 Ceres and 2 Pallas) are smoother than the Moon at decimeter scales but much rougher than the Moon at some much larger scale.  There is at least a five-fold variation in the radar albedoes of MBA's, implying substantial variations in these objects' surface porosities or metal concentrations.  The highest MBA albedo estimate, for 16 Psyche, is consistent with a metal concentration near unity and lunar porosities.

The diversity of NEA radar signatures is extreme.  The radar albedo of 1986 DA is twice that of Psyche and strongly suggests that this Earth-approacher is a ~2-km metallic fragment with hardly any regolith; it might be the source of some of our iron meteorites.  The radar polarization signature of 2101 Adonis is most unusual, resembling that of Jupiter's icy satellite Callisto more than that of any other radar-detected planetary target.  NEA polar silhouettes range from slightly non-circular to highly elongated and distinctly non-elliptical.  Delay-Doppler resolution of 1627 Ivar has yielded the first two-dimensional images of an asteroid; they show this ~7-km object to be elongated, irregular, non-convex, and bifurcated.  The radar signatures of NEA's often seem extraordinarily complex compared to those of large MBA's, and suggest an abundance of exotically shaped objects in the near-Earth population.

Echoes from 1986 JK, detected at 11 lunar distances from Earth three weeks after its discovery, yield Doppler-frequency measurements that will help to ensure optical recovery of this asteroid.  "Radar astrometry" of NEA's is important even for asteroids with an extensive optical-astrometric history, because a handful of radar measurements can shrink the positional error ellipsoid of the prediction ephemeris by a factor $\geq 2$ for decades.

# EARTH - RADAR STOKES PARAMETER MEASUREMENTS AND INTERPRETATIONS.

Jakob J van Zyl and Howard A. Zebker
Jet Propulsion Laboratory
California Institute of Technology
4800 Oak Grove Drive
Pasadena, CA 91109

We have converted a conventional synthetic aperture radar system into an imaging radar polarimeter by by employing two orthogonally polarized antennas and recording both the amplitude and phase measurements of the received electric fields. This enables us to measure the complete complex scattering matrix for each individual resolution element in the radar image. This sytem was used to measure the scattering matrices of a number of lava flows in the Snake River Plain, Idaho.

Knowledge of the scattering and Stokes matrices allows one to decompose the scattered waves into polarized and unpolarized parts. Images of the polarized and unpolarized energy shows that the return from the rougher lava flows contain more unpolarized energy than the returns from the smoother areas. We interpret this behavior as indicative of the increased role of multiple scattering as the surface gets rougher.

The polarization signatures measured with the JPL imaging polarimeter allow us to determine the dominant scattering mechanism for each flow. We find that the signatures are similar to those predicted by models of scattering by slightly rough dielectric surfaces. Specifically, the smoothest lava flows are modeled quite well by even the first order rough surface model, while at least a second order model is required to interpret the signatures of the rougher flows. At present we do not have complete, quantitative measurements of the actual surface roughness, however, we do have photographs and crude surface-height template measurements that indeed indicate a qualitative agreement between the radar observations and the ground-truth measurements of r.m.s. height.

J2-9    LUNAR RADAR IMAGES AT 15-M RESOLUTION
1620    S.H. Zisk
        MIT Haystack Observatory
        Westford, MA  01886

     New 5-m-resolution radar measurements of the lunar surface
have yielded range-doppler images with a projected surface
resolution (pixel size) of 30 to 60 meters. About 6 areas were
mapped between June and October, 1987.   Each map covers a
rectangular area of about 30 by 400 km. These data are being used
to further our understanding of the present geologic properties
and past history of the lunar surface, specfically regarding
volcanism and impact as major formative processes.  They will be
used as well to investigate the details of radar backscattering
from planetary surfaces, which is of particular interest for the
interpretation of the imminent Magellan mission to Venus.

J2-10    MULTI-STATION RADAR IMAGES OF VENUS AT MODERATE
1640     AND HIGH RESOLUTION

R. F. Jurgens and M. A. Slade
Communications Systems Research Section
Jet Propulsion Laboratory
Pasadena, CA 91109

During the past three years, the Goldstone radar system has undergone a significant upgrade such that radar ranging data can have a time resolution as fine as 0.3us. The first radar observations of Venus with this system show that interferometric fringes can be obtained without serious degradation, and that images can be formed with resolutions near 1 km. The new images cover the region from 280 to 5 degrees longitude and are near the equator. Resolutions vary from 1 to 4 km depending upon the distance to the planet.

We have also processed several of the observations from the 1980 and 1982 series and have reprocessed some of the 1978 series. Some earlier observations that were defective due to one of the interferometer stations being bad have been processed with a new generalized multistation algorithm that allows selecting the number of operation stations. The first images have been selected to provide multiple coverage with our earlier images. Distinct features found in these series of images have been used to calculate a new and much more accurate pole position and spin rate for Venus.

Several of the images made from the older data have shown some remarkable features that possess either very high or very low effective cross sections. These features have little topography associated with them, so that the scattering anomalies cannot be associated with the usual quasispecular scattering from slopes in the kilometer scale size. Preferentially aligned slopes in the 10 to 100 meter size cannot be ruled out; however, we believe these anomalies may be due to changes in the Fresnel reflection coefficient. Enhancements as much as 500% have been observed on one feature and would indicate Fresnel reflection coefficients in the order of 80 to 90%. Metallic material could also cause such reflections. Pioneer Venus data show no large anomalies in this region except for a slight increase in the Fresnel reflection coefficient, thus ruling out large variations in effective rms roughness. A temperature anomaly should be expected, however, the resolution of the PV radiometer may be inadequate to show the anomaly. Further studies of these regions will be required, especially the low reflection areas which have not received much attention.

Plenary Session    0830-Weds.    Duane G0-30

Session A-3   1355-Weds.   CR1-42
ANTENNA AND EM FIELDS MEASUREMENT
Chairman: Motohisa Kanda, Electromagnetic Fields Division, National
Bureau of Standards, Boulder, CO 80303

A3-1     **AN OPTICALLY LINKED ELECTRIC AND MAGNETIC**
1400      **FIELD SENSOR FOR POYNTING VECTOR MEASUREMENTS**
         **IN THE NEAR FIELDS OF RADIATIING SOURCES**
         L. D. Driver and M. Kanda
         Electromagnetic Fields Division - 723.03
         National Bureau of Standards
         325 Broadway, CO   80303

A unique, single-element antenna sensing scheme is described
which can simultaneously measure the electic, magnetic, and
time-dependent Poynting vectors of electromagnetic (EM)
fields. The electric and magnetic responses are separated by
a 0/180 degree hybrid junction; these rf voltages along with
relative phase and frequency information are transmitted to a
remotely located vector analyzer by a pair of well-matched
fiber optic downlinks; and the remote receiver displays (1)
the electric dipole response, (2) the magnetic loop response,
and (3) the time phase difference between the two, which can
be used to determine the time-dependent Poynting vector.
Both a theoretical analysis and a discussion of experimental
measurements performed are presented which describe the
capabilities and performance of a working prototype of the
antenna measurement scheme. The results indicate that a
properly characterized isotropic version of this system can
function properly in the near-fields of EM sources to
thoroughly characterize such fields and to describe the
resulting energy flow.

A3-2      NUMERICAL CALCULATION AND EXPERIMENTAL
1420      VERIFICATION OF NEAR FIELDS FROM HORNS
          Don W. Metzger
          Kaman Sciences Corporation
          P.O. Box 7463
          Colorado Springs, CO 80933
          Ronald M. Sega, John D. Norgard
          University of Colorado
          Department of Electrical Engineering
          Colorado Springs, CO   80933-7150

The testing of system response and vulnerabilty to
high power microwaves necessarily involves the creation
of the highest possible power microwaves.  In order to
simulate actual threats, testing should be performed in
the far-field region where the propagating waves are
plane waves.  However, to maximize the power density at
the test aperture, the system is often located in the
near-field.  Additionally, it is often impossible to
locate the test object in the far-field due to size
constraints of the anechoic chamber.  Thus, an accurate
prediction of the near-field region is necessary.

An extension of Silver's solution for the fields
produced by a distribution of currents provides the
basis for this method of calculating near fields.  The
horn is treated as a distribution of source currents
which can be determined from a generalized distribution
of E and H fields.  The currents lie on a planar surface
from which the wave is launched with a phase correction
to account for the horn flare.

Experimental   verification   of   the   near-field
calculations   was   accomplished   through   the   infrared
imaging method currently in use at the University of
Colorado at Colorado Springs.   In this method, when a
lossy dielectric sheet is illuminated by the microwave
source, it heats.  The sheet can then be viewed using an
infrared   camera   and   the   electric   field   pattern   is
determined.  The agreement between theory an experiment
is very good and will be presented.

A3-3    **NBS EFFORTS ON ELECTRIC FIELD PROBES FOR**
1440              **MILLIMETER WAVES**

J. Randa, M. Kanda, and D. Melquist
Electromagnetic Fields Division - 723.03
National Bureau of Standards
325 Broadway
Boulder, CO 80303

The National Bureau of Standards is pursuing research aimed at developing electric-field probes to operate in the frequency range 18 - 110 GHz. Work thus far has concentrated on two particular efforts: extension of the resistively tapered dipole design to higher frequencies and a new design based on a fiber-optically sensed temperature probe.

The resistively tapered dipole with Schottky diode detector is the basis of a previously developed probe which operates up to 18 GHz using dipoles of length 8 mm. This same design with shorter dipoles is being developed for a probe to cover the lower end of the frequency range of interest (up to about 40 GHz). Preliminary measurements of both frequency response and antenna pattern are encouraging up to at least 30 GHz.

The second design is intended to cover frequencies up to 110 GHz (and down to about 20 GHz). It consists of a thin resistive film deposited on the tip of a fiber-optically sensed thermometer. The optimal thickness and conductivity of the resistive film have been calculated, and measurements have been made on thin nichrome strips deposited on glass to test the feasibility of this probe configuration. The test results indicate that the heating of the strip can be detected, but that very high fields are required. This is due in part to the large ambient thermal fluctuations (of order $1^{o}$C) in the test environment. The effect of thermal isolation is estimated, as are the effect on the field due to the substrate and the effect of different input impedances for different resistive strip geometries.

A3-4
1520

THREE-DIMENSIONAL THEORETICAL
AND EXPERIMENTAL ANALYSIS
OF INTERNAL CYLINDRICAL FIELDS
COUPLED THROUGH A SLOT APERTURE

Paul E. Bussey, John D. Norgard,
and Ronald M. Sega
University of Colorado at Colorado Springs
Department of Electrical Engineering
Colorado Springs, CO 80933-7150

A modal expansion technique is used to predict the fields inside of a closed circular cylinder due to coupling through an axial slot aperture. The main interest is to determine which modes are excited in the cylindrical cavity, and the relative strengths of these modes. These results are then compared to experimental measurements made using an infrared technique developed at UCCS. The measurements are made so that the electric field vector can be determined, and the mode strengths calculated. The field distributions are obtained from heating of lossy dielectric sheets in a particular cylinder cross-section of interest. The lossy material is also cut so as to measure the amplitude of the given spatial electric field components. A comparison of theory and experiment is presented.

A3-5     DEVELOPMENT OF PHOTONIC PROBES FOR THE MEASUREMENT
1540     OF ELECTROMAGNETIC FIELDS

K. D. Masterson and L. D. Driver
Electromagnetic Fields Division,    MS/723.03
National Bureau of Standards
325 Broadway
Boulder, CO    80303

Fiber  optic,  all dielectric light guides provide wide
bandwidth,  EMI  immune,  and  unperturbing links over which
information  characterizing  electromagnetic  fields  can be
transmitted.   This  philosophy has been extended to include
the design of the field-sensing probe itself.

We  have  developed passive, all dielectric probes that
utilize   electric-field-induced  birefringence  in  certain
crystals  (esp.  $LiNO_3$) to measure field strengths down to 5
V/m at frequencies to 1.5 GHz(K.D. Masterson, High Bandwidth
Analog  Applications  of  Photonics, SPIE Vol. 720, 100-104,
1986).   The  physical and electrical characteristics of the
probe  are  described in detail, with particular emphasis on
results  obtained for increased bandwidths obtained with the
most recent version of the probe.

# MUTUAL COUPLING BETWEEN MICROSTRIP ANTENNAS

## S.R. Bhadra Chaudhuri, A.K. Bhattacharjee,
### D.R. Poddar & S.K. Chowdhury
Department of Electronics & Tele-communication Engineering
Jadavpur University,Calcutta 700 032, West Bengal, INDIA.

In the design of Microstrip Antenna Array the mutual coupling between microstrip elements have a marked effect on array performance. Rectangular microstrip antenna arrays have been used for various application e.g. in space vehicles, aircrafts etc. Generally, when a properly matched individual element is placed in an array, its terminal properties change due to mutual coupling effect. The properties such as side lobe level may increase, nulls may be shifted and grating lobes may appear. The antenna when scanned may show a degraded pattern which is also a function of scan angle.

Penard et.al. ( E. Penard, J.P. Daniel, Electronics letters, 8th July, 1982, Vol - 18; No : 14; pp. 605-607 ) used the cavity method and the equivalence theorem to determine the mutual coupling between H-plane coupled rectangular microstrip antennas. Jedlicka et.al. ( R.P. Jedlicka, M.T. Poe, K.R. Carver; IEEE Trans. on A.P. Vol. A P : 29, no : 1, January, 1982,pp. 147-149 ) reported measured data on the mutual coupling between microstrip antennas. The theory presented by Penard et.al. above involves the computation of a number of numerical double integrations and computation time is quite large.

A thorough investigation has been made by the present authors on the mutual coupling between rectangular half wave length microstrip antennas fed by a co-axial line at the centre of one of the radiating edges for a frequency ranging from 1 GHz to 8 GHz on various thickness of the substrate ranging from .1 to .305 cm. with the spacing between adjacent edges from $.005\lambda$ to $\lambda$ and di-electric constant chosen 2.5 to 2.55. The values of $\lambda_g$ for the antennas (the mutual coupling properties of which were investigated) were calculated from schneider's formula ( M.V.Schneider, G.Bernard and W.F.Bodtman, The Bell System Tech. Journal,1969) [Fig. 1] $S_{ij}$ ($i=j$ and $i \neq j$) of the above antennas were measured by an HP 8410 B Network Analyser.

A3-7   LOW-FREQUENCY REFLECTION FROM AN
1620   ARRAY OF PYRAMID-CONE ABSORBERS
Edward F. Kuester and Christopher L. Holloway
Dept. of Electrical and Computer Engineering
University of Colorado - Campus Box 425
Boulder, CO   80309

Pyramid-cone absorbers made from graphite-impregnated plastic foam are typically used to line the walls of anechoic measurement chambers. These cones operate on the principle of repeated plane-wave reflection between faces of neighboring cones, which results in an overall low reflection coefficient from a wall lined with such cones. When this physical picture is valid (i.e., when cone dimensions are at least a wavelength) then good suppression of reflected waves results.

For some purposes, it may be desirable to oprate a measurement chamber at frequencies where this "geometrical optics" picture does not apply. We present an analysis of plane-wave reflection from a periodic array of cone absorbers when the wavelength is large compared to the transverse spacing between cones. We show, using a method called homogenization, that the array of cones is equivalent, in the low-frequency limit, to a one-dimensionally inhomogeneous, anisotropic layer, whose permittivity is easily calculated from the bulk permittivity and geometrical dimensions of the cones themselves. The plane-wave reflection coefficient is then found rather easily.

Computed results show some interesting features of the reflection coefficient, apparently due to damped standing waves within the equivalent layer. A certain amount of experimental data is also available, which shows good comparison to the theory.

PDE-BASED METHODS FOR EM PROBLEMS IN OPEN REGIONS
Co-Chairmen: M.A. Morgan, Electrical and Computer Engineering Dept.,
Naval Postgraduate School, Monterey, CA 93943; and L.W. Pearson,
McDonnell Douglas Research Labs, St. Louis, MO 63166

B4-1      **REVIEW OF PROGRESS IN FINITE-DIFFERENCE EQUATION**
1400      **SOLUTION METHODS FOR ELECTROMAGNETIC WAVE INTERACTIONS**

**Allen Taflove**                    **Korada R. Umashankar**
EECS Department                      EECS Department
Technological Institute              Communications Laboratory
Northwestern University          University of Illinois at Chicago
Evanston, IL 60201                   Chicago, IL 60680

Contemporary high-frequency electromagnetics problems can involve wave interactions with complex, electrically large, three-dimensional structures. These structures can have shapes, material compositions, apertures, or cavities which produce near fields that cannot be resolved into finite sets of modes or rays.  Proper numerical modeling of such near fields requires sampling at sub-wavelength resolution to avoid aliasing of magnitude and phase information.  The goal is to provide a self-consistent model of the mutual coupling of the electrically small cells comprising the structure.

Two recent numerical modeling approaches for this purpose involve finite-difference equation solution methods.  The first, which we denote as finite-difference frequency-domain (FD-FD) methods, involves either a direct solution of the Helmholtz equation on a space grid containing the structure, or a solution of a transformed problem involving Debye potentials.  FD-FD methods generate a potentially large system matrix.  To date, published applications principally involve two-dimensional wave interactions.

The second approach, which we denote as the finite-difference time-domain (FD-TD) method, is a direct marching-in-time solution of Maxwell's time dependent curl equations, applying simple, second-order accurate, central-difference approximations for the space and time derivatives.  This achieves a sampled-data reduction of the continuous electromagnetic field in a volume of space over a period of time, simulating the actual waves by numerical analogs propagating in a computer's data space.  The resulting system of equations for the fields is fully explicit, so that there is no need to set up or solve a set of linear equations, and the required computer storage and running time is proportional to the electrical size of the volume modeled.  Recent FD-TD research progress includes:  1. Scattering models for three-dimensional reentrant structures spanning up to $9\lambda_0$ ; 2. Conformal models of curved surfaces;   3. Scattering models for two-dimensional, anisotropic structures;  4. Penetration models for narrow slots and lapped joints in thick screens;  5. Coupling models for wires and wire bundles in free space and in arbitrary metal cavities;  6. Penetration models for the electromagnetic fields within detailed, inhomogeneous tissue approximations of the complete human body (at UHF frequencies);  7. Microstrip / waveguide models;   8. Scattering models for relativistically vibrating mirrors;   9. Inverse scattering reconstruction of one-dimensional, spatially coincident profiles of $\epsilon$ and $\sigma$ ;   10. Inverse scattering reconstruction of two-dimensional conducting, homogeneous, and inhomogeneous dielectric targets from minimal TM scattered field pulse response data;  and 11. Large-scale computer software.

B4-2    A FINITE-DIFFERENCE FREQUENCY-DOMAIN APPROACH
1420    TO ELECTROMAGNETIC SCATTERING PROBLEMS

R. T. Ling
Mail Code 3812/82
Northrop Aircraft Division
One Northrop Avenue
Hawthorne, California   90250

A finite-difference, frequency-domain (FD-FD)
approach to electromagnetic wave scattering is
presented.  This approach evolved from recent pro-
gress [R. T. Ling, AIAA Journal, Vol. 25, pp. 560-
566 (1987), AIAA Papers 87-0487 and 88-0180] that
features the concept of generalized scattering
amplitudes, the application of boundary-fitted
curvilinear coordinate systems, and the use of
Debye potentials for 3-D obstacle scatterings.
The introduction of the radially non-oscillatory
generalized scattering amplitudes circumvents the
difficulties in dealing with oscillatory field
quantities in the infinite exterior scattering
region and allows the finite-difference method to
be applied to scattering problems in an effective
manner.  The radiation condition in terms of the
generalized scattering amplitude is very simple in
form and can be enforced exactly in the far field.
For a 3-D scattering problem the formulation in
terms of Debye potentials, expressed as functions
of body-fitted coordinates, not only decouples the
vector scattering problem into a combination of
two independent scalar scattering problems but
also makes the exact enforcement of obstacle sur-
face condition simple.  Specific examples with
numerical results validated by the eigenfunction
expansion method and the moment method are given
to illustrate the salient features of the FD-FD
approach.

# A TIME DOMAIN DIFFERENTIAL SOLVER
# FOR ELECTROMAGNETIC SCATTERING PROBLEMS

Vijaya Shankar and William Hall
Rockwell International Science Center
Thousand Oaks, California 91360

*Abstract*

The transverse magnetic (TM) wave form of the Maxwell equations written in conservation form is solved using a hyperbolic, finite-volume, upwind based multizone scheme originally developed for solving the Euler/Navier–Stokes equations of Computational Fluid Dynamics (CFD). The Maxwell equations are shown to represent a linearly degenerate set of hyperbolic equations with real characteristics with values $\pm c$, where $c$ is the speed of light. The electric and magnetic fluxes at a finite volume cell interface are computed using a characteristic subpath integration referred to as the Riemann Solver. A multistep Lax–Weindroff scheme which is second order accurate in both space and time is applied to solve the TM equations. At a material interface, the boundary condition requiring continuity of tangential total electric and magnetic field is satisfied, while at a perfectly conducting surface the total electric field is set to zero. At the far field, a first order accurate no–radiation boundary condition derived from the characteristic theory is applied. A near field–to–far field transformation is applied to the computed electric and magnetic fields to obtain the bistatic radar cross section (RCS). Results are presented for both time harmonic and transient electromagnetic scattering problems involving layered material mediums.

B4-4      THE TLM METHOD AND ITS APPLICATION
1500      TO OPEN AND BOUNDED FIELD PROBLEMS
          Michel M. Ney and Wolfgang J.R. Hoefer
          Laboratory for Electromagnetics and Microwaves
          Dept. of Electrical Engineering
          University of Ottawa
          Ottawa, Ontario, Canada K1N 6N5

Inspired by earlier network simulation techniques, Johns and Beurle introduced in 1971 a novel numerical method for solving general electromagnetic field problems. They modelled the propagation of fields in space by computing the progress of voltage and current impulses in a network of interconnected transmission lines. They showed that both fields and network variables obey the same differential equations as long as the mesh size is small compared with the wavelength.

The basic TLM algorithm describes the scattering of Dirac impulses at series and shunt nodes, a phenomenon which is equivalent to Huygens's principle in discretized form. The impulse response of the TLM network is computed in time steps equal to the transit time between nodes, and the frequency response is obtained therefrom via Fourier transform.

Lossless and lossy boundaries can be modeled by introducing suitable reflection coefficients in the TLM mesh. Since the mesh is discretized, boundaries are approximated by piecewise straight walls deployed halfways between nodes to preserve synchronism of scattering events. Open problems can be modeled as structures with absorbing boundaries. Dielecric and magnetic materials are simulated by loading shunt nodes with shunt stubs, and series nodes with series stubs, respectively. The simulated $\epsilon_r$ or $\mu_r$ values depend on the characteristic immittances of these stubs. Losses and anisotropy can be properly accounted for as well. Since the procedure is executed in the time domain, non-linear problems as well as situations involving time-variant material parameters can be treated with the TLM method.

In this paper, the TLM algorithm and the modeling of various boundary and material properties will be described briefly. Recent advances such as condensed nodes, graded mesh techniques, and error correction techniques will be discussed. Computational expenditures will be analyzed and compared with those of other numerical techniques. Finally, two applications of the method, one to an open problem (EMP response of an airplane), and one to a bounded problem (modeling of a finline T-junction) will be presented to illustrate the potential of the TLM method.

B4-5    **GENERALIZED COUPLED AZIMUTHAL POTENTIALS FOR**
1540    **ELECTROMAGNETIC FIELDS IN INHOMOGENEOUS MEDIA**

Michael A. Morgan
Electrical and Computer Engineering Department
Naval Postgraduate School, Monterey, CA 93943

The original coupled azimuthal potential (CAP) formulation
(Morgan, Chang & Mei, *IEEE Trans. Ant. & Prop.*, AP-25, pp. 413-417,
1977), has the advantage of using only two continuous potentials
to represent all field components in "arbitrary", but axially
symmetric, inhomogeneous material media.   It has been used as
the basis for several finite element numerical efforts involving
radiation, scattering and penetration problems.

A generalization of the original formulation is presented,
whereby the restriction to axisymmetric media is removed.   This
new methodology retains the advantage of vector field generation
in terms of only two scalar potentials.   Alternate forms for
solving the generalized CAP equations are considered, including
eigenfunction decomposition and circumferential natural basis
functions.   Numerical examples are presented for boundary
value problem solutions in 3-D using finite elements.   Finally,
the procedures for solving scattering problems using this theory
are discussed.

# RELATIVE ACCURACY OF FREQUENCY-DOMAIN INTEGRAL AND DIFFERENTIAL EQUATION FORMULATIONS FOR OPEN-REGION ELECTROMAGNETIC SCATTERING PROBLEMS

*Andrew F. Peterson*
*Electromagnetic Communication Laboratory*
*1406 W. Green St.*
*University of Illinois*
*Urbana, IL   61801*

*Steven P. Castillo*
*Department of Electrical Engineering*
*New Mexico State University*
*Las Cruces, NM   88001*

Open-region electromagnetic scattering problems can be formulated as integral or differential equations. The integral equation approach has been widely used, possibly because the Green's function appearing in the kernel of the integral operator implicitly accounts for infinite space and incorporates the radiation condition. Techniques for the numerical solution of integral equations usually involve fully-populated matrices. In contrast, differential equation formulations must explicitly enforce the radiation condition a finite distance from the scatterer. These methods generally require more unknowns than the integral formulations, but typically involve sparse matrices.

To evaluate the relative advantages of the integral and differential equation formulations in the context of numerical solutions, systematic comparisons have been carried out for several two-dimensional, open-region geometries. Numerical results indicate that both formulations provide similar accuracy when applied to identical scatterer models. However, the differential equation methods can have significant computational advantages because of the efficiency in treating sparse matrices. This suggests that differential equation methods may be better alternatives for numerical solution than the integral equation formulations currently in widespread use.

Examples illustrating the relative accuracy of integral and differential equation methods will be presented. The accuracy of the Bayliss-Turkel type of "near-field" radiation condition as a function of distance from the scatterer will be examined. Finally, efficient algorithms for treating sparse systems will be surveyed.

B4-7     TO BE OR NOT TO BE IN THE TIME DOMAIN
1620     Kenneth K. Mei
         Department of Electrical Engineering and Computer Sciences
         University of California
         Berkeley, CA   94720

Maxwell's differential equations in the frequency domain are ellip-tical, which results in classical boundary value problems.  In the time domain they are hyperbolic, the solutions of which march in time.  Nu-merically, the frequency domain differential equations require solutions of matrices; the time domain differential equations, if explicit, are spared from such endeavor.  Before the coming of super computers, almost all electromagnetic problems were solved in the frequency domain.  Now, there is a choice.  This talk enumerates the pros and cons of computations in either domain.  Depending on the objectives of the computation, one can make a rational decision in the computational domain.  However, individual familiarity and personal beliefs often are the dominant factors of to be or not to be in one particular domain.

B4-8      A FINITE-DIFFERENCE INTERPRETATION OF
          THE TRANSMISSION-LINE-MATRIX METHOD
1640
          Richard C. Booton, Jr., Chief Scientist
          TRW Electronic Systems Group
          TRW E2/3080
          One Space Park
          Redondo Beach, CA 90278

The finite-difference (FD) method and the transmission-line-matrix (TLM) method are recognized to be alternate approaches to the calculation of transient electromagnetic response. This paper demonstrates the equivalence of the two methods, provided two conditions are met. Initial conditions and boundary conditions must be assigned consistently. The ratio of time interval to space interval must have a certain value, namely the maximum value for which FD is a stable computational process. This value is $1/c\sqrt{2}$ for two dimensions and $1/c\sqrt{3}$ for three dimensions. The fact that the TLM solution satisfies the FD equations is demonstrated in detail for the two-dimensional case, and extension to three dimensions is summarized.

Equivalence of the methods is demonstrated by beginning with a single TLM pulse and utilizing the TLM rules to calculate pulse and nodal values for several time intervals. Direct comparison of the nodal values shows that the FD version of the scalar wave equation is satisfied for the ratio of time interval to space interval specified above. Superposition then shows that beginning with an arbitrary set of pulses, the same conclusion follows.

Nodal values for initial conditions for FD that correspond to the TLM pulses are determined from the TLM rules, as described above. Consistent boundary conditions for FD and TLM for Dirichlet and Neumann conditions are demonstrated. The TLM rules at boundary nodes are similar to one-dimensional transmission-line reflection at shorted and open terminations, respectively. Conditions for a boundary between two dielectrics present severe problems for TLM, which are not completely resolved herein, even though FD can handle the situation directly.

Another approach to the comparison starts with the discrete form of Maxwell's equations. If the nodal values correspond to the electric field, the magnetic field values can be shown to be proportional to the difference between the values of the pulses travelling in opposite directions.

B5-1
1400

# A BIVARIATIONAL APPROXIMATION FOR THE SCATTERING PARAMETERS OF A 90° MICROSTRIP-SLOTLINE CROSSOVER

Edward F. Kuester and Alexander Anger
Dept. of Electrical and Computer Engineering
University of Colroado - Campus Box 425
Boulder, CO  80309

One of the most challenging problems in the modeling of planar transmission lines is the characterization of the 90° microstrip-slotline crossover.   Here the microstrip rests on the top side of a dielectric substrate, while the slotline is cut into the ground plane on the bottom side of the substrate, at 90° to the microstrip axis.   A rough equivalent circuit model for this crossover has been known for some time [J.B. Knorr, IEEE Trans. MTT. 22, 548-554 (1974)], but this has been found to be insufficiently accurate for some close tolerance applications.

We present here a bivariational approximation to calculate the S-matrix of this junction.   A pair of coupled integro-differential equations is found for the unknown surface current density on the microstrip and aperture electric field in the slot.   A suitable formulation then results in a variational formula for any of the scattering parameters we desire.   The trial functions are the scattered currents and slot fields of the junction.   A simple choice of trial function involves the fundamental microstrip and slotline modes with adjustable amplitudes.   Substitution of this trial function into the variational principle yields terms which involve double Sommerfeld integrals and must be carefully handled numerically.   Results obtained in this way will be compared with others available in the literature.

B5-2
1420

## SIMPLE TRIAL CURRENT DENSITIES FOR THE BIVARIATIONAL ANALYSIS OF AN AIR-LOADED, SYMMETRIC STEP-IN-WIDTH MICROSTRIP JUNCTION

Robert T. Johnk and David C. Chang
Electromagnetics Laboratory
Campus Box 425
University of Colorado
Boulder, Colorado 80309-0425

One method for extracting the frequency-dependent S-parameters of an air-loaded symmetric step-in-width microstrip junction is the so-called bivariational technique. This approach involves the application of a simple trial current density to a bivariational functional in order to obtain a more accurate total current. The frequency-dependent S-parameters accounting for the junction radiation and reactance can be extracted from this corrected total current. This talk deals with the generation of a simple trial current density function for the bivariational analysis of an air-loaded symmetric step-in-width junction. Recent investigations of this junction have shown that the trial current density must be continuous throughout the microstrip junction. Our approach for generating such a trial current is based on the technique of conformal mapping. This method involves several steps. First, the conformal transformation for the dual electrostatic problem of a parallel-plate step in separation is solved for. This conformal transformation is then used in conjunction with a perturbation/iterational technique to compute exactly the first few static mode coefficients in both the wide-spaced and narrow-spaced parallel-plate regions. Higher mode coefficients are then derived from a simple recurrence formula, based on the edge condition. Once all of the necessary mode coefficients have been determined, we can convert them into a time-static current density using duality. The time-static current densities for the narrow and wide strip regions are now in the form of a simple Fourier series of exponential and trigonometric functions, and they are particularly suited for the bivariational analysis.

B5-3   **MODE-MATCHING FORMULATION FOR COMPLETE MODAL SPECTRUM**
1440   **OF DIELECTRIC WAVEGUIDES WITH UNIFORM SURROUND**
       D.P. Nyquist, E.J. Rothwell and P.F. Havala
       Department of Electrical Engineering
       Michigan State University
       East Lansing, MI  48824

Mode-matching techniques for quantification of discrete surface-wave modes supported by dielectric waveguides of wide-ly varying configurations have received exhaustive treatment in the recent literature.  The continuous component of the complete propagation-mode spectrum has, in contrast, received relatively little attention.  It is demonstrated, for the restricted class of arbitrarily-shaped, step-index guiding regions immersed in a uniform surround, that the mode-matching technique can be exploited to quantify the complete spectrum of such open-boundary waveguides.  Radiation fields arising from this description may be valuable in excitation, coupling and scattering problems associated with dielectric waveguides.

Let the guiding region be designated as $V_g$ and the sur-round as $V_s$.  All analysis is performed in the axial Fourier-transform domain; all quantities, e.g., $e(\rho,\zeta)= F_z\{E(\rho,z)\}$, are transforms depending upon transform variable $\zeta$.  Impressed current $j(\rho,\zeta)$ maintains impressed field $e^i(\rho,\zeta)$.  The latter field interacts with the guiding region, resulting in scat-tered field $e^s(\rho,\zeta)$.  Consequently the total field in either $V_g$ or $V_s$ is $e = e^i + e^s$.  If $j\varepsilon V_s$ then $e^i=0$ in $V_g$ while $e^i=0$ in $V_s$ when $j\varepsilon V_g$, i.e., $e^i\neq0$ in only one or the other of $V_g$ and $V_s$.  $e^i$ is known, through an appropriate 2-d Green's function $g_\zeta(\rho,\rho')$, for any given $j$.  Circular-harmonic expansions are exploited to represent $e^s$ in the guiding ($J_n$ Bessel series) and surround ($H_n^{(2)}$ Bessel series) regions.  Total tangential $e$ and $h$ fields are point matched at the guiding-region/surround interface, leading to a matrix equation for the system of expansion coefficients $[a_n(\zeta)]$ as $[E_{mn}(\zeta)][a_n(\zeta)] = [f_m^i(\zeta)]$ where the forcing vector implicates known impressed field components.

The spatial field is recovered as $E(\rho,z)=F_z^{-1}\{e(\rho,\zeta)\}$.  Evaluation of the inversion integral by appropriate complex $\zeta$-plane analysis leads to the complete propagation-mode spectrum excited by $j$.  Surface-wave modes arise from simple-pole sing-ularities at $\zeta =\zeta_p$, near which $a_n(\zeta)=\tilde{a}_n(\zeta)/(\zeta-\zeta_p)$ so the matrix equation requires $[E_{mn}(\zeta)][a_n(\zeta)]=0$ and $\det[E_{mn}(\zeta)]=0$ at $\zeta=\zeta_p$; this is the familiar mode-matching eigenvalue equation.  Inte-gration about branch points at $\zeta=\pm k_s$ leads to the radiation field as a continuous superposition of forced spectral solu-tions to the fundamental matrix equation.  Application of this quantification scheme to the dielectric rectangular waveguide is demonstrated.

B5-4   **ON SOMMERFELD-INTEGRAL ELECTRIC FIELD KERNELS FOR**
1520   **MICROSTRIP-BASED CIRCUITS**
       D.P. Nyquist, M.S. Viola, M.J. Cloud and M. Havrilla
       Department of Electrical Engineering
       Michigan State University
       East Lansing, MI  48824

Microstrip circuits are fabricated over the film/cover interface of a planar, layered conductor/film/cover surround environment. In an electric-field integral equation description of such circuits, the electric field tangential to metallic microstrip conductors, maintained by surface currents on those conductors, is required. A spectral approach through Hertz potentials leads to sommerfeld-type integral representations for required Green's function kernels.

Let the microstrip conductors reside at $y=0^+$, adjacent to the x-z film/cover interface plane. The field $e(x,\zeta)$ at the conductor surface, maintained by surface current $k(x,\zeta)$ on that conductor (both in the axial Fourier-transform domain; transform variable $\zeta$), is then

$$e(x,\zeta) = \lim_{y \to 0^+} (k_c^2 + \tilde{\nabla}\tilde{\nabla}\cdot) \int_{cond} \bar{\bar{g}}_\zeta (x,y|x',0) \cdot k(x',\zeta)dx'$$

where $k_c = n_c k_0$ ($n_c$=cover index), $\tilde{\nabla} = \nabla_{xy} + \hat{z}j\zeta$ and $\bar{\bar{g}}_\zeta$ is a Hertz potential Green's dyad in Sommerfeld-integral representation. It is convenient to pass the spatial integral and the differential operator, in turn, through the spectral integral over $\xi$, since the former operations can all be performed in closed form. This procedure is valid provided the details (source-point singularity) are handled carefully and the $y \to 0^+$ limit is performed lastly. In much of the recent literature, the latter limit is exchanged with the spectral integral; this invalidates the differential-operator exchange and leads to a divergent spectral integration. Consequently, uncertainty has arisen in the choice of appropriate expansion and testing functions for use in MoM solutions to associated EFIE's.

In fact, pulse basis functions and point matching lead to convergent spectral integrals if the $y \to 0^+$ limit is performed appropriately. MoM matrix elements are represented by

$$I_{\alpha\beta} = \lim_{y \to 0^+} \int_0^\infty W_{\alpha\beta}(\xi) e^{-p_c y} \frac{\sin(\xi\delta)}{\xi} \begin{pmatrix} \sin \xi x_m \\ \cos \xi x_m \end{pmatrix} \begin{pmatrix} \sin \xi x_n \\ \cos \xi x_m \end{pmatrix} d\xi$$

where $W_{\alpha\beta}$ is a complicated function of $\xi$ (carrying surface-wave poles of the surround) and $p_c = (\xi^2 + \zeta^2 - k_c^2)^{1/2}$. The most slowly convergent case is $\alpha = \beta = x$, where $W_{xx}(\xi) \hat{\alpha} \xi$ for large arguments, leading to an undamped oscillatory integrand when $y=0$. It is demonstrated, however, that the $y \to 0^+$ limit does indeed exist, and the convergence rates of the various $I_{\alpha\beta}$ are compared.

B5-5   ALTERNATIVE INTEGRAL FORMULATION FOR ANALYSIS OF MICROSTRIP
1540   TRANSMISSION LINES

J. M. Grimm and J. S. Bagby
Department of Electrical Engineering
University of Texas at Arlington, Arlington, TX   76019

For natural modes of an integrated microstrip transmission line, the axially-transformed surface current $\vec{k}(\vec{\rho}';\zeta)$ satisfies the well-known homogenous dyadic integral equation:

$$\hat{t}\bullet(k_c^2 + \nabla\nabla\bullet) \int_{\ell} \overset{\leftrightarrow}{g}(\vec{\rho}|\vec{\rho}';\zeta)\bullet\vec{k}(\vec{\rho}';\zeta)\ d\ell' = 0, \quad \vec{\rho}\ \varepsilon\ \ell$$

where $\overset{\leftrightarrow}{g}(\vec{\rho}|\vec{\rho}';\zeta)$ is the transformed Hertzian potential Green's dyad of the background structure, $k_c$ is the wavenumber in the cover region, $\zeta$ is the complex propagation constant of the mode, t is a unit-tangent to the transmission line, and $\ell$ is the cross-sectional contour of the line.

The Green's dyad components are typically given as inverse Fourier transforms with respect to $\xi$, the transform variable corresponding to the x direction.  The inversion integrals assume the form of Sommerfeld integrals and are notoriously difficult to compute.  Green's dyad component evaluation is further complicated due to surface wave singularities exhibited when the real part of $\zeta$ is less than the propagation constant of a surface wave mode in the background structure.

An alternative formulation for the Green's dyad components using complex $\xi$-plane analysis is presented here.  In this method, Cauchy's theorem is used to represent the Green's dyad components as a sum of residues at the surface wave pole singularities plus an integration along a hyperbolic branch cut in the complex-$\xi$ plane.  This alternative formulation has the advantage of replacing slowly-convergent Sommerfeld integrals with relatively well-behaved contour integrals.

This alternative Green's dyad formulation is used in the MOM solution of the integral equation above to analyze both narrow and wide microstrip configurations.  The above-described advantages are demonstrated for both cases via numerical results.

B5-6
1600

# APPLICATION OF METHOD OF LINES TO MULTIPLE STRIP PLANAR PROPAGATION STRUCTURES HAVING INHOMOGENEOUS LAYERS

M.A.Thorburn and V.K.Tripathi

Department of Electrical and Computer Engineering
Oregon State University
Corvallis, Oregon 97331-3202.

This paper deals with the propagation characteristics of a class of general multiple strip structures in layered medium having inhomogeneity in both transverse directions. Such structures have found applications in electro optical devices and the techniques developed can also be applied to study other useful problems such as microstrips near the chip edge in a monolithic circuit.

The method of lines which has been used in recent years to study general propagation structures and discontinuities (Schulz, AEU, 34, 176-178, 1980.,Schulz & Pregla, Radio Science, 16, 1173-1178, 1981.,Worm & Pregla, MTT-32, 191-196, 1984.,Diestel & Worm, MTT-32, 633-638, 1984.,Sherrill & Alexopoulos, MTT-S Digest, 327-329, 1987.) is extended in this paper to apply to problems having inhomogeneity in x direction. Both quasi TEM and frequency dependent full wave solutions are considered. For the quasi TEM case the Greens function interrelating the boundary charge and potential is used to compute the capacitance matrices and the structure properties. The complete full wave problem is formulated in terms of the general impedance matrix (Green's function ) of the structure which is used to solve for the eigen values ( propagation constants for the normal modes ), the current distribution, the line mode impedances and the field distribution of these structures. It is shown that these parameters can be used to compute all the multiport properties such as the scattering matrix elements of general coupled strip structures.
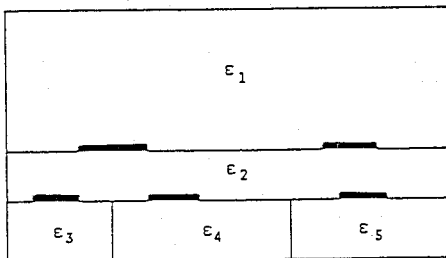


CROSS SECTION VIEW OF A GENERAL STRUCTURE

B5-7    RADIATION FROM TRANSMISSION-LINE "PIGTAIL" CONNECTIONS
1620

H. Hejase
Department of Electrical Engineering
University of Kentucky
Lexington, Kentucky 40506

A. T. Adams
R. F. Harrington
Department of Electrical and Computer Engineering
Syracuse University
Syracuse, NY 13244

The shielding effectiveness of a "pigtail" connection between a coaxial transmission line and a ground plane is treated rigorously by the method of moments, as a function of the type and number of pigtails and frequency. The type of pigtail connection is shown to be crucial with regard to radiation and shielding effectiveness, even though the pigtail itself does not radiate significantly. All pigtails are not equal, even though they may be short electrically. A short pigtail is significantly better than a longer one. A "sloppy" pigtail connection may actually enhance radiation. Multiple pigtails yield signficant improvement over the single pigtail for short pigtails.

A useful equivalent circuit representation of the pigtail problem is given. The pigtail impedance obtained by the method of moments is compared with that obtained by a quasi-static method with agreement to within a few percent for electrically short pigtails. Results have been compared with other theoretical results and with experiment, with good agreement.

# Spectrum Estimation via Maximum-Likelihood
# Generation of Toeplitz Constrained Covariances
# Using the Expectation Maximization Algorithm

*Michael Turmon and Michael I. Miller*

Electronic Systems and Signals Research Laboratory
Department of Electrical Engineering
Washington University
Saint Louis, Missouri 63130

## ABSTRACT

We consider the spectrum estimation problem in which we observe the single $G \times 1$ vector $y_G$ from a zero-mean Gaussian stationary random process with unknown $G \times G$ Toeplitz covariance $K_G$. The probability density function describing $K_G$ is thus

$$g(y_G; K_G) = (2\pi)^{-\frac{G}{2}}(\det K_G)^{-\frac{1}{2}}\exp(-\frac{1}{2}y_G^\dagger K_G^{-1} y_G) \quad , \tag{1}$$

with † denoting hermitian transpose. The maximum likelihood problem is to maximize this function with respect to all Toeplitz $K_G$.

To ensure the existence of a nonsingular estimate when given only one data vector $y_G$, we perform the maximization subject to the further constraint that $K_G$ be Toeplitz with a circulant extension of period $N > G$. We generate the estimates iteratively using the expectation-maximization algorithm. Within the context of this algorithm, we choose the incomplete data to be $y_G$, which data are a part of the larger unobserved $N \times 1$ complete data vector $y_N$. This complete data vector is from a stationary periodic process of period $N > G$ with $N \times N$ circulant covariance $K_N$. It has been shown [Miller and Snyder, *Proc. IEEE*, July 1987] that the constrained MLE $K_G$ in the set of $G \times G$ Toeplitz covariance matrices with $N$-periodic extension is the convergence point of the iteration sequence given by

$$K_G^{(p+1)}(\tau) = \frac{1}{N}\sum_{m=0}^{N-1} E\{y(m)y^*(<m+\tau>_N)| \; y_G, K_G^{(p)}\} \quad , \tag{2}$$

where $< >_N$ denotes modulo $N$. It has been shown that the Toeplitz estimates defined by (2) are monotonic in the likelihood of (1) and remain in the set of positive-definite Toeplitz covariances. Furthermore, all the limit points of (2) are stable and satisfy the necessary conditions for maximizing likelihood over the constrained set of Toeplitz matrices with $N$-periodic extensions.

## C1-2 1440 COMPONENTS OF VARIANCE INTERPRETATION OF SPECTRUM ESTIMATION

Louis L. Scharf and Li Du
Department of Electrical Engineering
University of Colorado - Campus Box 425
Boulder, CO   80309

In this paper we offer a number of alternative interpretations for D.J. Thomson's multiple window spectrum estimators.   Each interpretation is coupled to the solution of a detection, estimation, or identification problem that is closely related to the problem of estimating a spectrum in a narrow band.  We show that the key step in narrow band spectrum estimation is the projection of the data onto a low rank˙ subspace where its power may be accurately estimated.

C1-3
1540

**Time-frequency localization operators - a geometric phase space approach.**

Ingrid Daubechies
A.T.&T. Bell Laboratories
600 Mountain Avenue
Murray Hill  NJ 07974

In mathematical techniques which require good resolution in both time and frequency domains, it is customary to use the Slepian functions (prolate spheroidal wave functions) associated with the appropriate time and frequency windows, and the corresponding eigenvalues.

This paper shows how a different picture, more geometrical in nature, leads to different families of functions. In particular, if the domain of interest in time-frequency is a disk or an ellips, then the associated eigenfunctions and eigenvalues become Hermite functions and incomplete gamma-functions, respectively. These also have the virtue of being much easier to calculate than the Slepian functions and their corresponding eigenvalues.

C1-4
1620
HARMONIC ANALYSIS ON SYMMETRIC SPACES: Audrey Terras, Dept. of
Mathematics, Univ. of California, San Diego, CA

E1-1  **VARIABILITY OF THE HIGH-ALTITUDE EMP**
1400

Conrad L. Longmire
Mission Research Corporation
ABSTRACT

Classification has severely limited the amount of information on high-altitude EMP (or HEMP) that has reached the public. A result has been the development of the misimpression that the HEMP can be well characterized by giving a single pulse shape with a maximum amplitude. A possible logical consequence is the idea that electrical and electronic equipment hardened and tested to this single pulse will, with high probability, be hard to HEMP in general. The author believes that this idea is almost certainly wrong and at least requires proof with regard to specific equipments. The author's view is prompted by the nonlinearities in the coupling of HEMP into equipments, in the processes of upset and damage, and in some hardening techniques (e.g., limiting).

Classification of HEMP environments stems from the classification of some aspects of the outputs of nuclear weapons such as the actual rise time of the gamma output pulse. We have avoided that problem by assuming a gamma pulse with zero rise time and nominal pulse width and quantum energy. The calculated HEMP as a function of azimuth and ground range for a single burst at 400 km altitude over the central U.S. is presented in this paper. The wide variability in pulse shape and amplitude in these results and the consequent difficulty in selecting a single representative pulse are discussed. The author asks for the advice from the audience as to what kind of HEMP information would be most useful in hardening of systems.

E1-2      NORM LIMITERS COMBINED WITH FILTERS
1440      C. E. Baum
          Air Force Weapons Laboratory
          Kirtland AFB
          Albuquerque, New Mexico   87117-6008

   In the general formalism of electromagnetic
topology the propagation through and reflection
from subshield penetrations of signals is impor-
tant.   This paper considers the characteristics
of linear filters and nonlinear devices idealized
as norm limiters which can be used at such pene-
trations.   Both frequency-domain and time-domain
concepts are employed to limit undesirable signal
penetration and reflection.

E1-3
1500

# EARLY TIME PERFORMANCE AT LARGE DISTANCES OF PERIODIC ARRAYS OF FLAT-PLATE CONICAL WAVE LAUNCHERS

D. V. Giri
Pro-Tech, 125 University Avenue, Berkeley, CA 94710

and

Carl E. Baum
Air Force Weapons Laboratory/NTAAB
Kirtland AFB, New Mexico 87117

## Abstract

Many techniques have been investigated for the purpose of launching transient electromagnetic (EM) waves and the results have been incorporated in the design of various categories of EMP simulators. One such technique involves configuring many sources into an array. The source array synthesizes an appropriate aperture field distribution to launch a desired type of wave. The individual sources are interconnected in some series-parallel fashion, via conducting surfaces which have a significant impact on the early-time rate of rise in the distant field. Both planar and non-planar arrays have been considered in the past.

In this paper, we consider some possible geometries of unit cells in the distributed source or distributed switch wave launchers. Attention is focussed on one aspect of performance, i.e., the rate of rise in the far field (for assumed ideal step-function sources) of candidate unit cell designs. The unit cells considered are planar-conical or non-planar wave launchers. There are perhaps many module or unit-cell designs one may consider, each being associated with its own boundary value problem. Two illustrative examples are presented. Formulae for the early-time rate of rise are developed, tabulated and plotted, as a function of normalized geometrical parameters of an individual launcher and the array.

E1-4
1540

SYNTHESIS OF ANISOTROPIC LENSES FOR
INHOMOGENEOUS TEM PLANE WAVES RELATED
TO THE DIFFERENTIAL GEOMETRY METHOD

A. P. Stone
University of New Mexico
Department of Mathematics
Albuquerque, NM 87131
C. E. Baum
Air Force Weapons Laboratory
Kirtland AFB
Albuquerque, NM 87117

This talk is concerned with the equivalence of two methods
for the design of lenses for TEM plane waves, such as might ex-
ist on certain types of transmission lines. The transition re-
gion can be used to specify lenses for transitioning TEM waves,
without reflection or distortion, between these transmission
lines. The desired transmission is to be frequency independent
and the lens design is based on frequency independent solutions
of Maxwell's equations. One approach to the design of transi-
tion regions is a differential geometric one, in which a scal-
ing method creates an equivalence between two classes of elec-
tromagnetic problems. An alternative approach requires that
differential impedances be matched at all lens-waveguide bound-
aries and also that a plane wave front in one region should go
into a plane wave front in another region. These two methods
of EM lens design may be shown to be equivalent. In the case
of differential geometric scaling, one finds that for a TEM
wave propagating in one of the coordinate directions that both
differential-impedance matching and transit-time conservation
is obtained at the lens boundaries. On the ther hand, if one
starts with the impedance-matching and transit-time require-
ments, then arriving at the differential geometric conditions
requires more effort. In order to obtain these geometric con-
ditions, one must first consider the general case of transport
of waves through a set of ducts connecting surfaces which form
the boundaries for a lens. One then examines the use of these
ducts to reorder positions on a wavefront and then considers
two possible ways of arriving at an EM lens design, each the
dual of the other.

E1-5        RETURN-STROKE INITIATION

1600        Dr. Carl E. Baum
             Air Force Weapons Laboratory
             Kirtland AFB
             Albuquerque, New Mexico  87117-6008

The far fields from a lightning return stroke are a function of the spatio-temporal distribution of the return-stroke currents. This paper introduces a conical-transmission-line model of the return stroke immediately following leader closure. Based on this model, return-stroke speed is computed and shown to be near c at early times following leader closure. In turn the early-time far fields are also computed. This early-time speed is but one factor influencing the relationship between the return-stroke currents and the far fields. These factors are reviewed and shown to give a wide variation to this relationship, thereby making it difficult to infer return-stroke currents (with any accuracy) from the far fields.

# Comparison of Lightning Models for Channel Currents and Electromagnetic Fields

Maj. R. L. Gardner
Air Force Weapons Laboratory
Kirtland AFB, NM 87117

## Abstract

Many different models have been presented in the literature to predict the electromagnetic fields due to lightning. They generally fall into two categories. The first type is a model of the current in the lightning channel. These models vary from simple curve fits of current waveforms to elaborate nonlinear, nonuniform transmission line models. The second type of model is designed to predict the fields due to the currents predicted by the first type. These types of models vary from simple $1/r$ style radiating dipole models to elaborate propagation codes which include finitely conducting earth effects, scattering from discontinuities, etc.

Models presented in the literature are described and compared in this paper. The information assembled here should aid researchers as they search the literature for lightning models that contain the appropriate physics. Tradeoffs in computational expense compared to modeling detail will be apparent.

E1-7    A CHANNEL ADAPTIVE HIGH THROUGHPUT METEOR
1640    SCATTER COMMUNICATION SYSTEM

A. K. Gupta and J. R. Herman
GTE Government Systems Corp.
One Research Drive
Westborough, MA  01581

The present paper discusses an adaptive high throughput meteor scatter communication system, which maintains a constant high data-rate over the trail life-time despite time-varying path losses, time-varying doppler and multipath spread during this time.  The proposed system employs the coding and the interleaving in addition to the M-ary incoherent FSK signalling with waveform diversity, utilized in the earlier proposed system (A. K. Gupta and M. D. Grossi, Proc. of Ionospheric Effects Symposium, Alexandria, VA, 282-296, 1981; A. K. Gupta, National Radio Science Meeting, Houston, TX, Abstract, 1983).

A formula for varying M-ary signal alphabet, to provide a constant high data rate, is also provided for trade-off analysis with respect to specified performance, meteor burst channel parameters, data rate, code rate, code diversity, etc.

F1-1
1400

# SSM/I POST-LAUNCH RADIOMETRIC SENSITIVITY, STABILITY AND BEAM POINTING ACCURACY

G. A. Poe and J. P. Hollinger
Space Sensing Branch
Naval Research Laboratory
Washington, DC 20375-5000

Results are presented of the radiometric sensitivity and stability and antenna beam pointing accuracy of the SSM/I instrument over the first six months of operation. Both hot load and cold reflector calibration data are analyzed to estimate the sensitivities for all seven channels and the orbital drift of the gains of the radiometers. The RMS instrument noise is well within instrument specification and the radiometer gain is very stable over all data examined.

In addition the repeatability of the SSM/I brightness temperatures is determined by examining numerous histograms of data collected over many months of selected geographical regions, the Congo Basin, the Amazon Basin, the Libyan Desert and the Sargasso Sea. These data substantiate the excellent radiometric stability of the SSM/I.

The possibility of reducing fluctuations in the radiometer calibration data due to instrument noise are presented along with a suitable calibration algorithm to perform the filtering. The reduction of the radiometer delta-G over G are presented in terms of the number of scans of calibration data averaged.

Estimates of the antenna beam pointing accuracy are presented which were derived by comparing the radiometric signatures of land/water boundaries and with well known geographical maps.

# VALIDATION/CALIBRATION OF THE SSM/I ABSOLUTE CALIBRATION ACCURACY

J. P. Hollinger and G. A. Poe
Space Sensing Branch
Naval Research Laboratory
Washington, DC 20375-5000

Two approaches are being used to validate the absolute calibration of the SSM/I: 1) comparison of SSM/I brightness temperatures with those from the aircraft borne SSM/I simulator and 2) comparison with an environmental microwave radiative transfer model.

The Naval Research Laboratory RP-3A aircraft with the SSM/I simulator radiometer instrument is used to underfly the SSM/I satellite sensor. The SSM/I simulator is a non-scanning set of radiometers at the same frequencies and polarizations (19.4 Ghz H and V, 22.235 Ghz V, 37.0 Ghz H and V and 85.5 Ghz H and V) viewing the earth's surface at the same incidence angle as the conical scan angle of the SSM/I. The underflights were concentrated in the open ocean under various sky conditions since the ocean surface provides a set of significantly polarized brightness temperature signatures. Locations were chosen well away from land to avoid antenna sidelobe contamination and were at 8 km altitude above nearly all of the atmospheric absorption. Flight lines were in the form of a cross with 150 km legs to enable spatial and temporal comparison with the SSM/I footprints.

Ocean regions with very low 85.5 Ghz brightness temperatures where clear/dry atmospheric conditions were known to prevail were selected for comparison with model generated brightness temperatures. Environmental conditions used in the model were obtained from buoys and ships where possible and estimated otherwise. The estimates were based on climatology for that latitude and time of year as well as a study of other satellite weather data for the area.

F1-3     **STATUS REPORT ON THE SPECIAL SENSOR**
1440     **MICROWAVE/IMAGER CLOUD AMOUNT**
         **VALIDATION**
         G.W. Felde and R.W. Conant, Jr.
         Air Force Geophysics Laboratory
         Atmospheric Sciences Division
         Satellite Meteorology Branch (AFGL/LYS)
         Hanscom AFB, MA  01731

The new Special Sensor Microwave/Imager (SSM/I) is a seven channel, four frequency, linearly polarized, passive microwave radiometer which is onboard a polar-orbiting spacecraft launched in June 1987. The SSM/I provides estimates of several surface and atmospheric parameters. The Air Force Geophysics Laboratory is validating the cloud amount parameter (percent cloud coverage). Hughes Aircraft Company developed two algorithms for estimating cloud amounts from SSM/I brightness temperatures. One is applicable over snow backgrounds; the other over land backgrounds. However, it is not possible to obtain cloud amount estimates for land covered with vegetation. No cloud amount estimation algorithms for ocean or oceanic ice backgrounds were required to be developed; even though the potential over both of these backgrounds is good.

The ground truth cloud amounts used for validation are obtained from interactive computer analyses of 1.5 nautical mile resolution visible and thermal infrared meteorological satellite data. These data are from the scanning radiometer called the Operational Linescan System (OLS). The OLS is onboard the same spacecraft as the SSM/I and thus there is a good temporal match between the two data sources. Ground truth sites are located over North America and Greenland. Statistical comparisons between SSM/I and OLS cloud amount values are being generated. Two sets of validation statistics are presented, one for land backgrounds and one for snow backgrounds.

## PRELIMINARY RESULTS ON THE VALIDATION OF ICE ALGORITHMS FOR THE SSM/I

Rene O. Ramseier
Atmospheric Environment Service
(AES)/Center for Research in
Experimental Space Science (CRESS)
York University
4700 Keele Street
North York, Ontario M3J 1P3

Cathryn Bjerkelund
Norland Science and Engineering LTD

Irene Rubenstein
CRESS

The validation of the SSM/I ice algorithm is part of the total valida-tion/calibration effort being coordinated by the Naval Research Laboratory and commenced June 28,1987 with ice information (ground truth) obtained from the Beaufort and East Greenland Seas. The results to be presented will cover the melt season, (the most difficult period for ice interpretation), the onset of freezing, and the early part of the winter. The surface obser-vations are based primarily on data obtained from Side Looking Airborne Radars (SLAR) as part of the operational ice reconnaissance activities of AES, and from ship observations (visual and 37 GHz H and V) of brightness temperatures in Baffin Bay and East Greenland Seas, respectively.

The SSM/I ice algorithm developed by Hughes Aircraft Company and coded to run operationally at the Fleet Numerical Oceanography Cen-ter and the Air Force Global Weather Center, currently employs only the 37 GHz vertically and horizontally polarized channels. Preliminary results indicate that the algorithm provides ice edge, ice concentration and ice type (age) that agree reasonably well with surface observations. Due to restrictions imposed on the creation of the Hughes algorithm in the late seventies and the scientific advances since that time efforts are underway to improve the current algorithm using the 19.35 GHz channels with the 37 GHz channels in a AES/PHD algorithm.

# SSM/I WIND SPEED VALIDATION

John C. Wilkerson
NOAA/NESDIS
Washington, D.C.


Mark A. Goodberlet
Calvin T. Swift
Kuo Hua Hsush
University of Massachusetts
Amherst, Massachusetts

## Abstract

The accuracy of ocean surface wind speed from the Special Sensor Microwave Imager (SSM/I), launched in June 1987, is assessed by comparing SSM/I-derived winds with coincident wind speeds measured from moored ocean buoys operated by the National Data Buoy Center, NOAA.  The SSM/I environmental extraction (D-matrix) algorithm, developed by Hughes Aircraft Company, retrieves wind speed by latitude/climate zones using brightness temperatures at 19, 22 and 37 GHz as independent variables in a series of 11 linear regression equations.

Evaluation of performance is presented for 6 of these equations representing summer and fall conditions from the tropics to the arctic. Where the operational algorithm fails to retrieve winds to the accuracy goal of 2.0 m/s RMS, new sets of coeffects for the equations are derived from independent data to remove the constant and scale biases and bring the measurement within specification.

Case studies of tropical storms over the Pacific Ocean reveal the limits of sensor capability to recover winds in the presence of clouds, light rain and high gradient zones.  Global maps of SSM/I-derived wind speeds are analyzed over 7-day periods to demonstrate self-consistency of the data and to show regional and seasonal characteristics of the ocean wind field.  Histograms of SSM/I-derived wind speeds are compared to typical distributions of global wind observations for various latitude bands and seasons to reveal the quality and consistency of the SSM/I global data set.

F1-6
1600

## SIMULATED AND ACTUAL SAR IMAGES: A COMPARISON

Robert O. Harger and Can E. Korman

Electrical Engineering Department

University of Maryland

College Park, MD 20742

The synthetic aperture radar (SAR) images obtained with the Jet Propulsion Laboratory's L-band system in the TOWARD oceanographic experiment are compared with images generated by a simulation program implementing a SAR ocean imaging model based on two-scale hydrodynamic and electromagnetic scattering approximate models. The primary means of comparison here is an estimate of the best focus parameter than uses a sub-image cross-correlation technique.

The focus parameter estimates for the actual and simulated images both show (i) a reversal in sign with reversal in dominant long wave direction relative to the SAR direction, (ii) a magnitude increase with an increase in magnitude of the angle between the dominant long wave and SAR axes, and (iii) an independence of the altitude and also the range-to-velocity ratio. These behaviors are in agreement with a related analytical prediction. All equivalent velocity estimates are of the order of the dominant long wave phase velocity, normalized by the SAR vehicle velocity. The comparisons agree well qualitatively though there are some quantitative differences.

Experimental observations over about a decade may indicate that the two-scale, or WKB, hydrodynamic model underestimates the strength of the interaction between the long and short waves. It was found that an increase in this strength by about an order of magnitude rendered much better agreement in the images and their estimated spectral densities of the simulated and actual SAR images.

F1-7      ANTENNA PATTERNS FROM A CROSS ANTENNA
1620      Andrew S. Milman
          Radar Science Laboratory
          Advanced Concepts Division
          Environmental Research Institute of Michigan
          Ann Arbor, MI 48107

Microwave radiometric imaging of the earth from space will provide important meteorological information about water in all of its forms: liquid water, water vapor, and ice.  Microwave images can provide information about soil moisture and sea surface temperature, for example, in the presence of clouds and the absence of sunlight.  In order to get high spatial resolution (1 to 5 km) at the low frequencies (1.4 to 18 GHz) needed for these measurements, an antenna is needed with an aperture of 20 m or more.  This requirement can only be met with sparse antenna arrays.

Of the possible sparse array radiometric antennas, the most promising seems to be the cross antenna; it is two linear arrays placed at right angles to each other.  Because there are two continuous arrays of antenna elements, beamforming techniques can be used to synthesize a beam of size $\lambda / D$, where $\lambda$ is the wavelength and $D$ the length of one arm of the cross, thus allowing the use of very wide rf bandwidths and therefore good radiometric sensitivity.

With any array antenna, there is the worry that there might be severe problems with side lobes.  We can show, however, that

1) The antenna pattern can be modified either by processing the image from the radiometer; or by

2) Weighting the signals from the different antenna elements (i.e., tapering the array).

These two processes will yield equivalent results.  We can also show that any antenna pattern we want can be synthesized for the cross antenna, subject only to the limitation that an aperture of finite size imposes.
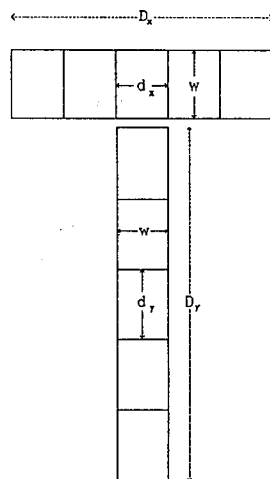
# SEA-BED PROPAGATION OF ELECTROMAGNETIC FIELDS FROM HARMONIC DIPOLE SOURCES LOCATED ON THE SEA FLOOR

A.C.Fraser-Smith[1], A.S.Inan[2], O.G.Villard, Jr.[1]

[1] STAR Laboratory
Stanford University
Stanford, California 94305

[2] Science and Engineering Research Center
Bilkent University
P.O.B. 8, 06572 Maltepe, Ankara, Turkey

Electromagnetic fields generated by vertical and horizontal, electric and magnetic dipoles located along the sea/sea-bed interface are considered. The interface is assumed to be a plane boundary separating two semi-infinite conducting media representing the sea and the material comprising the sea bed. All the components of the electric and magnetic fields derived previously for harmonically-varying current dipole sources are numerically evaluated and compared with those that would be produced under the same conditions in sea water of infinite extent. It is found that (1) the fields can propagate to longer distances along the sea floor because of the lower sea-bed conductivities, and (2) new field components are produced as a result of the presence of the sea/sea-bed interface. Some of these new components are larger at longer distances than the other field components; they are also more sensitive to the conductivity of the sea bed at low frequencies. The results could have applications in undersea communication and geophysical prospecting.

G3-1      MEASUREMENT OF ELF FROM MODULATION OF THE POLAR
1400      ELECTROJET FROM THE HIPAS FACILITY NEAR FAIRBANKS,
          ALASKA
          A. J. Ferraro and H. S. Lee
          Communications and Space Sciences Laboratory
          Department of Electrical Engineering
          University Park, PA  16802
          J. V. Olson
          Geophysical Institute
          University of Alaska at Fairbanks
          Fairbanks, Alaska  99775-0800

     ELF and VLF electromagnetic waves were generated from
modulation of the polar electrojet in the frequency range of
200 Hz to 5000 Hz using the HIPAS heater facility near
Fairbanks, Alaska.   The HIPAS (High Power Auroral Stimulation)
facility is operated by UCLA (Dr. A. Wong, Director) and
during the period of June 10-25, 1987 extensive measurements
were made at ELF and VLF for the first time using that
facility.   During strong electrojet conditions, locally
detected magnetic field strengths up to $6 \times 10^{-9}$ Gauss were
obtained while during quieter current conditions, $2 \times 10^{-10}$
Gauss were obtained.   This compared with $1.5 \times 10^{-11}$ Gauss
measured in 1981 by Ferraro and Lee due to modulation of the
dynamo current system near the Arecibo Observatory in Puerto
Rico.

     The results of ELF frequency stepping, polarization and
beam swinging experiments will be described.

G3-2    HIGH LATITUDE D-REGION ELECTRON DENSITIES ESTIMATED
1420    FROM STEPPED FREQUENCY ELF GENERATED FROM THE
        MODULATED POLAR ELECTROJET

A. J. Ferraro
Communications and Space Sciences Laboratory
Department of Electrical Engineering
University Park, PA  16802

The HIPAS (High Power Auroral Stimulation) heater
facility near Fairbanks, Alaska was used for the first time in
June 1987 to generate and measure ELF/VLF from modulation of
the polar electrojet.  ELF frequency stepping in the range of
200 Hz to 5000 Hz was performed several times with good
signal-to-noise ratios.  This paper explores the potential of
using such data as a means of estimating D-region electron
densities.  Since magnitude and phase can be scanned versus
frequency in a few minutes, such D-region sounder data can be
interpreted with full wave solutions to estimate a model
D-region for the electron densities.  A sweep frequency
polarimeter will be described for performing such experiments.

G3-3    ILLUMINATION OF IONOSPHERIC IRREGULARITIES
1440    WITH HIGH-POWER RADIO WAVES

Paul A. Bernhardt
Naval Research Laboratory
Washington, DC 20375-5000

Lewis M. Duncan
Clemson University
Clemson, SC 29634

Craig A. Tepley
Arecibo Observatory
Arecibo, PR 00613

New observations of plasma structure were made during
the January-February 1987 heating campaign at Arecibo, Puerto
Rico. The airglow excited by the 400 KW HF transmitter was
recorded with an intensified charge-coupled-device (CCD)
camera filtered at the red-line (630.0 nm) of atomic oxygen.
Images of the airglow show 1) the radiation pattern of the
transmitting antenna, 2) natural field-aligned
irregularities, and 3) heater induced cavities. The
irregularities drift with the $\underset{\sim}{E}$ x $\underset{\sim}{B}$ velocity of the plasma.
If the relative motion between the neutrals and plasma is
large, irregularities or cavities steepen due to the E x B
gradient drift instability.

G3-4
1500

# LARGE F-REGION ELECTRON-TEMPERATURE ENHANCEMENTS GENERATED BY HIGH-POWER HF RADIO WAVES

F.T. Djuth[1], A.L. Newman[1], B. Thidé[2], H.M. Ierkic[3], M.P. Sulzer[3], H.C. Carlson[4], G.P. Mantas[5]

[1]Space Sciences Laboratory, The Aerospace
   Corporation, El Segundo, CA   90245
[2]Uppsala Ionospheric Observatory,
   S-755 90, Uppsala, Sweden
[3]Arecibo Observatory, P.O. Box 995,
   Arecibo, PR   00613
[4]Air Force Geophysics Laboratory, Hanscom
   Air Force Base, MA   01731
[5]University of Patras, Greece

During recent experiments conducted at Arecibo, Puerto Rico, large (1000–2000 K) enhancements in electron temperature have been observed when high-power radio waves reflect near the nighttime F-region peak.  The electron temperature enhancements are accompanied by significant (50–300 K) increases in ion temperature, large (10–15%) reductions in electron density, and strong HF-induced spread F.  To determine the cause of the large HF-induced temperature enhancements, we performed a theoretical study which utilized an F-region thermal response model described by (G. P. Mantas et al., J. Geophys. Res., 86, 561–574, 1981).  The results indicate that low collisional cooling rates combined with strong thermal conduction along geomagnetic field lines play a key role in elevating F-region temperatures under current nighttime observing conditions at Arecibo.  The observed temperature enhancements are attributable to low electron densities at the F-region peak.  Because the induced temperature perturbations are so large, these experiments allow one to directly measure atmospheric cross sections and reaction rates that are difficult to determine by other techniques.

G3-5       IONOSPHERIC MODIFICATIONS DUE TO LIGHTNING INDUCED
1540       ELECTROMAGNETIC WAVES

C.P. Liao, K.M. Groves, D.R.Rivas, M.C. Lee
Massachusetts Institute of Technology
Cambridge, Massachusetts 02139
S.P. Kuo
Polytechnic University
Farmingdale, New York 11735

It is generally believed that lightnings can produce sig-
nificant ionospheric effects. For example, lightning induced
atmospheric gravity waves have been suggested to trigger the
equatorial spread F. Enhanced radar eches were constantly
recorded at the equator during lightning storms by the Jicamar-
ca radar operated at the frequency of 50 MHz. These radar
echoes were detected by the radar whose beam angle is 90  with
respect to the geomagnetic field in the ionospheric F region.
They were seen to have fast rise time and decay time, indicating
the excitation of short-lived meter-scale ionospheric irregula-
rities. This phenomenon was termed " explosive spread F " first
by Woodman and LaHoz (1976). Close correlation between the
occurrence of lightning storms and the observation of explosive
spread F was further confirmed by observations made by Woodman
(1984) and LaHoz (1984) independently. We examine the interac-
tions of lightning induced VLF waves with the ionospheric
plasmas as a potential mechanism generating the short-lived
meter-scale ionospheric irregularities. The process under
consideration involves a parametric instability that can con-
currently excite lower hybrid wave modes. The predicted plasma
wave characteristics will be compared with observations and
other mechanisms will be commented.

G3-6     RADIO WAVE SCATTERING FROM ARTIFICIAL PLASMA LAYERS
1600     M.C. Lee, D. Thurairatnam, E.R. Williams
         Massachusetts Institute of Technology
         Cambridge, Massachusetts 02139

Conceptualized plasma layers generated by high power radio waves in the atmosphere have been investigated theoretically by A.V. Gurevich and coworkers with intention to extend the capability of ionospheric radio communications. The required power is very high and not achievable with any existing radar facilities. However, laboratory experiments have been conducted for corroborating the concepts and the predicted plasma characteristics. We note that the plasma layers generated in the chamber experiments often have rough surfaces. It is also expected that the conceptualized plasma layers created in the atmosphere by radio waves cannot have smooth surfaces. In this paper we investigate the effect of roughness on the radio wave scattering from the artificial plasma layers. This problem has been analyzed theoretically. The results shall be compared with our recent radar observations of lightning induced plasmas. The theoretically expected wavelength dependence of power reflectivity is clearly indicated in our radar experiments though the lightning induced plasmas may have very different shapes in comparison with the electromagnetic wave produced plasmas.

# STUDY OF IONIZATION OF THE LOWER IONOSPHERE
# BY TWO CROSSED RADIO PULSES
# (LABORATORY SIMULATION)

Y.S. Zhang and S.P. Kuo
Polytechnic University, Route 110, Farmingdale, N.Y. 11735

Experiments have been set up to produce a plasma in a large chamber which simulate the ionization process of the lower ionosphere by strong radio pulses. The chamber is a 2' x 2' x 2' cube of plexiglass that is filled with argon gas to a pressure range from 50m torr. to 1.8 torr. Microwave beams are fed into the cube by two s-band microwave horns placed at right angles to adjacent sides. The scheme of using two crossed high power microwave beams is employed to generate an ionized layer in the center of the cube where the beams intersect. This approach enables us to simulate how to scan the ionized layer in the atmosphere, and also to minimize beam energy loss before reaching the designated region for ionization.

The microwave power is generated by a single magnetron tube (OKH1448) driven by a soft tube modulator. The magnetron produces 1 MW peak output power at a frequency of 3.59 to 3.7 GHz. The modulator uses a pulse forming network (PFN) having a pulse width of 1.1 microseconds and a repetition rate of 60 cycles.

The detailed arrangement of the experimental set up will be described. Also, plasma has already been produced, and the experimental results which clearly demonstrate the success of this scheme will be presented.

G3-8
1640

# IONOSPHERIC MODIFICATION OVER ARECIBO DURING THE SPACELAB 2 MISSION

P.A. Bernhardt
Naval Research Laboratory
Washington, DC 20375-5000

C.A. Tepley and M.P. Sulzer
Arecibo Observatory
Arecibo, PR 00613

W.E. Swartz and M.C. Kelley
Cornell University
Ithaca, NY 14853

On July 30, 1985, the Orbital Maneuvering Subsystem (OMS) of the Space Shuttle deposited 279 kg of exhaust near the peak of the night-time F-layer. The Arecibo incoherent scatter radar recorded the resulting disturbance in the plasma densities. The expanding exhaust vapors produced a plasma hole with density enhancements on the top and bottom sides. The enhancement disappeared after 30 seconds. The depletion lasted for over 300 seconds when it was convected through the bottomside F-layer. The long-lasting hole was produced by chemical reactions between the neutral exhaust and the ambient plasma. Excited states of atomic oxygen were produced during the chemical process. Measurements by photometers and intensified imagers showed that most of the ionospheric modification occurred 80 km downstream from the center of the engine burn. This was the distance required for the supersonic exhaust to come to rest in the rarefied environment of the upper atmosphere. Revised theoretical models are required to explain the results from the Spacelab 2 experiment.

H1-1       DIRECTIONAL INFORMATION IN DOPPLER-
1400       BROADENED VLF WAVE SPECTRA

H.G. James
Communications Research Centre,
P.O. Box 11490, Station "H",
Ottawa, Ontario K2H 8S2
Canada

The spectrum of Doppler-broadened signals received on ionospheric spacecraft from VLF transmitters on the ground has been found to depend on the direction $L$ of the receiving dipole antenna. The received spectrum is interpreted as corresponding to a distribution of quasi-electrostatic waves whose wave vectors lie close to the whistler-mode resonance cone. In typical observations from the ISIS-II VLF receiver, the carrier frequencies lie between 10 and 20 kHz, and the plasma and gyrofrequencies are much greater than these transmitter frequencies. The result is that the resonance cone lies within a few degrees of the perpendicular to the terrestrial magnetic field $B_0$. When, as a consequence of satellite cartwheel spin, the angle $(L, B_0)$ becomes small, the dipole discriminates against waves whose $E$-vectors are in the spin plane, near the resonance cone and therefore nearly perpendicular to the dipole.

At moderately high latitudes where broadening is observed, the magnetic field direction is roughly vertical. Because the spacecraft velocity is horizontal, the discrimination against $E$-vectors in the spin plane on one side of the resonance cone is a discrimination against Doppler components with a particular sign. As $(L, B_0)$ passes through its minimum, the received spectrum evolves from one with enhanced positive Doppler components to one with enhanced negative Doppler components, or vice versa. The result is a characteristic downturn or upturn in the frequency-time signature of a VLF tone at constant carrier frequency. The angle between the satellite-spin and orbit-normal vectors determines uniquely whether an upturn or downturn obtains. This holds for both northbound and southbound passes in both hemispheres.

Theoretical calculations of the temporal variation of the Doppler spectrum based on the quasi-electrostatic postulate agree with observations from ISIS II. In certain cases, better fits to the observations are obtained with $k$ vectors confined to a narrow range of azimuths about $B_0$ rather than distributed evenly throughout all azimuths.

H1-2
1420

ULF/ELF/VLF PROPAGATION FROM A SPACEBORNE
ELECTRODYNAMIC TETHER TO A SATELLITE-BORNE
RECEIVING TERMINAL
Mario D.Grossi
Harvard-Smithsonian Center For Astrophysics
Cambridge, Massachusetts 02138

An electrodynamic tether, such as the forthcoming Shuttle-
borne TSS-1, will generate e.m. waves at ULF, ELF , VLF, and possib-
ly in other bands. These waves are expected to leak to the Earth
surface. However, because the losses incurred in crossing the iono-
sphere/atmosphere boundary are substantial ( at ULF/ELF only 1% of
the power  leaks through at night, and only 0.1 % in day time),
experimenting with this propagation path requires a long integration
time, and this precludes the measurement of short-time features of
the e.m. waves.

We are investigating an experimental configuration that will
avoid boundary-crossing, by using a satellite-borne receiver in
Earth orbit. We could therefore keep the integration time very
short, thus detecting rapidly-varying phenomena in the propagation
path. Even more important, we would also maximize the probability of
receiving above noise the e.m. waves radiated by the tether.

In the 16 hours or so that TSS-1 will radiate, a SAN MARCO
satellite ( designed and constructed in Italy by PSN), suitably
instrumented, could be injected in orbit and perform propagation
measurements with path lengths up to several thousands Kilometers,
achieving  various terminal-to-terminal geometries and magneto-
conjugacy  conditions. The instrumentation would consist  of re-
ceivers and magnetic-dipole antennas in three bands : (a) 3 to 30
Hz (ULF);  (b) 30 to 300 Hz (ELF); and (c) 3 to 30 KHz (VLF).

The orbital mechanics problems in performing effectively this
space science mission are several and far from simple. We are help-
ed by the fact that SAN MARCO  has a choice of orbital inclinations
from equatorial to polar, and a reasonably broad height  range. An
important requirement is that we cross at least once the tube of
flux of the geomagnetic line of force where TSS-1 is located and
is radiating. We would also like to explore the effect of L-conju-
gacy on propagation, and to measure path losses across lines and
shells. This experiment would provide a thorough check of propaga-
tion theory for the ULF, ELF and VLF bands in the magneto-ionic
medium of the Earth ionosphere.

The results of this experiment would be of value in assessing
the ability of an electrodynamic tether to function as generator/
radiator of e.m. waves,an assessment that is relevant both from
a scientific and  from an application standpoint.

H1-3   3-DIMENSIONAL IONOSPHERIC RAY TRACING:
1440    AN APPLICATION OF SCIENTIFIC DATA
        VISUALIZATION
        Denis J. Donohue
        Space, Telecommunications and Radioscience Laboratory
        Stanford University
        Stanford, California 94305
        James L. Green
        NASA Goddard Space Flight Center, Code 630.2
        Greenbelt, Maryland 20771

In this talk we describe a fully 3-dimensional computer ray tracing program which has been specially developed for ionospheric propagation studies. The program was initially written by Stan Shawhan at the University of Iowa in the mid-1960's and has been used in investigating propagation and source region characteristics of the earth's auroral kilometric radiation and Jupiter's decametric and kilometric emmisions. The program has now been modified for calculating ray paths of electromagnetic radiation in earth's ionosphere and incorporates several new developments including high resolution display graphics. The recently developed International Reference Ionosphere (IRI) model is used to describe earth's complex ionospheric plasma distribution. The IRI determines the electron density and temperature as well as the composition of 5 species of ions ($H+$, $He+$, $O+$, $NO+$ and $N2+$) at any point in the ionosphere.

For display of the ray path calculations, a powerful graphics package has been developed on a Silicon Graphics IRIS workstation which gives a complete 3-dimensional perspective of the ray paths and magnetic field lines and permits arbitrary rotation and spatial scaling of the image. This technique greatly facilitates the interpretation of complex 3-D ray paths in the ionosphere and will aid in the comparison of the ray path calculations to shuttle and satellite based wave observations and future wave generation experiments.

The talk will include a description of the ray tracing program, corresponding plasma and magnetic field models, and graphic displays. A videotaped demonstration of the IRIS display will also be shown.

G/H1-1        IONOSPHERIC EFFECTS ON TARGET DETECTION BY AN
1540          INTERFERENCE-CLUTTERED MULTI-CHANNEL SYSTEM
              A. K. Gupta
              GTE Government Systems Corp.
              One Research Drive
              Westborough, MA   01581

In this paper, modern detection theory principles are applied
to determine the effects of a propagation channel, such as Ionosphere,
on the fixed target detection in an interference environment by a
multi-channel system (such as diversity, phased-array antenna,
multibeam antenna system, etc.).  The ionosphere is assumed to
transform a deterministic signal to a Gaussian signal with Rayleigh
amplitude and random phase.  The interference in this paper is modelled
as correlated white noise.  The problem therefore reduces to that of
detection of a known vector signal in correlated vector noise and to
that detection of a Gaussian signal in correlated vector noise.

The determination of Ionosphere effects involves the development
of optimal receivers and the analysis of probability of detection for
a deterministic channel and for a random channel in an interference
environment.  The difference in optimal performance (by employing
corresponding optimal receivers) may be attributed to Ionospheric
effects.  Various forms of optimal receivers are discussed in this
paper, some of which may be easily adapted in real-time.  The formulas
for performance analysis are also useful in determining the number
of channels required to counteract the ionospheric effects in the
interference environment.

The approach considered in this paper can be generalized to the
problems involving WSSUS ionospheric propagation channel with
multipath and/or doppler spread, and phase-only ionospheric effects
in various interference environments.

G/H1-2
1600

# Propagation Effects on Space-based Radar

Suman Ganguly
Center for Remote Sensing
8200 Greensboro Drive, Suite 503
McLean, VA 22102

This paper describes the results of a preliminary study regarding the effects of ionosphere and atmosphere on the design of a space-based radar. Manifestation of primary concern is the severe random fluctuations of electron densities in the E and F regions of the ionosphere. These irregularities can produce scintillations in amplitude and phase of a signal propagating through the medium; they also produce radar clutter for signals that are scattered from these irregularities. Several other issues that would be of concern for the design of a SBR are addressed. We describe these relevant processes and provide recommendations for understanding them. It is stressed that the design of the SBR is intimately connected with these propagation issues, and theses issues must be an integral part of the design of the SBR architecture.

J3-1      IMAGE RECONSTRUCTION FROM COHERENCE: J.L. Yen, Univ. of Toronto,
1400      Toronto, Ontario M4S 1A7 Canada

J3-2      NOISE IN IMAGES OF VERY BRIGHT OBJECTS: R.D. Ekers, National Radio
1420      Astronomy Observatory, Socorro, NM 87801

J3-3      REDUCTION OF SCANNING NOISE IN RASTER SCANNED DATA
1440      D. T. Emerson
          National Radio Astronomy Observatory
          949 North Cherry Avenue
          Tucson, AZ 85721

In many branches of science a 2-dimensional image of an object under study is obtained by raster-scanning a sensor across the region of interest. In general, because of unavoidable instrumental offsets and drifts, the baselevel of each individual linear scan has to be corrected. The most commonly used technique is to subtract a linear or higher order baseline derived from regions of each linear scan believed to be free from emission.

This suffers from errors resulting from:
(1)  the necessary assumption of emission-free regions. This requires prior knowledge of the object, or that an unreasonably large area be sampled;
(2)  random noise levels which may cause errors in the derivation of baselines, and
(3)  the danger of distorting real features by an unwise choice of zero regions or by the use of higher order baseline fits.

This paper describes an alternative derivation of baseline corrections, making use of two or more data sets taken with different scanning angles. The data are treated in the Fourier domain, providing a unique, analytic, non-iterative and computationally efficient solution to the problem.

J3-4
1500

A COMPARISON BETWEEN FULLY FILLED APERTURE AND NON-REDUNDANT MASK IMAGING: T. Nakajima, California Institute of Technology, Pasadena, CA 91125

J3-5     SELF-CORRECTION OF TELESCOPE SURFACE ERRORS
1520     USING A CORRELATING FOCAL PLANE ARRAY

P. J. Napier and T. J. Cornwell
National Radio Astronomy Observatory
P.O. Box O
Socorro, New Mexico  87801

In recent years the technique of "self-calibration" has dramatically improved the quality of radio images obtained with synthesis telescopes by removing the effects of atmospheric phase fluctuations and other aberrations.  In this paper we point out that self-calibration can be extended to remove the effects of various aberrations, including reflector profile errors, from images obtained in the focal plane of large single reflector telescopes.  Focal plane self calibration requires that the spatial coherence function of the image be measured with a focal plane array attached to a correlator.  Some of the practical difficulties to be solved in applying the technique include satisfying the focal plane spatial sampling theorem and building sufficiently large correlators.

J3-6    VLA OBSERVATIONS OF SPECKLES IN INTER-PLANETARY
1540    SCINTILLATION
        T. J. Cornwell, K. Anantharamaiah[1] and R. Narayan[2]
        1 National Radio Astronomy Observatory
          P. O. Box 0
          Socorro, NM 87801
        2 Steward Observatory
          Tucson, AZ 85721

Historically, the scintillation patterns due to scatter-
ing in the solar wind have been studied via the fluctuations
in total power received either at a single point as a function
of time, or at many points simultaneously.  However, extra
information is available from measurements of fluctuations in
the coherence function measured by an interferometric array.
Snapshots of sufficiently short integration (less than 10-50
msec) should freeze the scintillation pattern on the ground.
An image made by an interferometric array in that time will
therefore show "speckles" similar to those seen in optical
imaging through the Earth's atmosphere.  The radiation from
the different speckles must be coherent, and so the usual
theory of interferometric imaging of incoherent objects does
not apply.  However, in the special case of an unresolved
background scattered source, the effect of the coherence is
particularly simple: for an array of N elements there are no
longer $N(N-1)/2$ independent numbers per integration, but
rather only N.  These numbers may be thought of as the (com-
plex) gain introduced by a scintillation pattern lying over
the array.  The speckles must therefore be removable by
self-calibration of the observed snapshot coherences.  Fur-
thermore, given a sufficient number of telescopes, the scat-
tering screen can be visualized directly by appropriate
transformation of the array element complex gains.

We have performed this experiment using the VLA to
observe the radio source 3C279 at elongations of a few degrees
from the Sun.  We can confirm the existence of "speckles," and
their removal by self-calibration.  We will show examples of
both, and we will discuss the possible applications.

J3-7    WIDE FIELD IMAGING: L. Baath, Onsala Space Observatory, Onsala,
1600    Sweden, and California Institute of Technology, Pasadena, CA 91125

J3-8     TIME SERIES ANALYSIS WITH **CLEAN**
1620     David H. Roberts
         Astronomy Department 105-24
         California Institute of Technology
         Pasadena, CA 91125 USA, and
         Physics Department*
         Brandeis University
         Waltham, MA 02254 USA

We discuss a method of time series spectral analysis which is especially useful for unequally-spaced data. Based on a complex, one-dimensional version of the **CLEAN** deconvolution algorithm widely used in two-dimensional image reconstruction, this technique provides a simple way to understand and remove the artifacts introduced by missing data. We describe the method, give several examples, and point out various analogies with the conventional use of **CLEAN**.

This work has been done in collaboration with J. W. Dreher and J. Lehár of MIT.

*Permanent address.

J3-9       KALMAN FILTERING VISIBILITY AMPLITUDE OF HAT
1640       CREEK MILLIMETER-WAVELENGTH INTERFEROMETER DATA

Yong-Seon Koh, Yi Zheng, and John P. Basart
Department of Electrical and Computer Engineering
Iowa State University, Ames, IA  50011

ARIMA modeling and Kalman filtering techniques were
applied to extended sources observed with the Hat Creek
Millimeter Interferometer. Atmospheric fluctuations
frequently prevent the dynamic range in the maps from
exceeding 100. The dominating disturbance to the Hat Creek
System is to the visibility amplitudes. Methods such as
self-calibration cannot be used for this data since the data
are recorded on only three baselines simultaneously. An
alternative to self-calibration is to do model-based
filtering of the signal on each baseline separately. Then
models for the signal (source), the system noise, and the
atmosphere must be determined. These can be complicated to
find for extended sources. Models for the source are
obtained from the CLEAN components after they are transformed
to the spatial frequency domain. The difference between the
CLEAN component time series and the data time series will be
dominated by atmospheric noise. Applying time series
analysis to this difference series, we get a model for the
atmosphere. Finally, receiver system is modeled as white
noise. After putting all three models into a state-space
formalism, we filter the original data series. The results
from applying our procedure to simulated data and to real
data from the Hat Creek Interferometer will be discussed.

J3-10     KALMAN FILTERING VLA PHASE DATA WITH SOURCE
1700      MODELING
          Patrick L. Anderson, Yi Zheng, and John P. Basart
          Department of Electrical and Computer Engineering
          Iowa State University
          Ames, IA  50011

We have previously applied the Kalman filter to VLA phase data in both the spatial and spatial-frequency domains. Filtering in the frequency domain included phase models for the atmosphere, system, and a point source. This work has been continued to include modeling and filtering an extended source in the uv plane which is reported here. We model the source, atmosphere, and system as ARIMA (autoregressive integrated moving-average) processes. ARIMA processes are known to provide good short-term predictions for time-series data. The phase model is obtained for an extended source using the CLEAN components which are transformed from the spatial domain to the frequency domain in a baseline-time series. This time series is then modeled as an ARIMA process. The source phase model is subtracted from the measured phase to form residual phases. The model of the atmosphere is given by describing the residuals of the source model and the measured phase as an ARIMA process. ARIMA models of the source, atmosphere, and system are written in state-space form for application of the Kalman filter. These models provide the covariance matrices and state-transition matrices used in the Kalman filter. The phase is modeled and filtered baseline-by-baseline.

Results of the Kalman filter and self-calibration will be compared using simulations and actual data from the VLA. It is expected that the Kalman filter can be used in situations where self-calibration does not sufficiently reduce the phase noise.

Session A-4   0855-Thurs.   CR1-40
MEASUREMENTS OF THE PROPERTIES OF MATERIALS
Chairman: Sedki M. Riad, Dept. of Electrical Engineering, Virginia
Polytechnic Institute and State University, Blacksburg, VA 24061

A4-1
0900

# DIELECTRIC SPECTROSCOPY USING A WIDEBAND DIELECTRIC FILLED CAVITY

Mohammad A. Saed and Sedki M. Riad
Department of Electrical Engineering
Virginia Polytechnic Institute and State University
Blacksburg, Virginia 24061

This paper concerns the development of a Wideband Dielectric Filled Cavity (WDFC) to be used for characterizing dielectric materials over the HF to microwave frequency region. The cavity is completely filled with the dielectric material to be characterized.

Two configurations are presented:

1. The WDFC is adapted to the end of a transmission line. The measured reflection coefficient is used to compute the complex permittivity.

2. The WDFC is placed between two transmission lines. The complex permittivity is computed from the reflection coefficient or the transmission coefficient information. However, both the complex permittivity and the complex permeability can be computed if a combined reflection - transmission measurement is performed.

The WDFC technique has several advantages over other methods which require the sample to be inserted in an air line. In those methods, the sample has to be precisely cut to fit in between the inner and outer conductors causing two problems to occur. The first problem is that samples with rough edges will result in air gaps between the sample and the conductor surfaces introducing significant errors. The second problem is the possible damage of the air line's conductor surfaces because of the sample's rough edges. Such problems are minimized in the proposed structure.

This paper presents the concept of the proposed technique. Results of computer simulation as well as experiments involving the measurement, in the time domain, of the complex permittivity and the complex permeability of some materials are also presented.

A4-2   TIME DOMAIN MEASUREMENT OF ANECHOIC
0920    CHAMBER REFLECTIONS

E. N. Clouston, Dr S. Evans,
Cambridge University Engineering Department,
Trumpington St. Cambridge CB2 1PZ  U.K.
Dr P. A. Langsford, Marconi Research Ltd. U.K.

Time domain techniques have been developed and demon-
strated for the measurement of anechoic chamber reflect-
ivity, and for the accurate location of the sources of
reflections.  They allow detailed study of any particu-
lar area of the absorber on the chamber walls.

Broadband reflectivity information is available from
a single measurement of the pulse transmitted directly
between two antennas and the ensuing reflections from
the chamber walls.  In a chamber large enough for the
reflections to be delayed by more than 10ns, the trailing
edge of the direct signal had dropped enough for reflect-
ivity levels up to 50dB down to be measured above 1GHz or
43dB down above 500MHz.  The noise dominated the result
above 2GHz, but this can be extended to 4GHz by use of an
amplifier in front of the sampling oscilloscope.

Frequency domain techniques (J. Appel-Hansen, IEEE
Trans. AP-21(4), pp.490-498, 1973) rely on careful scan-
ning to detect the worst interference between different
reflections.  The time domain approach can separate them
from each other, so the reflectivity can be measured
without moving the antennas at all; variation with ant-
enna position can then be investigated.

The path length is available from the delay of any
reflection, but the direction can only be calculated from
the change in delay when one of the antennas is moved.
This can be done for any reflection which can be identi-
fied in both records, and high-pass digital filtering can
help.  But to be sure of separating out the reflections
from a particular area, the antennas must be moved close
to it, and this is limited by the reflections overlapping
the trailing edge of the direct signal.  This was solved
by rigidly fixing two antennas 2m apart on a wooden beam,
and measuring the direct signal between them.  This was
then subtracted from subsequent records, to leave the
reflections, including those which had been superimposed
on the direct signal.

Although frequency domain techniques offer a better
dynamic range, the time domain approach offers a simple
reflectivity measurement, which gives a safe overestimate
from a single measurement.  It is also far more versatile
in locating the sources of reflections.

A4-3    LOSS CALCULATION IN SYMMETRICALLY SPHERICAL WITH CIRCULAR
0940 APERTURE UNSTABLE OPTICAL RESONATORS USING DIFFERENT TECHNIQUES

M. H. RAHNAVARD, J. ZARE MOODI
Electrical Engineering  Department
Shiraz University, Shiraz, Iran
Telephone Number: Iran, Shiraz  34064-2712

Unstable Optical resonator is used in medium and high power laser. In stable resonator when Fresen number is greater than 0.5 all of the energy is not absorbed by 1st mode but energy is absorbed in higher order modes. In unstable resonator with proper gain it is possible to have mode with lowest power loss and this mode will absorbe most of the energy from the laser material and it is possible to have optical resonator with smaller length. For this reason power loss calculation is important in unstable optical resonators.

At first Fox and Li calculated power loss in infinite strip cylinderical and spherical resonators with circular aperature for Fresnel number greater than 10 by scalar theory of diffraction using iterative method (Fox, A. G. and Li, T. H. 1964. Quantum Electronic I11, 8, 1262). By using geometrical optics Siegman calculated power loss in optical resonators for large Fresnel number (Siegman, A. E. 1965. Proc. IEEE. 53, 277). Sanderson and Striefer calculated power loss by Gaussion Quadrature and Cornu spiral methods (Sanderson, R. L., and Streifer, W. 1969. Appl. Opt. 8, 2129).  In the first method the integral is converted to a matrix. Using QR-method eigen value and eigen vector of the matrix is evaluated.  Eigen vectors are electric field modes and power loss in each mode is equal to one minus absolute value of the eigen value of that mode. Siegman and Miller found eigen values for spherical resonator with circular aperture for Fresnel number greater than 13 using Prony's method (Siegman, A. E. and Miller, H. Y. 1970. Appl. Opt. 9, 2729). Santana and Felson calculated eigen value using waveguide theory (Santana, C. and Felsen, L. B. 1976. Appl. Opt. 9, 1470).

As Fresnel number gets larger resulting series from the integral has more elements.  The number of elements in the series is usually between 6 to 10 times the Fresnel number (Siegman, A. E. and Miller, H. Y. 1970. Appl. Opt. 9, 2729). So power loss evaluation in optical resonators with Fresnel number greater than 10 takes a long time. Except Santana and Felson (Santana, C. and Felsen, L. B. 1976. Appl. Opt. 9, 1470) all of the works which is done based on scalar theory of diffraction. In this paper physical optics in exact form and with Fresnel approximation, scalar theory of diffraction without approximation, geometrical theory of diffraction and physical theory of diffraction are used in analyzing and power loss calculation of symmetrically spherical with circular apperture unstable resonators.

A4-4    IMPEDANCE EFFECTS ON ELECTROMAGNETIC SUSCEPTIBILITY*
1020    R. J. King and W. C. Ng
        Lawrence Livermore National Laboratory
        Livermore, California  94550

The in situ measurement of transient or cw voltage,
current, or energy coupled to the input of a susceptible elec-
tronic subsystem at frequencies above a few tens of MHz cannot
be measured without disturbing the coupling cable, wire, etc.
Using state-of-the-art frequency domain instrumentation and
signal processing techniques, means for calculating these
electrical quantities is described.

From cw measurements of the self-impedance ($Z_A$) and
received voltage across 50 ohms at the coupling terminals of a
generic test object, a Thevenin equivalent circuit model is
derived.  Using this model, the electrical parameters are com-
puted for several interesting load impedances.  Of interest
are two worst cases where the load impedance is the complex
conjugate of $Z_A$ and the conjugate pure reactance of $Z_A$.
Another case of particular interest is where the load impe-
dance is that of an electronic unit representing that of a
typical subsystem designed for operation at much lower fre-
quencies.  These three cases are compared with the voltage,
current, and energy at a 50-ohm load.  It is concluded that
the electrical quantities for the two conjugate cases can be
one or two orders of magnitude larger than that for the 50-ohm
case as might be expected.  However, it is somewhat surprising
that the smoothed electrical quantities at the input of the
electronic units tested are comparable to those for the 50-ohm
case.  The spectral energy density responses are generally
within a factor of two (± 3 dB), but may be as large as a
factor of three (± 5 dB) over narrow frequency bands.

Examples are given showing both spectral and temporal
electrical quantities at the electronic system input for
assumed electromagnetic transients incident on the exterior of
the coupling system.

A4-5
1040
NEAR-FIELD STATEMENT OF MONOSTATIC-BISTATIC THEOREM
David G. Falconer, Ph.D.
Remote Measurements Laboratory
SRI International
333 Ravenswood Avenue
Menlo Park, CA 94025

Over the years we have developed several enhancements and
extensions of Kell's monostatic-bistatic theorem (MBT).  This
approximation (*Proc. IEEE*, v. 53, n. 8, p. 983, August 1965),
which we use regularly in our anechoic-chamber measurements of
radar cross section (RCS), states that one can estimate a tar-
get's bistatic RCS pattern at the wavenumber k by measuring
its monostatic one at the bisecting angle at the reduced wave-
number $k' = k \cos(\theta/2)$, where $\theta$ is the bistatic angle.  We
have extended Kell's version of the MBT by introducing a phase
adjustment, $\exp[i2(k - k')R]$, that allows one to estimate the
phase (as well as the RCS) of the bistatic scattering ampli-
tude.  Similarly, we have developed an amplitude modification,
$k/k'$, that provides an estimate of the bistatic scattering am-
plitude for extended (rather than point) scatterers.  Finally,
we have derived a new version of the MBT that is suitable for
near-field scattering conditions, i.e., for ranges $R < 2D^2/\lambda$,
where D is the nominal target diameter.  In the near-field
case, it is necessary to measure the monostatic pattern at
both the reduced wavenumber $k'$ and the reduced range $R' = R$
$\cos(\theta/2)$.  The required phase adjustment and amplitude modifi-
cation are similarly changed to $\exp[i2(kR - k'R')]$ and unity,
respectively.

It is often difficult to measure the monostatic RCS pat-
tern at both the reduced wavenumber and reduced range required
under a Kell-type derivation.  Accordingly, we have developed
an alternate form for the near-field MBT that requires no
wavenumber or range reductions during measurement of the mono-
static pattern and no phase adjustments or amplitude modifica-
tions of the recorded data.  This version of the MBT, however,
places a slightly stricter requirement on target geometry,
namely that $\theta < \sqrt{\lambda/H}$, where H is nominal thickness of the
scattering body when viewed at the bisecting angle.

We have validated our work by comparing the above approx-
imations with the RCS and phase patterns predicted by an op-
tically oriented model for a square plate and a modal solution
for a long right circular cylinder.

A4-6
1100

Millimeter Wave Transmitted Power Through
Illuminated Semiconductor Panel
Scanned with Strip of Shadow

M. H. RAHNAVARD, A. HABIBZADEH
Electrical Engineering  Department
Shiraz University, Shiraz, Iran

One of the needs in air traffic is to know the environmental situation under any weather condition. Visble and IR radar will fail in adverse weather because of high attenuation but there are several windows in millimeter wave region with low attenuation in bad weather condition (Weibel, C. H. and Dressel, H. O. 1967, Proc. IEEE, 55, 497). One of the method to convert millimeter wave to visible light is by using illuminated semiconductor Panel. Semiconductor panels are used as image convertors in both transmission and reflection mode of operation (Jacobs, H. et. al. 1967, J. Opt. Soc. 57, 913). In both cases the response of illuminated panel is important. Excess carrier in semiconductor panel under stationary illumination is obtained by Levin et. al. (Levin, B. J. 1968, IEEE letters, 56, 1230, Mavaddat, R. and Levin B. J. 1967, J. of Applied physics, 40, 5324). Using the above result reflection coefficient and attention coefficient for this case is also studied (Mavaddat, R. 1970, IEEE Trans. on Microwave Theory and Techniques, 18, 360, Mavaddat, R., 1971, IEEE Transaction on Microwave theory and Technique, 19, 555), Practically, the response of semiconductor panel to moving illumination is required. Excess carrier in moving spot illuminated semiconductor panels is studied and profiles of excess carrier for moving strip illuminated semiconductor panel vs. different parameters is obtained. (Rahnavard, M. H. et. al., 1975, Journal of Applied physics, 46, 1229). In this paper using the excess carrier results, transmitted power through illuminated semiconductor panels scanned with shadowed strip as a function of scanning velocity, position, thickness of the strip and time is studied and the resultant curves are plotted.

B6-1       MAXWELLIAN AND CAVITY ELECTROMAGNETIC FIELDS
0840             WITHIN CONTINUOUS SOURCES
                    Arthur D. Yaghjian
              Electromagnetics Directorate
              Rome Air Development Center
              Hanscom AFB, MA 01731-5000

The free-space operational definitions of the electric and
magnetic field in terms of the forces on a test charge are in-
applicable, without some modification, within continuous sources
because the definitions require that the test charge be exterior
to the sources producing the measured electric and magnetic
fields.  The free-space definitions can be modified in the
source region by specifying that the test charge be placed
in an infinitesimal free-space cavity formed by removing the
sources within the cavity while maintaining the sources out-
side the cavity.  These cavity-defined electric and magnetic
fields depend, in general, on the geometry of the cavity (i.e.
on its shape, its orientation, and the position of the test
charge within the cavity) even though the size of the cavity
approaches zero.  In other words the cavity-defined electromagnetic
fields within a continuum are not necessarily unique unless the
geometry of the cavity is specified, and do not necessarily
equal the Maxwellian fields, i.e., the unique fields defined
mathematically by Maxwell's equations for continuous sources.

Maxwell, in Articles 395-400 and 604-605 of his treatise,
used the cavity definitions of electric and magnetic fields
within continuous polarized media, related the fields in cavi-
ties of various shapes to the Maxwellian fields, and specified
the "narrow crevasse" cut perpendicular and parallel to the
direction of magnetization as the cavities that should be
used to operationally define the two magnetic field vectors (B
and H, respectively) in the source region.  For these particular
cavities the respective cavity-defined magnetic fields equal
the Maxwellian magnetic fields.  Maxwell studied the subject in
detail only for the magnetic fields within magnetic polarization,
but stated in Article 60 that the electric field within electric
polarization (and also, as we show, the time-harmonic electric
field within volume current) can be treated in the same manner
"to the greatest advantage."

Here, Maxwellian and cavity electromagnetic fields are
derived within a continuous source distribution of volume
current or electric and magnetic polarization densities by
direct, rigorous differentiation of the vector potential.
The derivation, which uses only operations of vector calculus,
reveals naturally the contributions from interior and exterior
source regions.  Results are obtained for static and arbitrarily
time-varying fields as well as for time-harmonic fields.

B6-2    A TRANSVERSE APERTURE-INTEGRAL-EQUATION METHOD
0900    FOR NUMERICAL EVALUATION OF EDGE DIFFRACTION BY
        SEMI-INFINITE STRUCTURES
        L. W. Pearson, McDonnell Douglas Research
        Laboratories, R. A. Whitaker, McDonnell Douglas
        Aerospace Information Services,  P.O. Box 516
        St. Louis, MO 63166

With a few exceptions, analytically tractable canonical prob-
lems for edge diffraction are limited to impenetrable struc-
tures.  Recently Herrmann (I.E.E.E. Trans. Antennas Propa-
gat., AP-35, 53, 1987) suggested an approach that employs
signal processing methods in angular space as a means for
isolating the diffraction at a single edge of an object
comprising penetrable materials.

In this presentation, we propose an alternative formulation
for numerical computation of diffraction at the edge of a
semi-infinite section of a stratified structure.  The strati-
fied structure could comprise a number of layers of material
with different electrical properties and one or more perfect-
ly conducting sheets, the only restriction being predicated
upon whether an analytic Green's function can be determined
for all points in the associated infinite planar structure.
It is believed that the method can be extended to structures
comprising anisotropically conducting sheets, for example in
some fiber composite materials (L. W. Pearson, "Reflection
and Propagation Characteristics of Multiple Layers of Aniso-
tropic Admittance Sheets," National Radio Science Meeting,
Blacksburg, VA, June, 1987).

The problem is formulated as an aperture integral equation in
the infinite-extent plane transverse to the structure and
passing through the edge at which diffraction occurs.  The
aperture field at large distances from the edge can be pre-
dicted asymptotically and subtracted from the total unknown
field so that one solves for a difference unknown that decays
as a function of transverse distance from the edge.  The as-
ymptotic fields affect the excitation vector for the numeri-
cal system and are a function of the angle of incidence, but
these fields may be represented in spectral-domain analytical
forms that may be computed efficiently.

B6-3        SPECTRAL DEFECTS IN THE PARAXIAL
0920        GAUSSIAN BEAM METHOD

I.T. Lu, X.J. Gao and L.B. Felsen
Dept. of Electrical Engineering/Computer Science
Polytechnic University
Route 110, Farmingdale, NY  11735

Discretization in terms of paraxial Gaussian beams, pioneered in seismology (Cerveny, J. Geophys. Res., 58, 44-72, 1985) provides an attractive numerical algorithm for tracking source-excited high frequency wavefields through complicated propagation and scattering environments.  However, the algorithm is flawed by an arbitrariness in the choice of the beam and stacking parameters, and also by spectral deficiencies arising from the paraxial approximation.  These deficiencies have been made evident, and explained from a spectral perspective, in a test problem involving acoustic radiation in a half space separated by a plane interface from an exterior medium with higher propagation velocity (I.T. Lu, L.B. Felsen and Y.Z. Ran, Geophys. J. R. astr. Soc., 89, 915-932, 1987).  From comparison with a reference solution generated by numerical integration of an exact spectral integral, it was shown that retention of full complex spectra removes the deficiencies.  These considerations are now transferred to the electromagnetic case and illustrated by additional numerical examples.  They are also extended to the case of an anisotropic exterior that can support ordinary and extraordinary waves.  Conclusions from these studies permit a critical assessment of the validity of the paraxial Gaussian beam method.

# THREE DIMENSIONAL FIELD EXPANSION IN THE MOST GENERAL ROTATIONALLY SYMMETRIC ANISOTROPIC MEDIUM.

J. Cesar Monzon
Damaskos, Inc.
P. O. Box 469
Concordville, PA 19331

A material region characterized by tensors $\varepsilon$ and $\mu$ and possessing general rotational symmetry is found to be specified by six parameters. A field expansion in spherical coordinates is described for the solution of three dimensional electromagnetic problems. The analysis reveals that the angular dependence is dictated by spherical harmonics whereas the radial functions satisfy a set of coupled second order ODE. A total of eight different radial functions are obtained and described in detail, including asymptotic representations.

The present field expansion is specially useful for material geometries conformal with spherical coordinates such as the one shown in the figure, but can, however, be employed for arbitrary geometries when used in combination with an alternative volumetric method. The utility of our method resides in the fact that once the tangential field components are specified on the surface, then an explicit expression for the field at any point in the interior is known.

Numerical results are presented.
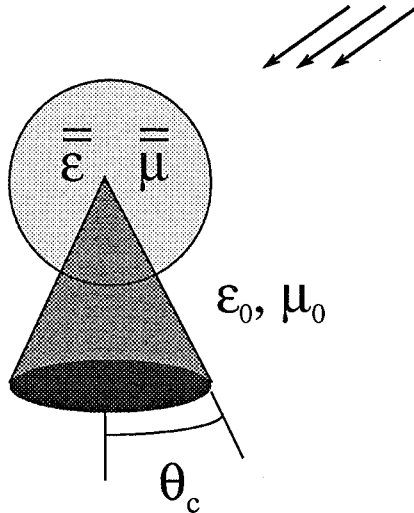
B6-5    TIME DOMAIN DECONVOLUTION OF TRANSIENT
1020    RADAR DATA

E. Rothwell, K. M. Chen, D. P. Nyquist
and P. Ilavarasan
Department of Electrical Engineering and
Systems Science
Michigan State University
East Lansing, MI 48824

Accurate measurement of the transient response
of conducting radar targets hinges on the ability to
remove the effects of the transmit-receive charac-
teristics of the measurement system.  This requires
deconvolving the transmitting and receiving antenna
responses, as well as the response of the receiving
equipment and the propagation path, from the measured
data.  Simple deconvolution algorithms involving
matrix inversion of time-sampled data and division of
Fourier spectra are known to be ill-conditioned.  A
new time domain technique has been developed, which
is shown to be better conditioned than the simpler
algorithms.

Let $c(t)$, $e(t)$, and $h(t)$ be three waveforms
obeying the convolutional equation $c(t)=e(t)*h(t)$.
Also, let $\{e_n\}$ and $\{c_m\}$ be measured versions of the
waveforms, sampled with a time interval $T_s$ within a
truncation window $[0,T_w]$. Finally, let $C(t)$ and $E(t)$
be appropriately interpolated continuous verisons of
$\{e_n\}$ and $\{c_m\}$.  Then, an approximation $H(t)$ to $h(t)$
can be found by solving the convolutional integral
equation $C(t)=E(t)*H(t)$, $0<t<T_w$.

A solution to the integral equation is obtained
by expanding $H(t)$ in a set of basis functions and
employing the method of moments.  A prudent approach
to chosing expansion and weighting functions is to
expand $H(t)$ in a Fourier series over $[0,T_w]$ and apply
Galerkin's method.  Since the basis and weighting
functions span $[0,T_w]$, the integrals in Galerkin's
method perform a smoothing operation on the measured
data, reducing the sensitivity of the resulting mat-
rix equation to random noise.  In addition, estimates
of the highest frequency present in $H(t)$, from know-
ledge of the sample interval $T_s$ and the highest
frequency passed by the measurement system, is easily
incorporated into the representation of $H(t)$ via its
Fourier components.

B6-6
1040

FRESNEL EQUATIONS FOR A DIELECTRIC-CHIRAL INTERFACE

S. Bassiri, C.H. Papas
Electrical Engineering Department
California Institute of Technology
Pasadena, California  91125
and
N. Engheta
The Moore School of Electrical Engineering
University of Pennsylvania
Philadelphia, Pennsylvania  19104-6390

Propagation of plane electromagnetic waves in a lossless, reciprocal, chiral medium will be discussed in this talk.  Such a medium is described electromagnetically by the constitutive relations $D = \varepsilon E + i\gamma B$ and $H = i\gamma E + (1/\mu)B$.  The constants $\varepsilon, \mu, \gamma$ are real and have values that are fixed by the size, shape, and the spatial distribution of the elements that collectively compose the medium.  In this talk the problem of reflection from, and transmission through a semi-infinite chiral medium will be addressed by obtaining the Fresnel equations.  The conditions for the total internal reflection of the incident wave from the interface, and for the existence of the Brewster angle are obtained.  The effects of the chirality on the polarization and intensity of the reflected wave from the chiral half-space will be shown and illustrated by employing the Stokes parameters.  The propagation of electromagnetic waves through an infinite slab of chiral medium is formulated for oblique incidence and will be presented analytically for the case of normal incidence.

B6-7      DYADIC GREEN'S FUNCTION AND
1100      DIPOLE RADIATION IN CHIRAL MEDIA

S. Bassiri and C. H. Papas
Electrical Engineering Department, 116-81
California Institute of Technology
Pasadena, California 91125
N. Engheta
The Moore School of Electrical Engineering
University of Pennsylvania
Philadelphia, Pennsylvania 19104

The radiation emitted by an oscillating dipole in an unbounded, lossless, chiral medium that is described electromagnetically by the constitutive relations $\mathbf{D} = \varepsilon\,\mathbf{E} + i\,\gamma\,\mathbf{B}$ and $\mathbf{H} = i\,\gamma\,\mathbf{E} + (1/\mu)\mathbf{B}$ is calculated. The constants $\varepsilon, \mu, \gamma$ are real and have values that are fixed by the size, shape, and spatial distribution of the elements that collectively compose the medium.

From these constitutive relations and from the time-harmonic Maxwell equations $\nabla \times \mathbf{E} = i\omega\,\mathbf{B}$ and $\nabla \times \mathbf{H} = \mathbf{J} - i\omega\,\mathbf{D}$, it is seen that the wave equation for such a medium is $\nabla \times \nabla \times \mathbf{E} - \omega^2 \mu\varepsilon\,\mathbf{E} - 2\,\omega\mu\gamma\,\nabla \times \mathbf{E} = i\,\omega\mu\,\mathbf{J}$ where the source term $\mathbf{J}$ is the current density of the oscillating dipole and where $\mathbf{E}$ is the electric vector of the radiated field.

The desired solution of this wave equation is found by the Green's function method, that is, by first constructing the dyadic Green's function and then evaluating the expression $\mathbf{E}(\mathbf{r}) = i\omega\mu \int \Gamma(\mathbf{r},\mathbf{r}') \cdot \mathbf{J}(\mathbf{r}')\, dv'$. The dyadic Green's function $\Gamma$ and the components of the radiated electric field $\mathbf{E}$ are obtained in closed form. The components of the radiated $\mathbf{B}$, $\mathbf{D}$, and $\mathbf{H}$ fields can be derived from knowledge of $\mathbf{E}$ by using the Maxwell equation $\mathbf{B} = (1/i\omega)\,\nabla \times \mathbf{E}$ and the constitutive relations. The wave impedance of the medium and the radiation resistance of the dipole are also obtained. The effects of the chiral medium on the polarization and intensity of the dipole radiation are discussed.
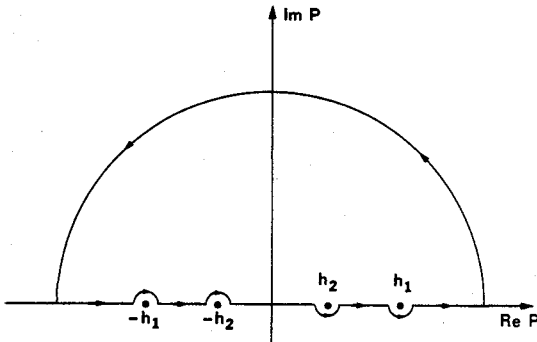


Path of integration in complex p-plane for right-handed ($\gamma > 0$) chiral medium.

## B6-8
## 1120
# ELECTRIC FIELD COMPUTATION IN A REGION OF UNIFORM CURRENT DENSITY

R. Clark Robertson
The Bradley Department of Electrical Engineering
Virginia Polytechnic Institute and State University
Blacksburg, VA   24061

The calculation of the electric field within a current-carrying region by the Green's dyadic method, given by

$$\vec{E}(\vec{r}) = \int_{V'} \vec{J}(\vec{r}') \cdot \vec{\vec{G}}(\vec{r} \,|\, \vec{r}') dV'$$

where the integration is over the volume of the current density and $\vec{\vec{G}}(\vec{r} \,|\, \vec{r}')$ is the appropriate Green's dyadic, requires that the normal Green's dyadic be modified to take into account the principal value of the Green's dyadic (J. Van Bladel, IRE Trans. on Antennas and Propagation, AP-9, 563-566,1961). This is a result of the singular nature of the portion of the Green's dyadic corresponding to an infinite homogeneous region. For the special case of a uniform current density, commonly encountered in the application of the method of moments when pulse functions are used as subsectional basis functions and Dirac delta functions are used as testing functions, the Green's dyadic method can be successfully used to evaluate the electric field inside the current density without invoking the concept of principal values or the necessity of excluding the singularity in the integrand from the volume of integration. This can be shown by comparing the expression obtained by the Green's dyadic method for the electric field at the center of a region of uniform current with that obtained by the method of retarded potentials. The use of principal values is avoided by using a volume of integration such that the singular part of the Green's dyadic is a perfect differential of the variable of integration that corresponds to the direction of current flow. If this integration is performed first, then the remaining integrations can be performed without reference to an excluded region, and the result is identical with that obtained from the retarded potential method. With reference to the moment method, integration of the Green's dyadic over the various subregions is naturally expressed in Cartesian coordinates since the subregions are usually either cubes or rectangular parallelepipeds. As a result, the expression of the singular part of the Green's dyadic as a perfect differential of one of the variables of integration is natural. Hence, the evaluation of the contribution of the singular cell can proceed without special care being taken to exclude the origin from the region of integration.

# Low Frequency Response of a Current Loop
# in 3-D Conductive Inhomogeneity

W.C. Chew
Department of Electrical and Computer Engineering
University of Illinois
Urbana, IL 61801
R.L. Kleinberg
Schlumberger-Doll Research
Ridgefield, CT 06877

When a current loop is radiating low frequency fields in an axially symmetric, conducting inhomogeneity, a common approximation for calculating the response is the geometrical factor theory. However, when the inhomogeneity is general, and non-axially symmetric, the geometrical factor theory breaks down. Even the more general Born approximation is ineffective in such a geometry because of the Maxwell-Wagner charge build up at the interface.

In this paper, we will discuss the range of validity of the Born approximation. We will also discuss a variational solution to such a problem, which is valid beyond the range of Born approximation. The variational solution provides a calculation that is in much better agreement with experiment than the Born approximated solution, or the geometrical factor theory when compared with experiments. It can be used to ascertain the response of a current loop in the vicinity of three dimensional inhomogeneity easily.

As an illustration, we use such a theory to ascertain the response of a microinduction sensor over vertically stratified inhomogeneities.

C2-1    **FINE STRUCTURE IN RF SPECTRA OF LIGHTNING**
0840    **RETURN STROKE WAVE FORM**

**K. Rinnert**
MPAE, Katlenberg-Lindau 3, FRG
**L.J. Lanzerotti, D.J. Thomson, C.G. MacLennan**
AT&T Bell Laboratories, Murray Hill, NJ 07974
**E.P. Krider**
University of Arizona, Tucson, Arizona
**M.A. Uman**
University of Florida, Gainesville, Florida

We have calculated the power spectra of the RF signals for a number of lightning return strokes measured during a thunderstorm which occurred in Lindau in August, 1984. The purpose is to quantify the periodicities recognized in the "subsidiary peaks" which have been observed to follow the onset, fast transition to peak amplitude, of return strokes. The RF data are obtained with the engineering unit of the Galileo Probe lightning experiment. The impulse signal is first removed from the data and the RF power spectra are then calculated using four prolate spheroidal data windows in the time domain and a fast Fourier transform algorithm. The RF spectra definitely show fine structure; there are two or three distinct peaks in the spectra in many of the return strokes. These peaks often occur at frequencies of ~40 and ~70 kHz, but can be quite variable in frequency in the range 0–120 kHz. We present a series of such RF spectra and show how the periodicities of the subsidiary peaks vary during the course of the thunderstorm.

C2-2
0920
## THE COHERENT SIGNAL-SUBSPACE METHOD FOR THE DETECTION AND ESTIMATION OF THE DIRECTIONS OF MULTIPLE WIDEBAND SOURCES

*M. Kaveh*

Department of Electrical Engineering, University of Minnesota,
Minneapolis MN

This presentation addresses the problem of detecting and estimating the directions of arrival (doa) of multiple co-channel, possibly fully correlated wideband signals received by an array of sensors. The Coherent Signal-subspace Method (CSM) relies on an approximately coherent combination of spatial signal subspaces of the temporally narrowband components of the received signal vector. A two-step algorithm is described. First, initial "low-resolution" doa estimates are used to align the signal sub-spaces and generate an enhanced spatial covariance matrix estimate. In the second step of the algorithm, appropriate narrowband signal-subspace methods are used for detection and the estimation of the doa's. The presentation also includes a discussion of some unconventional approaches to the characterization of the performances of detectors and estimators for this class of problems.

C2-3    **MULTIPLE-WINDOW    TRANSFER    FUNCTION**
1020    **ANALYSIS**
**of ELECTROMAGNETIC DATA**
**David J. Thomson**
AT&T Bell Laboratories, Murray Hill, N.J. 07974

We discuss the estimation of transfer functions from electromagnetic data using variants of the multiple-window method. The theory upon which estimation of magnetotelluric transfer functions is founded depends on numerous statistical assumptions: *A-1* A unique solution exists and the data is temporally stationary enough for time averages to converge; *A-2* The dominant incident field is a homogeneous plane wave; *A-3* The vertical magnetic field depends linearly on the two components of the horizontal field.

Because EM data is rarely either stationary or Gaussian, robust estimation procedures have been introduced which impose additional constraints in the form of data segmentation. This implies that we can choose segment lengths so that for a majority of segments: *A-4* Features of the spectral matrix are resolved, and; *A-5* The data is essentially stationary within the segment.

In this paper we study the influence and interactions of these assumptions on the estimated transfer function and describe tests for their violation. Most of these tests are generalizations and extensions of procedures known in multivariate analysis. Such tests are sensitive to departures from normality but if A-5 is valid the transformed data will be reasonably Gaussian even if the original data is not. Induced voltage on Transatlantic cables and data from the EMSLAB array are used as examples.

C2-4
1100

ESTIMATING THE PARAMETERS OF A GENERALIZED CHIRP SIGNAL IN THE PRESENCE OF NOISE: R. Kumaresan, Electrical Engineering Dept., Univ. of Rhode Island, Kingston, RI 02881

F2-1    ESTIMATION OF ZENITH CLEAR-AIR ABSORPTION
0900    FROM GROUND PARAMETERS FOR 10 TO 300 GHz
K.C. Allen and S.D. Hector
National Telecommunications and
Information Administration
Institute for Telecommunication Sciences
Boulder, Colorado 80303

A data base of monthly mean atmospheric profiles for 37 cities was used to analyze the relationship between zenith clear-air absorption and ground level meterological parameters. The absorption rate was computed at each profile height and integrated with respect to height to estimate the zenith attenuation. A nonlinear least squares fit was then applied to the ground level parameters and zenith attenuation. Through an analysis of residuals, the functional form of a good estimator of zenith attenuation in dB from the ground parameters of pressure, P, temperature, T, and water vapor pressure, e, was found to be

$$A = \frac{a_1 P e (a_3 + T^2)}{a_2 + T} + a_4 P^2 (a_5 - T) \qquad (1)$$

where the $a_i$'s are frequency dependent. The first and second terms in (1) give the water vapor and oxygen absorption, respectively. The RMS error of (1) for the data base is about six percent or less for most frequencies. Because the zenith attenuation was computed up to only 30 km in height, the results must be used with caution near the oxygen lines (50-70 GHz and near 118 GHz).

A second approach to estimating the zenith attenuation by multiplying the ground level attenuation rate, $\alpha_o$, by an effective height, $h_a$,

$$A = \alpha_o h_a, \qquad (2)$$

was also investigated. A strong dependence of the effective height on the ground level attenuation rate was discovered. For the profiles in the data base, $h_a$ ranged from 2.3 to 4.4 at 44 GHz. An effective height functionally dependent on the ground level attenuation rate or meterological parameters and frequency makes (2) a good estimator of zenith attenuation.

F2-2      MILLIMETER WAVE TEMPORAL SPECTRA FOR SPHERICAL WAVE
0920      PROPAGATION THROUGH ATMOSPHERIC TURBULENCE
          R.J. Lataitis, S.F. Clifford, R.J. Hill, J.T. Priestley
          NOAA/ERL/Wave Propagation Laboratory
          325 Broadway
          Boulder, CO   80303

In atmospheric turbulence, refractive-index fluctuations produced by local small-scale variations in the temperature and humidity randomly perturb the amplitude and phase of a propagating wave.  Clifford (J. Opt. Soc. Am., 61, 1285-1292, 1971) has derived the temporal frequency spectra for the amplitude, phase, and phase-difference fluctuations of a spherical wave propagating through weak refractive turbulence.  At millimeter wave frequencies, humidity fluctuations can also produce small scale absorption fluctuations.  We use an extended theory to include this effect.  The theory is compared to results from a joint NOAA-GIT (National Oceanic and Atmospheric Administration-Georgia Institute of Technology) millimeter wave propagation experiment performed over a period of two years (1983-1985) in Flatville, Illinois.  Millimeter waves of frequencies 116, 119, 142, 173, and 230 GHz were propagated over a 1.4 km path at a height of 4 m over a flat open field.  The propagation path was well instrumented to provide an accurate comparison with meteorological conditions.  The agreement between experiment and theory is good and indicates that small scale absorption fluctuations may dominate the low frequency portion of the amplitude spectrum while refraction fluctuations dominate at higher frequencies.  The entire phase difference spectrum appears to be dominated by refraction fluctuations.  Several episodes of large scale (whole path) absorption variations were also recorded.  These appear to be non-stationary phenomena that can dominate the low frequency behavior of the spectra and are not explained by the theory.

F2-3        USE OF DIFFERENTIAL PROPAGATION PHASE CONSTANT TO
0940        ESTIMATE LIQUID WATER IN A MIXTURE OF HAIL AND RAIN
            D.S. Zrnic', N. Balakrisnan, M. Sachidananda
            National Severe Storms Laboratory
            1313 Halley Circle
            Norman, OK  73069

The differential phase constant $K_{DP}$ is defined as the difference between phase constants of horizontally and vertically polarized waves that propagate horizontally. This constant can be estimated with coherent polarimetric radars. $K_{DP}$ has a unique property which allows discrimination between statistically isotropic and anisotropic scatterers. In a mixture of randomly oriented scatterers (such as hail) with aligned scatterers (such as rain drops) $K_{DP}$ is only affected by the aligned scatterers, whereas differential reflectivity is affected by both. This is because on the average the phase shift after propagation through randomly oriented scatterers is the same for horizontally and vertically polarized electric fields, whereas horizontally-polarized electric fields propagating through rain experience relatively larger phase shifts. We show theoretically the differential phase constants expected in various mixtures of rain and hail. Also we show data consisting of reflectivity factor Z, differential reflectivity $Z_{DR}$, and $K_{DP}$ which can be reconciled by the simultaneous presence of hail and rain.

F2-4
1000

CLIMATOLOGICAL ANALYSIS OF RAIN AND CLOUD
ATTENUATION OF MILLIMETER WAVES

E. J. Dutton
National Telecommunications and
Information Administration
Institute for Telecommunication Sciences
325 Broadway
Boulder, CO   80303-3328

Rainfall observational data are processed by least-squares curve-fitting to call attention to some of the desirable aspects of such fitting.  The curve-fitting techniques are illustrated for annual rainfall and worst-month rainfall distributions, but are as readily applicable for distributions of rain-caused attenuation or scattering.

Then analysis of specific rain attenuation data observed at Huntsville, AL at 28.8, 57.7, and 96.1 GHz is discussed. These data are used to construct the third part of a CONUS-wide climatology for use in obtaining the distribution of specific attenuation at geographic locations within these zones.

Finally, the feasibility of determining zenith cloud attenuation distributions at millimeter-wave frequencies, basically using radiosonde observations as the main indictor of cloud location and occurrence, is examined.  A 5 year sample for Washington, D.C. is examined and results presented.

F2-5
1040

RADIOMETRIC AND RADAR MEASUREMENT OF RAIN IN
HEAVY CELLS

D. C. Hogg
Colorado Institute for Research in Environmental
Sciences
University of Colorado
Boulder, CO 80309

Computations of 6 GHz brightness temperatures generated
by heavy rain cells embedded in an absorbing troposphere are
given.  It is assumed that the cell dimensions are measured
by a companion radar.  The radiometric measurement is made on
and off the cell.  The elevation angle of the radiometric
beam is taken to be 2 degrees and the raindrop sizes repre-
sented by a Laws-Parsons distribution.  For a 2 km diameter
cell of rainrate 100 mm per hr located at a range of 75 km,
the brightness is about 80 K of which only a 1.5 K correction
is required for the clear-air brightness from beyond the
cell.  A 6 GHz measurement is also discussed.

F2-6    AN ACOUSTIC SOUNDER FOR MONITORING QUALITATIVE
1100    TEMPORAL VARIATIONS IN VERTICAL RADIO REFRAC-
        TIVITY PROFILES IN THE LOWER TROPOSPHERE
        S.M. Babin and J.R. Rowland
        The Johns Hopkins University/Applied Physics Labora-
        tory, Johns Hopkins Road, Laurel, Maryland 20707

        Low altitude gradients in radio refractivity can have
dramatic effects on radar propagation at sea.  Detailed quan-
titative refractivity data can be gathered using helicopters
and rocketsondes.  A method is needed for continuously moni-
toring detailed qualitative changes in vertical refractivity
profiles over the ocean surface so that one would know when
more detailed quantitative studies were needed to predict
radar propagation.  One possible technique for doing this is
by means of a small high frequency acoustic sounder.  Since
the absorption of sound in air is highly dependent on humidity,
such an acoustic sounder could conceivably measure vertical
humidity profiles.  Assumptions about the temperature profile
would allow a description of the refractive index profile.
The characteristics of a small multiwavelength high frequency
acoustic sounder suitable for making humidity measurements to
an altitude of 200 meters are presented.

F2-7
1120

LOW COST ROCKET PROBES FOR USE IN
RADAR PROPAGATION STUDIES
J. R. Rowland
The Johns Hopkins University/
Applied Physics Laboratory
Johns Hopkins Road
Laurel, Maryland   20707

Recent development of computer models that have the
capability of predicting radar performance under ducting
conditions at sea has produced a need for high resolution
profiles of microwave refractivity.  In the past, radiosondes
have been used to make the types of measurements required for
the radar models.  Conventional radiosondes are carried by
balloon and telemeter temperature, pressure and relative
humidity at sampling intervals of several hundred feet altitude.
In order to accurately calculate the effects of these meteoro-
logical parameters on the radar at low altitudes, however,
measurements with a vertical resolution of a few feet extending
all the way to the water surface are generally required.
Conventional balloon carried radiosondes launched at sea from
ships suffer from contaminated measurements in the vicinity
of the ship due to the microclimate surrounding the ship.  In
addition, essential measurements at altitudes below the normal
deck level at which the radiosonde is released cannot be
obtained by these radiosondes.  For this purpose, a simple
low-cost disposable rocketsonde system has been developed.
The prototype rocketsonde system was developed using mass
produced off-the-shelf hobby rocket components.

Rocketsondes have been used to support several radar
propagation tests.  On a number of occasions they have been
launched from boats at sea.  Test firings have been made from
boats as small as 23 feet in length.  Several tests in Puerto
Rico and a test at Kwajalein Atoll in the Marshall Islands
have demonstrated the reliable shipboard use of the rocket-
sondes.  This paper contains a description of the rocket system
and the results of field comparisons with other sensors.

F2-8      USER EXPERIENCE WITH A MODEL ROCKET RADIOSONDE:
1140      John F. Cavanagh, Code F405, Naval Surface Warfare Center, Dahlgren,
          VA 22448-5000

During February of 1987, NSWC conducted sea backscatter measurements using the
TRADEX, ALCOR and MMW radars at the KREMS facility on Kwajalein Atoll in the
Marshall Islands. Refractive profiles were measured in support of these experiments by
means of a radiosonde system launched from a research vessel located near the
illuminated surface.

The rocketsonde system is under development by the Applied Physics Laboratory of
Johns Hopkins University. Representative profiles will be presented showing
evaporation ducts and surface ducts. Comments concerning the employment of this novel
device will be offered along with suggested features for incorporation into future
versions.

The ocean surface was also monitored during the radar experiments. The research vessel
was used to deploy and recover a wave rider bouy. Samples of ocean wave directional
spectra derived from the buoy data will be presented.

G4-1    COUPLING, ENERGETICS, AND DYNAMICS OF
0900    ATMOSPHERIC REGIONS (CEDAR) - AN NSF
        INITIATIVE

T. L. Killeen, Vice-Chair CEDAR Science Steering Committee
Space Physics Research Laboratory
Department of Atmospheric and Oceanic Sciences
The University of Michigan
Ann Arbor, Michigan 48109.

The Aeronomy and Upper Atmospheric Facilities Programs of the National Science Foundation's (NSF's) Atmospheric Sciences Division have jointly sponsored a new initiative aimed at providing a more detailed understanding of the physical, chemical, dynamic and radiative processes that control the Earth's upper atmosphere, ionosphere, and near-space environment. The multi-year program was designed through the efforts of many scientists from numerous institutions both within and outside the US. The CEDAR program features the development and utilization of "state-of-the-art" ground-based optical and radar instrumentation to attack a series of scientific problems associated with the vertical and global coupling between atmospheric regions. At present a series of campaigns are being undertaken using existing equipment, and these will be followed by data analysis workshops. A five year plan of equipment development and upgrading for both optical and radar diagnostic techniques has been initiated. In this talk we review the current and evolving state of the CEADR program and focus on several of the individual scientific topics that will be addressed over the next few years.

G4-2    IONOSPHERIC EXPERIMENTS WITH MOTHER-SON
0940    ROCKET PAYLOADS
H.G. James
Communications Research Centre,
P.O. Box 11490, Station "H",
Ottawa, Ontario K2H 8S2
Canada

The National Research Council of Canada and NASA are studying proposals for innovative radioscientific experiments in the ionosphere. In the OEDIPUS campaign, it is proposed to launch two high-altitude sounding rockets instrumented with plasma diagnostics. Both will be flown from Andoya, Norway, during periods of auroral activity. A unique feature of each payload will be a long insulated conducting tether connecting the two subpayloads. The separation vector will be parallel to the local magnetic field direction and up to 1 km in length. This system will be deployed in flight and will be used to stimulate various plasma phenomena and to make passive observations of the ambient auroral plasma. The major scientific objectives for this program will be:

1) to measure the reponse of the long probe in the ionospheric plasma;

2) to seek new insights into plane- and sheath-wave propagation in plasmas; and

3) to make passive observations of the auroral ionosphere utilizing the long probe, in particular to measure the component of the natural dc electric field parallel to the magnetic field.

The OEDIPUS-A rocket will stress active probe and wave techniques, points 1) and 2), on a flight in winter 1989 with an apogee of about 650 km. The theme of the OEDIPUS-B rocket one year later will be the passive investigation of the parallel electric field and associated spontaneous plasma phenomena, point 3). The apogee will be 1000 km.

WISP Rocket is the name of a complementary investigation using a double payload comprising a separated transmitter and receiver (no tether), to be launched from Wallops Island in summer 1989. The characteristics of a 40-m transmitting dipole in a magnetoplasma will be investigated, including its impedance and radiation efficiency. This will be carried out at very low frequencies (VLF) on a trajectory with an an apogee of about 400 km.

All the above experiments are preparation for the Waves In Space Plasmas (WISP) investigation on Shuttle/Spacelab. All the rocket trajectories will be such that the payloads will spend a significant fraction of their operational lifetimes in the ionospheric F region, i.e., at WISP orbital altitudes. The preparatory rocket exeriments and WISP have a number of common scientific topics: plasma-wave fundamentals observed with a bistatic transmitter-receiver geometry; antennas and probes in plasmas; and natural wave-particle interactions.

G4-3
1000

WORLDWIDE ACOUSTIC GRAVITY
WAVE STUDY (WAGS) - Overview
of Results
Paul E. Argo
Los Alamos National Laboratory
Los Alamos, NM 87545 and
Robert Hunsucker
Geophysical Institute
University of Alaska
Fairbanks, AK  99701

The Worldwide Acoustic Gravity Wave Study
(WAGS) was conducted during the month of October
1985.  Some of the topics of interest were:  AGW
generation mechanisms, ion-neutral coupling, effects
of AGW dispersive propagation, measurements of
attenuation constants, and effects and conditions of
wave ducting.

The days of October 14-19 were designated as
high priority days, and the collection of high-time
resolution data was encouraged.  The geomagnetic
indices for these days indicated moderate activity,
and the data are in fact showing "enhanced" acoustic
gravity wave activity.

Some interesting results include:  (1) the
periodicity measured in aurorally generated AGW's
may mirror source variations rather than atmospheric
filter processes; (2) in several large scale AGW's
no systematic variation of period with the
propagation distance were observed.

The potential for future campaigns will be
discussed.

G4-4      THE WORLD IONOSPHERE/THERMOSPHERE STUDY
1040      C. H. Liu, Dept. of Electrical and Computer Engineering
          University of Illinois, Urbana, IL 61801

The World Ionosphere/Thermosphere Study (WITS) is an international, interdisciplinary program of research organized by SCOSTEP for the period July 1987 to December 1989. Its aim is to increase substantially our understanding of the global dynamics of the ionosphere and thermosphere as a coupled system with coupling to the magnetosphere and middle atmosphere. Both large-scale dynamics and small-scale structures will be studied in the global sense. The current status of the program will be reported and the scientific goals and planned campaigns of WITS projects will be discussed.

G4-5      THE INTERNATIONAL REFERENCE IONOSPHERE
1120      Dieter Bilitza
          Goddard Space Flight Center, code 633,
          Greenbelt, MD 20771, U.S.A.

The International Reference Ionosphere (IRI) is a URSI/COSPAR sponsored project to establish reliable standard models of ionospheric density and temperature parameters based on the world-wide ionospheric data base. The IRI models are continously checked with new measurements and up-dated if necessary. We discuss the latest edition, IRI-86, with special focus on the electron density model.

Comparisons with groundbased and spacecraft data are used to show the extent of agreement between measurements and model, and to indicate areas where more work is needed.

We review the recent progress in empirical and semi-empirical modeling of the ionospheric bottomside, topside and F peak regions and its implications for the IRI.

G4-6    SUNDIAL:   A CONTINUING INTERNATIONAL PROGRAM
1140    IN SOLAR-TERRESTRIAL PHYSICS

E. P. Szuszczewicz, Director
Experimental Space Programs and Applications
Plasma Physics Division 157
Science Applications International Corporation
1710 Goodridge Drive
McLean, Virginia 22102

SUNDIAL is an international effort combining
theoretical modelling with coordinated ground-based
and satellite-borne measurement programs. The
overall objective is the development of a
comprehensive understanding and an associated
predictive capability for the cause-effect
relationships which control the quiescent and
disturbed global-scale ionosphere. While the focus
is the ionospheric state at any place, at any time,
and under any condition, the program requires and
measures solar and interplanetary inputs, and works
to establish a detailed understanding of the
interactive roles that the ionosphere plays with
the magnetosphere and the thermosphere. The
program has emphasized the importance of truly
world-wide simultaneous measurements, making sure
that coverage allows separation of UT and LT
effects, and making possible important comparisons
between Northern and Southern hemisphere
observations. SUNDIAL has established the extended
campaign mode as its normal operational procedure,
with data collected on a minimum eight-day, around-
the-clock basis. For its first three campaigns
this has made it possible to observe the global-
scale ionosphere transition from a stable,
quiescent state to that of considerable
disturbance....and then back again to a quiescent
condition. This has provided a valuable data set,
immensely amenable to comparisons with large scale
numerical and empirical modes, and adaptable to
SUNDIAL requirements which seek to quantitatively
define "quiet," "average," and "progressively
disturbed" ionospheric conditions for each of the
seasons within a given period of the solar cycle.
(Supported by NSF Grant #ATM8617560.)

H2-1      OBSERVATION OF ELF PLASMA WAVES GENERATED
0900      BY PULSED ELECTRON BEAMS

R. I. Bush, G. D. Reeves, T. Neubert, P. M. Banks
STAR Laboratory, Stanford University
Stanford, CA  94305
D. A. Gurnett
Department of Physics and Astronomy, University of Iowa
Iowa City, IA  52242
W. J. Raitt
Center for Atmospheric and Space Sciences, Utah State
University
Logan, UT  84322

The Spacelab-2 payload was flown on the STS 51-F Shuttle mission in July and August of 1985, and the Vehicle Charging and Potential Experiment (VCAP) was included as part of the experiment complement. One of the VCAP investigations involved the injection of electron beams with an energy of 1 keV and a beam current of 100 milliamperes into the ionospheric plasma. The electron beam could be square wave modulated to frequencies over 30 kHz by switching the high voltage supply accelerating the electrons. Observations of plasma waves produced by the pulsed electron beams were made by the wave receiver instruments on the Plasma Diagnostic Package (PDP) which provided wide band measurments of both the electric and magnetic field fluctuations up to 30 kHz.

As part of the investigations of the Orbiter environment, the PDP was released from the Orbiter for a six hour period, and the Orbiter was maneuvered into different positions relative to the PDP. During the PDP freeflight, a VCAP sequence designed to emitted electron beams in the ELF pulsing regime was initiated a total of 8 times. In this ELF pulsing sequence, the electron beam was pulsed at 7 different frequencies between 9.5 Hz and 610 Hz. A significant difference in the measured magnitude of the electric and magnetic signatures of the pulsing frequencies was observed between ELF sequences initiated upstream (with respect to the plasma flow) of the Orbiter than for those sequences initiated downstream of the Orbiter. Comparisons of the plasma wave generation efficiency will be presented as a function of the relative positions of the electron beam source and the PDP.

H2-2
0920

AN ANALYSIS OF THE AMPLITUDE OF VLF
RADIATION GENERATED BY A SQUARE WAVE
MODULATED ELECTRON BEAM IN SPACE
G.D. Reeves, P.M. Banks, K.J. Harker, T. Neubert,
R.I. Bush
Space, Telecommunications and Radioscience Laboratory
Stanford University, Stanford, California 94305
D.A. Gurnett
Department of Physics and Astronomy
University of Iowa, Iowa City, Iowa 52242
W.J. Raitt
Center for Atmospheric and Space Science
Utah State University, Logan, Utah 84322

During both the STS-3 and Spacelab-2 space shuttle missions a square wave modulated, 1 keV, 100 mA electron beam was injected in the ionospheric plasma and the resulting electric and magnetic fields measured with an array of plasma diagnostic instruments including a wide-band spectrum analyzer. The results of both missions showed that a square wave modulated electron beam generates narrow-band emissions at the pulsing frequencies and harmonics of those frequencies and broad band emissions throughout the 0-30 kHz frequency range.

Up to this time analysis of the wave emissions was necessarily qualitative because the recorded signals were kept within strict limits by an automatic gain control circuit. Digitization of the wide-band signals and numerical processing allows us to remove the effect of the AGC and study the amplitude of the wave emissions for both the electric and magnetic antennas.

Results of this analysis will be presented for periods of the Spacelab-2 mission during which both the fast pulsed electron generator (FPEG) and the University of Iowa Plasma Diagnostics Package (PDP) were located in the orbiter cargo bay and for periods when the FPEG was on the orbiter and the PDP was released as a free-flying satellite out to distances of several hundred meters. Results for the flux tube connection when the orbiter and the PDP were located on the same magnetic field line while the FPEG was pulsed at 1.22 kHz will be presented in detail. The amplitude of the wave emissions will be compared with the predictions from the theories of model systems [Harker and Banks, 1986., and Al'pert, 1983] and with the amplitude of emissions during a DC flux tube connection [Gurnett et al., 1986]

H2-3
0940
COHERENT CERENKOV RADIATION FROM THE SPACELAB-2
ELECTRON BEAM

W. M. Farrell, D. A. Gurnett and C. K. Goertz
Dept. of Physics and Astronomy
The University of Iowa
Iowa City, Iowa   52242

During the Spacelab-2 (SL-2) mission, the plasma wave
instrument onboard the Plasma Diagnostics Package (PDP)
detected intense whistler-mode radiation from a 1 keV - 50
mA D.C. electron beam.  It is believed that coherent
Cerenkov radiation from bunches of beam electrons is
responsible for the whistler-mode radiation, where an
electrostatic beam-plasma instability forms the coherently
radiating bunches.  In this paper, we present a detailed
model of the coherent Cerenkov emission process from the
SL-2 electron beam.  A one-dimensional computer simulation
of the beam propagating through the ionospheric plasma is
used to model the expected phase space structure of the beam
electrons.  In the simulation, bunching of the beam by a
beam-plasma instability is clearly evident. The coherent
Cerenkov radiated power from the modeled beam is calculated
to be $\sim 10^{-8}$ W/Hz from a 200-meter beam segment, and is
about a factor of 10 greater than those measured.  It will
be demonstrated that the electrostatic instability in the
beam is vital to raising the wave powers above incoherent
levels since it forms the highly coherent electron bunches.
Increasing the radiation efficiency by pulsing the beam in
the whistler-mode range of frequencies will also be
discussed. Based on the results of this study, it is
concluded that coherent Cerenkov radiation processes from
the SL-2 electron beam can account for the detected
whistler-mode power levels.

H2-4      CORRELATION OF UPPER HYBRID WAVES WITH ELECTRON
1000      CONICS
          J.D. Menietti, H.K. Wong, C.S. Lin, J.L. Burch
          Department of Space Sciences
          Southwest Research Institute
          6220 Culebra Road
          San Antonio, TX  78284

          D.A. Gurnett
          Department of Physics and Astronomy
          University of Iowa
          Iowa City, IA  52242

Electron conical distributions have been observed by the Dynamics Explorer 1 (DE-1) and VIKING satellites in the mid-altitude polar magnetosphere.  Wong et al. (talk presented at the Fall American Geophysical Union meeting, 1987) have shown that such distributions can be generated by electrostatic upper hybrid waves.  Numerical solutions of the diffusion equation, for this mechanism, have been performed and the results compared to particle data obtained by the High Altitude Plasma Instrument (HAPI) on board DE-1.  Velocity-space contours of the numerical results compare favorably to the data for local plasma parameters.  We have performed a survey of the data obtained by the HAPI and the Plasma Wave Instrument (also on board DE-1) that seems to indicate the presence of upper hybrid waves when electron conical distributions are present.  These results support the concept of the generation of electron conics by upper hybrid waves.

H2-5
1040
ORIGIN AND THE NONLINEAR EVOLUTION OF THE
ELECTROSTATIC WAVES OBSERVED DURING THE AMPTE
SOLAR WIND RELEASES
N. Omidi
Institute of Geophysics and Planetary Physics
University of California, Los Angeles
Los Angeles, CA 90024-1567
K. Akimoto
Earth and Space Sciences Division and
Applied Theoretical Physics Division
Los Alamos National Laboratory
Los Alamos, NM 87545
D.A. Gurnett and R.R. Anderson
Department of Physics and Astronomy
The University of Iowa
Iowa City, IA 52242

    To understand the generation and the nonlinear evolution of the
electrostatic waves observed during the AMPTE (Active Magneto-
sphere Particle Tracer Explorers) solar wind releases a detailed
investigation is conducted. Previous linear studies have suggested
that two distinct sets of instabilities may be responsible for the
generation of these waves. One set consists of ion-acoustic type
instabilities, while the other group corresponds to the modified two
stream instabilities and requires the solar wind flow to be across
the ambient magnetic field. In order to establish which set of
instabilities are more viable for the generation of the observed
electrostatic waves, a detailed linear Vlasov theory has been
conducted. In addition both the plasma wave as well as the mag-
netic field measurements by the IRM (Ion Release Module) spacecraft
are used to correlate the frequency and the power of the observed
waves with the magnitude and the direction of the solar wind
magnetic field. The results of these analyses indicate that the
ion-acoustic type instabilities are responsible for the generation of
the observed waves. In order to investigate the nonlinear evolution
of these instabilities and discern their role in the coupling of the
released ions to the solar wind, one-dimensional electrostatic
simulations have been performed. The results show that both the
solar wind protons and the released ions may be heated and
accelerated in the directions oblique to the solar wind flow
velocity.

# PLASMA INSTABILITIES OF A FINITE-SIZE ELECTRON BEAM-PLASMA SYSTEM

C. S. Lin and H. K. Wong
Department of Space Sciences
Southwest Research Institute
San Antonio, TX 78238

It is well known that for an infinite homogeneous electron beam-plasma system, the electron beam mode has a much larger growth rate than the whistler wave. However, for the case of a finite size beam, which is more realistic in space and laboratory experiments than homogeneous beams, it is not clear how the finite size effects will affect the growth of these waves. In this work, the electromagnetic dispersion equation of a bound beam-plasma system is derived by assuming that a electron beam with finite radius is imbedded in a cold uniform background plasma. The background plasma can either be bounded or unbounded, depending on the physical situations. The beam drifts along the background magnetic field line with constant velocity, and the self magnetic field by the beam is considered to be negligible. The solutions of the dispersion equation indicate that the growth rate of the beam mode is strongly suppressed around the electron cyclotron frequency if the cyclotron frequency is less than the electron plasma frequency. However, the whistler mode seems to be less affected by the finite size effects. These instabilities are examined for various frequency and plasma regimes. The relevance of these instabilities to wave emissions observed during electron beam injection experiments from the Space Shuttle will be discussed.

H2-7    COMPARISON OF RADIOWAVE AND VEHICLE
1120    CHARGING PROCESSES OBSERVED WITH
ROCKETS AND THE SPACE SHUTTLE
P.M. Banks, T. Neubert, P.R. Williamson,
R. Bush, G. Reeves, B. Gilchrist and W.J. Raitt
Space, Telecommunications and Radioscience Laboratory
Stanford University
Stanford, CA 94305

This paper will review a collection of interesting space plasma effects observed during the past seven years of experiments with rockets and the Space Shuttle. The question of vehicle charging in response to active electron beam emissions will be covered, showing the complexity of environmental effects. This includes unexpected responses to dramatic changes in background plasma density, hot thruster clouds, and cold nitrogen jet firings. In addition, a review will be given of ELF and VLF wave generation experimental results obtained from the CHARGE-2 rocket and, in collaboration with the University of Iowa, the PDP and VCAP experiments on Spacelab-2. These too, have strange features which are difficult to explain on the basis of present understanding of how electron beams generate waves in the ionosphere.

J4-1      NEW  RESULTS  ON THE PROPERTIES OF TYPE III RADIO
0840      BURSTS IN THE INTERPLANETARY MEDIUM

Robert G. Stone
Laboratory for Extraterrestrial Physics
NASA Goddard Space Flight Center
Greenbelt, MD 20771

Results are presented on two basic problems in the interpretation of
kilometer type III radio observations; 1) Why trajectories in the
interplanetary medium derived from type III positions disagree with expected
trajectories along the spiral magnetic field. 2) New evidence that kilometer
type III radio emission is more generally observed at the harmonic and less
often at the fundamental of the local plasma frequency. The ISEE-3 radio
experiment monitors solar radio emissions from 2 MHz to 30 kHz
corresponding to radial distances from about 10 solar radii to 1 AU from the
sun. Utilizing a spinning dipole parallel to the ecliptic and a dipole along the
spin axis, the azimuth, elevation, and percent modulation of the radio
emission at each observing frequency is determined. Because type III exciter
electrons propagate along interplanetary magnetic field lines, tracking type
III radio emission should provide a 3-D "snapshot" of the large scale
interplanetary magnetic field configuration. But trajectories derived from the
observed azimuths generally describe paths through the interplanetary
medium that eventually track back to the observer at low frequencies rather
than following the expected spiral field path through the interplanetary
medium. It was recently demonstrated that the finite size of the  source and
the directivity of the radiation can account for this observed behavior.
Azimuths of the radio sources at low frequencies are shown to be
systematically displaced from the azimuths of the centroid of the type III
exciter electron beam. A method has been developed that derives the source
locations using observed characteristics of the radio burst This yields
trajectories that are consistent with the interplanetary magnetic field
configuration.

The most recent considerations of whether type III bursts are observed at
the fundamental of the plasma frequency, at the harmonic or at both, was
presented by Dulk et. al.(G. A. Dulk, J.L. Steinberg, and S. Hoang, Astron.
Astrophys., 141, 30-38, 1984). They believe "the evidence for harmonic
emission is not as strong as that for fundamental emission in at least some
bursts." We studied  Type III events whose trajectories crossed 1 AU
(observed azimuth passed through  90 degrees) less than one day to the
west of the observer . The observing frequency for 1AU  is compared with
ISEE-3 in-situ density measurements assumed to be the same as at the
time of the type III event. For 50 events analyzed, only harmonic emission is
seen. We suggest that harmonic emission is the rule, and that the
fundamental is so directive that it is seen only when the observer is looking
along the direction of the  electron beam.

# KILOMETER WAVE RADIO BURSTS FROM BEHIND THE SUN

George A. Dulk
Department of Astrophysical, Planetary and Atmospheric Sciences
University of Colorado
Boulder, CO 80309–0391

One of the common types of radio radiation at kilometer wavelengths occurs when streams of multi-keV electrons originate near the Sun's surface and propagate out through the corona and interplanetary space. The flux densities attain values as high as 100 GJy, making the bursts easy to detect with receivers such as were on the Voyager and ISEE–3 spacecraft. A newly-found characteristic of these "type III" bursts is that they are visible to sensitive radio instruments irrespective of the locations of the radiating sources, be they in front of or behind the Sun.

Explanations of the radio emissions will be described in terms of recent ideas of the generation of plasma waves and the emission and propagation of radio waves in a severely inhomogeneous medium.

This work is in collaboration with Drs. A. Lecacheux, J.L. Steinberg and S. Hoang of the Observatoire de Paris, Meudon, France.

J4-3      STUDIES OF LARGE SCALE STRUCTURE OF THE SUN's UPPER
0920      CORONA FROM LOW FREQUENCY IMAGING OBSERVATIONS
          M. R. Kundu
          Astronomy Program
          University of Maryland
          College Park, MD   20742

We discuss the use of Clark Lake multifrequency radio-
heliograph for several studies of the large scale structure of
the Sun's upper corona.  The radioheliograph is used as a
coronagraph to study coronal streamers.  In particular, we
compare our streamer data with similar data obtained in white
light from satellite experiments, P78-1 solwind and SMM-C/P.
We study the rotation of streamers as they move across the disk
and show that they can be used to study 3-D structure of
coronal structures.  We study the propagation of type III-burst
producing electrons in coronal streamers and deduce electron
density distribution above streamers.  Using daily quiet sun
images, we produce synoptic charts and compare them with white
light synoptic charts, which reveal the existence of streamers
and coronal holes as bright features and voids.  Finally, we
show that slow ($\lesssim$ 100 km/s) coronal mass ejections events
(CME's) can have radio signatures associated with them.

J4-4       IMPORTANCE OF RADIO OBSERVATIONS TOWARDS THE
0940       UNDERSTANDING OF CORONAL MASS EJECTIONS
N. Gopalswamy
Astronomy Program
University of Maryland
College Park, MD   20742

We present the analysis of low frequency imaging
observations of coronal mass ejection events.  The observations
of nonthermal radio emission generally reveal the dynamics of
energetic particles and their inter-action with the associated
coronal mass ejection (CME) and the ambient corona.
"Precursor" type III bursts indicate the presence of particle
acceleration and heating during the onset phase of CME´s.
Positional analysis of the II bursts provides information about
the origin of the shocks - whether created by the CME or by the
flare explosion.  The moving type IV burst associated with a
CME can be used to study the nature of the plasmoid associated
with the CME and the characteristics of the nonthermal
particles trapped in the plasmoids.  Thus radio emissions at
various stages of the CME could be used to study the evolution
of the CME´s.

J4-5      URANUS RADIO EMISSIONS
1000      M.L. Kaiser
          Goddard Space Flight Center, Code 695
          Greenbelt, MD 20771

Uranus was very slow in revealing direct evidence of its magnetosphere. For both Jupiter and Saturn, polarized emissions of magnetospheric origin were detected by the Voyager Planetary Radio Astronomy instruments when the spacecraft were still several A.U. from their respective encounters. In contrast, the first Uranian emissions were not detected until just a few days before the Voyager-2 fly-by which occurred on January 24, 1986.

Radio observations in the immediate vicinity of Uranus showed that although the Uranian emissions were generally weaker than their Jovian and Saturnian counterparts, the were by no means simpler. Uranus' radio spectrum appears to consist of perhaps as many as six separate radio components originating from separate magnetospheric source regions and with a variety of emission mechanisms. These radio components are all in the band from a few kHz to about 850 kHz. In addition to the megnetospheric radio components, some signals above 1 MHz were detected which may originate in atmospheric discharges (lightning). The observational characteristics of each component will be described and the ongoing analysis effort aimed toward localizing the individual source regions will be reviewed.

J4-6
1020

# THE MAIN SOURCE OF RADIO EMISSION FROM THE MAGNETOSPHERE OF URANUS

Thomas D. Carr, Department of Astronomy, University
  of Florida, Gainesville, FL 32611.

Samuel Gulkis, Space Science Division, Jet
  Propulsion Laboratory, Pasadena, CA 91103.

We developed a geometrical model to account for
the main component of the modulated radio emission,
which was left elliptically polarized, observed
from about 20 to 900 kHz as Voyager 2 passed near
Uranus. We assumed cyclotron maser emission by
electrons descending within the $L=17$ magnetic
shell toward the boundary of the UV auroral region
seen on the dark side of the planet. In the model,
X-Mode radiation is emitted in a thick-walled
hollow-cone beam from each point within a sector of
the so-called auroral radio ring. The axis of each
hollow cone is tangent to the magnetic field at
the emission point. The radio ring at each observed
frequency is located just above the intersection of
the $L=17$ shell with the contour surface on which
the electron cyclotron frequency equals that
observed. The overall emission beam at a given
frequency is thus the sum of the hollow-cone beams
from all source points lying in the active sector
of the ring. With optimized sets of the adjustable
parameters, reasonably good fits to the main
features of the observed modulation patterns were
obtained. The Uranian radio emission, the Auroral
Kilometric Radiation (AKR) from Earth, the emission
from Saturn, and that from Jupiter are compared in
this frequency range. An electron density profile
model based on the similarity of the Uranian
emission to AKR was obtained.

J4-7
1040

INTERFEROMETRIC PHASE SCINTILLATION IN THE IPM
B. Dennison[1,2], S. Ananthakrishnan[3], R. S. Simon[2],
R. L. Fiedler[2]
1  Virginia Polytechnic Institute & State University
   Blacksburg, VA 24061
2  E. O. Hulburt Center for Space Research
   Naval Research Laboratory
   Washington, DC 20375
3  Tata Institute of Fundamental Research
   Ooctacamund 643 001, India

Using a global VLBI array operating at 327 MHz, we find strongly correlated scintillations in the fringe phase obtained on various baselines.  The magnitude of the fringe phase scintillations is approximately proportional to baseline length.  Cross correlation of the fringe phase on different baselines reveals maximum correlation at some small lag, whose value is dependent upon baseline pair.  We find that the lags of maximum correlation (for different baseline pairs) are fit very well by a model in which the phase fluctuation pattern is moving across the array with fixed velocity.  Since the fit velocity is 410 km/s, almost radially outwards from the sun, we confirm that the interplanetary medium is responsible.  The implied phase power spectrum is in good agreement with other observations.

These  results  have  important  implications  for  VLBI, particularly at low frequencies.  These implications will be discussed for existing arrays, as well as planned extensions into space.

J4-8      **THE GALACTIC PLANE AT 30.9 MHz**

1100      Namir E. Kassim

Astronomy Program

University of Maryland

College Park, MD 20742

The Galactic plane has been mapped with the Clark Lake TPT telescope at a frequency of 30.9 MHz with unprecedented resolution. The synthesized beam at the zenith is $13.0 \times 11.1$ arc–minutes. Contour maps have been produced for the region $350° < l < 250°$ with $|b| \leq 2° - 3°$, and a source list of nearly 700 discrete emission sources accompanies them. The survey has permitted the study of the interaction between small–scale Galactic nonthermal emission processes and their absorption by intervening ionized gas which was not possible with earlier lower resolution surveys.

Results from this study which will be presented include:

1. New SNRS. More than 60 discrete nonthermal sources which have been catalogued are probably either previously unidentified or missidentified Galactic SNRs. If so, these candidates could significantly increase the number of catalogued SNRs.

2. Known SNRs. The survey has permitted the construction of the accurate low frequency spectra of known Galactic SNRs. From these, low frequency optical depths towards 51 SNRs have been derived and used to determine the distribution of ionized gas in the ISM. Patchiness in the absorption towards distant SNRs places an upper limit on the density of any hot ($T \sim 8000K$), widely distributed ionized component of the ISM at 0.25 $cm^{-3}$. Taken together with 325 MHz recombination line observations, they indicate the presence of hot ($T \sim 3000 - 8000K$), low density ($n_e \sim 1 - 10$ $cm^{-3}$) ionized gas, probably associated with the outer envelopes of 'traditional' HII regions.

3. Numerous foreground HII regions were detected in absorption against the Galactic background. Combined with lower resolution observations these measurements have permitted a determination of the strength of the Galactic background and foreground emission towards the HII regions.

4. Patchiness in the distribution of extragalactic source counts at higher longitudes has been used to infer the presence of a low density ionized halo associated with a known HII region in the outer Galaxy.

5. No prominent new sources with steep spectra similar to the millisecond pulsars PSR $1937+21$ and PSR $1821-24$ have been found. This indicates that any such similar sources located along the Galactic plane must be at significantly lower flux densities.

Composite maps of the entire survey will be shown and a qualitative discussion of their morphology as a function of Galactic longitude will be given.

J4-9    THE LOW FREQUENCY SPACE ARRAY
1120

K.W. Weiler[1], B.K. Dennison[1,2], W.C. Erickson[3], K.J.
Johnston[1], M.L. Kaiser[4], R.S. Simon[1], and J.H.
Spencer[1]
1E.O. Hulburt Center for Space Research, Naval
 Research Laboratory, Washington, DC, 20375-5000
2Virginia Polytechnic Institute and State
 University, Blacksburg, VA, 24061
3University of Maryland, College Park, MD, 20742
4NASA Goddard Space Flt. Ctr., Greenbelt,MD 20771

At the lowest radio frequencies ($\leq$30 MHz), the Earth's
ionosphere transmits poorly or not at all.  This relatively
unexplored region of the spectrum is thus an area where high
resolution, high sensitivity observations can open a new
window for astronomy.  Also, extending observations down to
such very low frequencies approaches a fundamental physical
limit where the Milky Way becomes optically thick due to
diffuse free-free absorption.
     To obtain data at these frequencies requires the
difficulty and expense of placing radio telescopes into Earth
orbit, but the scientific rewards of a space mission are
likely to be great.  Even without considering the seren-
dipitous discoveries which have always accompanied the opening
of a new realm of frequency, resolution, or sensitivity in
astronomy, a low frequency telescope in space can:

1. map the entire sky, particularly the galactic
   background non-thermal emission;
2. survey the galactic diffuse ionized hydrogen
   absorption;
3. study of the interstellar plasma scattering
   and refraction;
4. study individual source spectra for energy
   production and absorption/loss mechanisms;
5. study the correlation between steep spectrum
   galaxy clusters and enhanced x-ray emission;
6. search for "fossil" radio sources;
7. image individual sources with high resolution;
8. study the impulsive emission from Jupiter and
   the Sun; and
9. search for cosmic coherent radiation.

A scientific justification and technical description is
developed for a Low Frequency Space Array (LFSA) operating at
deka-hectometer wavelengths to carry out high resolution, high
sensitivity full sky mapping and individual source imaging at
frequencies between 1.5 and 26.3 MHz.

J4-10
1140

# LOW-FREQUENCY RADIO ASTRONOMY WITH SMALL SATELLITES

D.L. Jones, T.B.H. Kuiper, M.J. Mahoney, and R.A. Preston
Mail Code 238-700
Jet Propulsion Laboratory
4800 Oak Grove Drive
Pasadena, CA. 91109

There are many important astrophysical questions which could be answered with observations at frequencies of a few MHz and angular resolution of an arcminute or better. Such data can be obtained with an interferometer array composed of several small satellites in Earth orbit.

A workshop was held at JPL in May 1987 to consider how small and simple the individual satellites for such a mission could be. Since then two spacecraft designs have been studied: 1. cylindrical, gravity gradient stabilized, with two orthogonal dipoles in the horizontal plane, and 2. spherical, unstabilized, with three orthogonal dipoles. In either design the satellites contain uncooled receivers for frequencies below $\approx$ 15 MHz, nearly omnidirectional antennas, a high quality crystal oscillator, and a low power telemetry transmitter. There are no gyros, thrusters, data recorders, or other moving parts, and no expendables. The weight of each satellite could be as low as 35-45 kg. This is important because the performance of the array depends strongly on the number of satellites.

For satellites without thrusters, careful deployment with velocities $\approx$ 1 cm/s is essential. Deployment is particularly simple in the case of spherical satellites, which can be dispersed spherically from the launch bus. This requires no special orientation of the bus. The array would then slowly disperse under the influence of the deployment velocities and various differential drag forces. In a 30000 km altitude circular orbit it should take at least a year for the size of the array to exceed 200-300 km, the maximum useful baseline length at a few MHz. For orbital heights $\geq$ 10000 km, a single small ground antenna could receive data simultaneously from all satellites in the array.

A number of specific areas are still being studied, including the optimal orbital parameters, radiation hardening (if a $\approx$ 10000 km orbit is chosen), methods for accurately determining the three-dimensional configuration of the array as a function of time, sensitivity limits, and the effects of man-made interference on data calibration.

Session A-5    1355-Thurs.    CR1-42
EMI MEASUREMENTS AND STANDARDS
Chairman: Edward K. Miller, Rockwell Science Center, Thousand Oaks, CA
91360


A5-1        NBS CALIBRATION PROCEDURES FOR HORIZONTAL DIPOLE
1400        ANTENNAS (25 to 1000 MHz)
            Dennis Camell and Ezra Larsen
            Electromagnetic Fields Division, 723.03
            National Bureau of Standards
            Boulder,CO 80303

     The theoretical basis and test procedures for
horizontally polarized dipole calibrations at the National
Bureau of Standards will be described.  Two different
techniques and two different test sites are used for these
measurements.  The standard antenna method uses the
calculation of a field strength level, from the response of a
simple half-wave dipole, to calibrate an antenna.  This
method is used at an open field site in the frequency range
of 125 to 1000 MHz.  The standard field method applies the
theoretical gain equations of waveguides to determine the
field strength level.  This latter method is used in an
anechoic chamber in the frequency range of 200 to 1000 MHz.
Procedures for both techniques are explained and measurement
setups are illustrated.  Measurement uncertainties are
discussed.

A5-2     ELECTROMAGNETIC SUSCEPTIBILITY TESTING OF ELECTRONIC
1420     SUBSYSTEMS BY DIRECT INJECTION*
         R. J. King and W. Ng
         Lawrence Livermore National Laboratory
         Livermore, California  94550

The lack of realistic threat-level transient electromagnetic simulators in the HF through the microwave frequency range mandates the development of clever techniques for evaluating the susceptibility of electronic subsystems. Even if such pulsed simulators existed, cost and size would limit the range of threat environment parameters, such as spectral frequency components which can be generated, threat engagement angles, polarization, and peak fluence levels. Therefore, there is strong motivation to:

(a) measure coupling down to the input terminals of a subsystem using low level (linear) cw techniques, and then

(b) use this information to properly inject high power pulses directly into the subsystem to achieve burnout or upset, and thereby establish susceptibility threshold levels. Having established such thresholds, there is a need to verify that the electronic subsystems can survive a real threat for full system analysis.

Accomplishing step (a) is now relatively routine.  Step (b) is a new challenge which this paper addresses.

A proposed direct injection technique for testing the electromagnetic susceptibility of electronic subsystems is outlined.  This technique accounts for the highly complex structure of the threat signal appearing at the terminals of the subsystem, and permits the susceptibility level to be precisely and continuously measured over a wide frequency spectrum.  It takes advantage of the high precision attainable from modern frequency domain instruments, as well as time domain pulsing to account for heat build-up within susceptible electronic components.  The technique uses linear cw coupling measurements made at the cable terminals which feed the subsystem.  It therefore includes the effects of the external EM threat parameters, e.g., spectral intensity of frequency components, polarization, and incidence direction.  Besides being useful for establishing electronic breakdown thresholds, the technique can be used for full system analysis to verify that the electronics can survive an assumed threat.

The instrumentation system is fully automated for data acquisition and control of test parameters.  Testing up to 200 W peak power has been done over the 1 to 18 GHz range, but the technique is sufficiently general that it can be adapted to any frequency range.

A5-3      ALTERNATIVE TECHNIQUES FOR SOME TYPICAL
1440      ELECTRIC FIELD MEASUREMENTS IN A SCREENROOM

J. E. Cruz and E. B. Larsen
Electromagnetic Fields Division
National Bureau of Standards
Boulder, Colorado 80303

This report deals with alternative techniques for several types of screenroom measurements to be considered by the U.S. Army for more accurate electromagnetic compatibility (EMC) testing. Most testing is performed in a shielded enclosure (screenroom) which leads to uncertainty in the measurement of emissions from electronic equipment, or the susceptibility of equipment to electromagnetic (EM) radiation. Possible alternative techniques for improved measurements in a screenroom have been developed by the National Bureau of Standards (NBS). These techniques are covered in this talk.

We present antenna factors determined in a screenroom which was partially loaded with radio frequency (rf) absorbing material, using the two-antenna insertion-loss technique. These antenna factors are compared with the antenna factors obtained in an unloaded screenroom, a fully loaded screenroom (anechoic chamber), and at an open field site. In addition, measurements at the eight corners of a cube were made in the partially loaded and fully loaded screenroom to determine the field deviation at the eight corners of the cube with respect to its center. Also, measurment improvements are quantified for electric field strength beneath a single-wire transmission line, in a partially loaded screenroom. Finally, electric field measurements were made on top of the grounded table in a partially loaded screenroom to determine the field strength variation above the table.

## ANALYSIS OF MODE STIRRED CHAMBERS USING GEOMETRICAL OPTICS

John M. Dunn

Department of Electrical and Computer Engineering
University of Colorado
Box 425
Boulder, Colorado, 80309

Mode stirred chambers are presently under consideration at a number of research laboratories as an attractive alternative to the more conventional anechoic chambers for use in the testing of systems in various electromagnetic environments (M.T. Ma et. al., Proc. of IEEE, 73(3), 388–411, 1978), (P.C. Corona et al., IEEE Trans. EMC, 18(2), 54–59, 1976). The mode stirred chamber typically consist of a rectangular test chamber with metal walls, and a stirrer, usually in the form of a large paddle or fan blade, near the ceiling of the chamber. The object under test is placed in the chamber and exposed to an electromagnetic field, during which time the stirrer slowly revolves. The average response of the object to the field is found by integrating the response over the time period of one revolution of the stirrer. The metal walls of the cavity allow a large field to be built up inside the cavity. At the same time the stirrer smooths out the sharp nulls of the field, usually present in such a resonant structure. The object under test can therefore be exposed to a high field level consisting of several different polarizations. It is therefore possible to test the object in a matter of hours instead of days.

The conventional thinking in the study of such chambers has been to decompose the field into a series of modes without the stirrer present, and to then regard the stirrer as coupling or mixing the various modes together, thus the name mode stirred chamber. It is shown that there are a large number of modes present in the chamber for reasonably high frequencies, typically several hundred. It is then not possible to carry the analysis much farther, and a random field is assumed. It is then possible to derive an approximate value for the Q of the chamber (B.Liu, et. al., NBS tech. note 1066, 1983).

The same formulas for the Q of the chamber can be derived in an alternative way using geometrical optics. This method has two advantages over the more conventional method of analysis using modes. The first is that the technique can be extended to chamber shapes other than rectangular. The second it that the posssibility of a better physical understanding of the fields in the chamber can be reached, leading to the possiblility of better chamber design.

In this talk, I will first explain the geometrical optical method of calculating the chamber Q, and will then go on to explain how a number of better designs are suggested.

A5-5      THE EFFECT OF A LARGE ROTATING SCATTERER
1540      IN A RECTANGULAR CAVITY
          D. I. Wu
          Electromagnetic Fields Division 723.03
          National Bureau of Standards
          Boulder, CO   80303
          D. C. Chang
          Department of Electrical and Computer Engineering
          University of Colorado
          Boulder, CO   80309

In a mode-stirred chamber, the field in the cavity is perturbed with a stirrer, i.e. a rotating scatterer, in such a way that it is uniformly random.  This uniformity feature is the governing characteristic of the mode-stirred (or reverberating) chamber widely used in the area of electromagnetic interference testing.  To establish a design guideline for the stirrer, it is essential that we understand the key mechanism which produces this uniform randomness. Since it has been shown that a small resonating stirrer of dimension less than a wavelength can not produce a statistically uniform field (D. I. Wu and D. C. Chang, URSI/AP Symposium, URSI Abstracts, p.55, June 1986), in this analysis we focus on the effect of a large body stirrer.

In treating a large body scatterer, we begin by examining the fundamental properties associated with a perturbing body in a cavity.  Using the concept of perturbation, we find that the key to effective perturbation lies not so much in resonance but in the shifting of eigenmode frequencies.  When the size of the perturbing body becomes large, the shifting may be large enough that the new perturbed modes no longer resemble the original unperturbed modes.  In effect, as the stirrer rotates, different perturbed modes may be excited, thus introducing randomness into the system.  To capture the essence of effective field perturbation as well as to minimize numerical complexity, we revert to a two-dimensional case for illustrative purposes.  The numerical complexity is further simplified by the use of a 2D Transmission-Line-Matrix (TLM) method.  The TLM method is a time domain numerical method where the propagation of plane wave in any medium or structure is modeled by a Cartesian mesh of transmission lines.  Plane wave propagation is manipulated by monitoring the voltage and current at every node throughout the mesh as time progresses.  The response in the frequency domain is obtained by performing the discrete Fourier transform on the output function.  Using the TLM method, the shifting of eigenfrequencies and the variation on the magnitude of the fields for different stirrer sizes are examined.  From this analysis, useful insights are drawn which include an analogy between the action of a large rotating scatterer and a frequency modulator.

A5-6
1600

# AIRCRAFT FIELD DEGRADATION AND ELECTROMAGNETIC COMPATIBILITY

Kenneth H. Cavcey and
Dennis S. Friday
Electromagnetic Fields Division
National Bureau of Standards
Boulder,Colorado 80303

This paper discusses the first tests undertaken to study the problem of field degradation in army aircraft (helicopters and one fixed wing airplane) due to the deterioration of electronic and electrical systems. The electromagnetic compatibility (EMC) of such systems were investigated by considering the aircraft as a collection of radio frequency sources. Methods to detect these sources were developed including the non-stationary noise that existed.

Next the collected data was studied to see if there existed any obvious factors derived from the data that one could use to correct potential problems that might affect flight safety. Emphasis was placed upon making such test methods appropriate, inexpensive, and easily performed by army field personnel. In addition applications to quality control or acceptance testing, as related to the Environmental Stress Screening (ESS) program, are examined.

B/F1-1    AN EXAMINATION OF THE "FULL-WAVE" METHOD FOR
1400      ROUGH SURFACE SCATTERING

Eric. I. Thorsos
Applied Physics Laboratory
College of Ocean and Fishery Sciences
University of Washington
Seattle, WA 98195

Akira Ishimaru
Department of Electrical Engineering
University of Washington
Seattle, WA 98195

The accuracy of Bahar's "full-wave" solution for scattering from rough surfaces (E. Bahar, IEEE Trans. Antennas. Propagat., AP-28, 11-21, 1980; Eqs. 4.10 and 6.5b) is examined for the case of the Dirichlet (zero field) boundary condition using one dimensional surfaces with a Gaussian roughness spectrum. This corresponds to scattering of horizontally polarized electromagnetic waves from perfectly conducting rough surfaces. The field quantity calculated is the bistatic scattering cross section, which is obtained with a Monte Carlo technique. The full-wave solution is compared to that obtained with the Kirchhoff approximation, with first order perturbation theory, and with exact numerical results obtained by solving an integral equation. The full-wave solution is found to agree closely with the Kirchhoff solution, except for grazing incident and scattered angles. The full-wave solution does not reduce to the first order perturbation solution as the rms surface height and slope become small. Also, exact numerical results begin to diverge from the Kirchhoff results as the surface correlation length is reduced below the radiation wavelength; in this region the full-wave solution continues to agree closely with the Kirchhoff solution, except for grazing incident and scattered angles. In summary, we find that the full-wave method is not an improvement over the Kirchhoff approximation for this case.

B/F1-2    A SIMPLE MODEL OF THE BACKSCATTER ENHANCEMENT
1420      EFFECT FOR RANDOM ROUGH SURFACES
          F. K. Schwering
          US Army CECOM, ATTN:  AMSEL-RD-C3-TA-1
          Fort Monmouth, NJ    07703

The backscatter enhancement effect is analytically demonstrated for a simple model of a random rough surface.  The model consists of a planar metal surface with a random distribution of scatter centers in the form of vertical dipoles (Fakir's bed).  For simplicity, the two-dimensional problem is treated where the dipoles are replaced by parallel, vertical ridges as indicated in Fig. 1; the incident plane wave is TM-polarized with regard to the ground plane.  The dipoles or ridges are assumed to be loss-less passive scatterers; the dipole moment per unit length of the $n$th ridge is $p_n = \alpha E_{zn}$ where $\alpha$ is a constant, which is the same for each ridge, and $E_{zn}$ is the vertical electric fieldstrength at the locaton of the $n$th ridge generated by the sum of the incident plane wave, the specular wave reflected by the ground plane, and the scatterfields of all other ridges.

The scatter problem for this surface is solved by an iterative procedure where the first term represents single scattering, the second term double scattering, etc.  These terms and the associated power patterns are obtained in the form of multiple sums which, however, can be substantially simplified on careful inspection.  In particular, the second order theory has been reduced to closed form analytical expressions.  The backscatter enhancement appears quite natural in this representation and no special effort is needed to extract it from the formulas.

The theory shows that, as expected, the backscatter enhancement is caused by second and higher order scattering, and that the maximum enhancement is limited to 3 dB which occurs when multiple scattering dominates over single scattering.  The theory shows, furthermore, that the backscatter enhancement will be clearly visible only if the average spacing d of the scatter centers is in the order of a wavelength or more while it becomes obscured as d is reduced.  Also, the backscatter lobe is much broader than the forward scatter lobe (which is caused by single scattering).  For given overall size of the scatter surface, the width of the forward lobe is independent of d, while the width of the backscatter lobe increases with $\sqrt{\lambda/d}$ as the number of scatter centers is increased and d is reduced.

Fig. 1

B/F1-3          EMISSIVITY OF A HALF SPACE ANISOTROPIC
1440                      RANDOM MEDIUM

Jay K. Lee and Saba Mudaliar
Department of Electrical and Computer Engineering
Syracuse University
Syracuse, NY 13244-1240
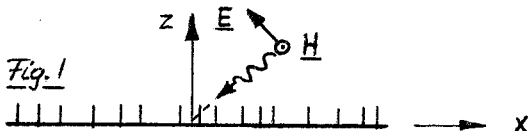
A model for calculating the emissivity of a half space anisotropic
random medium is presented here. We follow the multiple scattering
approach using the Dyson equation for the mean field along with the Bethe-
Salpeter equation for the covariance of the electric field. The modified
radiative transfer (MRT) equations thus constructed are solved under a
first order approximation to obtain the upward- and downward-travelling
incoherent intensities. The procedure is the same as followed by the
authors for calculating backscattering coefficients for the above-mentioned
medium (URSI Meeting, Blacksburg, VA, 1987). We provide analytic expres-
sions for bistatic scattering coefficients and compare them with those
obtained by the Born or single scattering approximation (Lee and Kong,
IEEE Trans., GE-23, 924-932, 1985). The structure is exactly the same
except for two changes. The single most striking feature observed due
to a multiple scattering approach is that the propagation constants which
appeared in the Born approximation results are replaced by "effective"
propagation constants. This is exactly what one would expect under the
first-order approximation to the MRT equations.

Secondly, we notice that there are some modifications in the terms
which contribute to backscattering. We observe that these are due to
"backscattering enhancement," which is a unique result of the wave theory
as compared to the phenomenological radiative transfer theory.

Using these expressions for bistatic scattering coefficients we
proceed to compute the emissivity through $e = 1 - r_c - r_i$ where $r_c$ is the
coherent reflectivity and $r_i$ is the incoherent reflectivity obtained by
integrating the bistatic scattering coefficients over the upper hemisphere.
A number of numerical results are presented to facilitate comparison with
the corresponding single scattering approximation results. Finally the
theoretical results will be used to explain a set of measured emissivity
data of terrain media which are electrically anisotropic and highly
scattering.

B/F1-4      BACKSCATTERING ENHANCEMENT BY RANDOMLY
1500        DISTRIBUTED LARGE PARTICLES
            Yasuo Kuga and Akira Ishimaru
            Department of Electrical Engineering
            University of Washington
            Seattle, Washington  98195

The experimental evidence of the backscattering enhancement due to randomly distributed particles was first reported by Kuga and Ishimaru (J. Opt. Soc. Am. A, 1, 831, 1984) and later by other groups. This enhancement was caused by the constructive interference of two waves traveling through identical multiple scattering paths in opposite directions. It is also known as the weak Anderson localization effect in solid state physics. We call this backscattering enhancement type I. The characteristics of enhancement type I are (1) it is most visible when the particle size is comparable to the wavelength, (2) the peak is observable only in densely distributed particles, and (3) the angular width of the peak is less than $0.1 - 0.2$ degrees and it is related to the transport cross section. When the particle sizes become much larger than the wavelength, backscattering enhancement type I is not observable. However, it has been indicated previously that the backscattering enhancement can be caused by large particles and turbulences (Kravtsov and Saichev, Sov. Phys., 25, 1982). This enhancement is also known as the double-passage effect and focusing effect. It has been indicated that this enhancement may occur in sparsely distributed random media, and therefore, it may be important for remote-sensing applications. We call this backscattering enhancement type II. In this paper we will show the experimental evidence of backscattering enhancement type II. The experiment was conducted using large particles (45 μm) and a HeNe laser ($\lambda = 0.475$ μm in water). Both the co-polarized and cross-polarized components were measured for optical distances of 0.5 to more than 100. Unlike enhancement type I, type II is most visible around a particle concentration of 1% and an optical distance of 15. It disappears in a dense concentration of particles. The shape of the peak in the cross-polarized components is substantially different from the one in the co-polarized components. The differences between enhancement types I and II will be discussed.

B7-1      USING THE EFIE IN THE PRESENCE OF CAVITY
1540      RESONANCES
Francis X. Canning
Rockwell International Science Center
Thousand Oaks, CA 91360

Hollow, perfectly conducting bodies support internal resonances at discrete frequencies, at which the total current flowing on the surface cannot be determined by the EFIE and the incident external field. The undeterminable component of the surface current, i.e., that associated with the cavity mode, does not radiate, so the scattered fields are determined by the EFIE.   However, it has been widely reported that Method of Moments (MoM) calculations based on the EFIE have severe numerical problems at such resonant frequencies. One may ask if a different numerical procedure, based on the EFIE, would circumvent these problems.   We will demonstrate such a procedure.   In addition, we will gain insight into the mechanisms by which moment method calculations based on the EFIE often fail near these resonant frequencies.

A matrix algebra technique called the Singular Value Decomposition (SVD) is used.   While the algorithms implementing this technique have existed for decades, this author's literature search found no references to its application to moment method problems. One purpose of this paper, therefore, is to describe how SVD applies to moment method problems, and to describe the information it provides about the MoM matrix.

We begin by describing what is known theoretically about the matrices used in the moment method.  We find that close to the resonant frequencies the numerical problem comes from a term that can be isolated. This term is the product of three numbers, two of which are close to zero and one which is very large. Numerical calculations are performed on a trivial test case, that of scattering by a conducting circular cylinder. The SVD is applied to these calculations, showing the cause of the numerical problems.  This detailed information suggests possible solutions, which we explore.

A HYBRID E-PULSE/LEAST SQUARES TECHNIQUE
FOR NATURAL RESONANCE EXTRACTION

E. Rothwell, K. M. Chen, D. P. Nyquist
and W. Sun
Department of Electrical Engineering and
Systems Science
Michigan State University
East Lansing, MI 48824

Interest in using natural resonances in the
discrimination of radar targets has prompted the
need for an efficient, automated technique for ex-
tracting the complex resonance frequencies of a tar-
get from a measurement of its transient response.  A
new scheme based on the E-pulse technique has been
developed, and is found to have the additional bene-
fits of random noise and mode content insensitivity.

An E-pulse waveform is defined to be a finite
duration signal which when convolved with a sum of
damped sinusoids produces a null result in the late-
time.  If $m(t)$ represents the measured transient
response of a target (assumed to be a finite sum of
damped sinusoids in the late-time), then the E-pulse
waveform $e(t)$ is the solution to the convolutional
integral equation $m(t)*e(t)=0$, $t>T_L$, where $T_L$ is the
beginning of late-time. The natural frequencies con-
tained in $m(t)$ are then the solutions to $E(s)=0$,
where $E(s)$ is the Laplace transform of $e(t)$.  By an
appropriate representation of $e(t)$, $E(s)=0$ becomes a
polynomial equation.

As there are many possible solutions for $e(t)$,
it becomes prudent to define the "best" solution as
that which minimizes the squared difference between
the measured waveform and a waveform constructed
using the natural frequencies found from solving
$E(s)=0$.  This criterion becomes the basis for an
automated method for determining the natural frequen-
cies which is insensitive to the presence of random
noise and to estimates of modal content.

Examples using the measured responses of various
radar targets are considered.

# The Calculation and Identification
## of the
## Complex Natural Resonances
## of a
## Circular Strip

*Jeffery T. Williams*

Applied Electromagnetics Laboratory
Department of Electrical Engineering
University of Houston
Houston, TX 77004, USA

*Donald G. Dudley*

Electromagnetics Laboratory
Department of Electrical and Computer Engineering
University of Arizona
Tucson, AZ 85721, USA

The circular strip is an ideal canonical scattering structure for use in system and target identification studies and in transient antenna range experiments. It offers a tractable theoretical solution, and it is relatively easy to model experimentally. In addition, the circular strip supports two distinct species of natural resonances: exterior resonances and interior resonances. The interior resonances suffer little radiation damping, whereas, the exterior resonances are more highly damped. Therefore, the circular strip provides an excellent model in which to compare the relative contributions of strong natural resonances and weak, highly damped resonances.

An electric field integral equation is formulated in terms of the current induced on the surface of the strip and solved using the method of moments (MOM). Using the MOM formulation, we determine the natural resonances of the circular strip. We show the pole trajectories for the first layer of exterior resonances for a wide range of strip height-to-radius ratios. In addition, we locate the strong interior resonances and relate them to the $TM_{0pq}$ modes of the circularly cylindrical cavity. We find that the interior resonances which correspond to the $TM_{0p0}$ cavity modes are weakly damped, dominating the scattered field response.

Using the transient scattered fields calculated from the MOM formulation as input and output data for a single input, single output identification algorithm, we identify the dominant poles in the scattered fields. We show that these dominant poles are those associated with the $TM_{0p0}$ interior resonances of the circular strip. We also show that by using intelligent filtering and source selection, resonances with higher damping can be identified.

# NATURAL RESONANCE EXTRACTION USING THE FINITE ELEMENT METHOD-DIELECTRIC PROLATE SPHEROIDS

Philip J. Moser
AVTEC Systems, Inc.
3025 Hamaker Court
Fairfax, VA  22031-2217

Michael A. Morgan
Naval Postgraduate School
Monterey, CA  93943

Anton Nagl and Herbert Uberall
The Catholic University of America
Washington, D.C.  20064

The Finite Element Code for Electromagnetic Scattering (M.A. Morgan and K.K. Mei, IEEE Transactions AP-27, pp. 202-214, 1979) has been adapted for finding resonances of axisymmetric penetrable bodies and applied to solid dielectric spheroids. These resonances are created by creeping waves both in the dielectric material and along its exterior surface and are distinctive to the material composition and body shape (H. Uberall, et al., J. of Applied Physics, September 15, 1985). Because of the flexibility inherent in the Finite Element Method, it is now possible to extend the research for resonances to penetrable bodies and is applicable to both homogeneous and non-homogeneous materials with both real and complex dielectric constants. This method has been applied to homogeneous real dielectric prolate spheroids and resonances found. From the resonances a scheme has been applied using phase matching techniques to obtain phase velocity dispersion curves and attenuation curves. The effects of the resonances on the body's radar cross-section can now be evaluated and their importance in target identification noted.

G5-1       SMALL SCALE ELECTRODYNAMIC STRUCTURE
1400       OF THE HIGH LATITUDE IONOSPHERE

James F. Vickrey
Geoscience and Engineering Center
SRI International
333 Ravenswood Avenue
Menlo Park, CA  94025

Traditionally, the study of ionospheric irregularities
at high latitudes has concentrated on fluctuations in
electron number density and/or integrated electron content.
This emphasis was driven largely by the fact that readily
available experimental diagnostics were limited to scintil-
lation measurements and occasional in-situ langmuir probe
observations.  Over the past several years, our knowledge
of the processes that control the formation and dissipation
of plasma structure have increased greatly.  This is a
result of improved theoretical modeling and more comprehen-
sive diagnostics.  We now know that the evolution of F-
region plasma structure is strongly affected by electro-
dynamic coupling to the E-layer below and to the magneto-
sphere above.  Information about the conditions in these
various altitude regimes is conveyed via electric fields
perpendicular to the geomagnetic field B and by magneti-
cally field-aligned currents.  Thus the spectral character-
istics of density fluctuations are intimately associated
with those of the electric and magnetic fields.  In this
review we will emphasize the electrodynamic coupling
processes along the magnetic field and their consequences
for the evolution of plasma structure.  We will also
present examples of the spectral forms of electric and mag-
netic field fluctuations and discuss the exchange of
Poynting flux between the magnetosphere and the ionosphere
as a function of scale size.

G5-2    NIGHTSIDE UV AURORAL IMAGES AND VHF/UHF
1440    SCINTILLATION
        Santimay Basu, R.W. Eastes, F.P. DelGreco, and
        R.E. Huffman
        Air Force Geophysics Laboratory
        Hanscom AFB, MA 01731
        Sunanda Basu
        Emmanuel College
        Boston, MA 02115

     The ultraviolet (UV) images and VHF/UHF beacon
transmissions obtained with the Polar Bear satellite at
Tromso and Sondrestrom Fjord were utilized to study the
relationship of UV emissions from the nightside aurora and
phase/amplitude scintillations on magnetically quiet days.
Preliminary results indicate that UV images of auroral
structure present near the local magnetic L-shell of the
observing station are associated with moderate enhancement
of scintillations.  This result probably indicates that the
quiet aurora creates weak F-region irregularities.  Under
such magnetic conditions, more intense scintillations are
often associated with increases in total electron content
(TEC).  Closely spaced transits of the HiLat satellite are
utilized to determine the nature of the energetic electron
precipitation.  Spectral characteristics of phase
scintillations associated with UV images are compared with
those observed in conjunction with TEC enhancements.

G5-3    IONOSPHERIC IMAGING USING COMPUTERIZED TOMOGRAPHY
1500    J. R. Austen, S. J. Franke, and C. H. Liu

Department of Electrical and Computer Engineering,
University of Illinois at Urbana-Champaign, Urbana
IL 61801-2991

A two-dimensional image of the electron density in the
ionosphere can be produced from TEC data by using
computerized tomography (CT) techniques.  The imaging of
large-scale structures such as the ionospheric trough and
equatorial bubble should be possible.   Different
reconstruction algorithms will be compared and the effects
of noise on the reconstruction will be discussed  Several
geometries will be compared using a set of ionospheric
models, and factors affecting the ultimate resolution of
this technique will be investigated.  Images produced from
simulated TEC data as well as from actual data will be
presented.

G5-4        Conjugate Radar Studies of High Latitude
1540               Ionospheric Irregularities

R.A. Greenwald, K.B. Baker
Johns Hopkins University/Applied Physics Laboratory
Johns Hopkins Road
Laurel, MD 20707

J.R. Dudeney, M.J. Pinnock
British Antarctic Survey
High Cross Madingly Road
Cambridge, CB3 OET, U.K.

At the present time all authors of this paper except the speaker are in Halley Bay, Antarctica where they are assembling the southern half of the Polar Anglo-American Conjugate Experiment (PACE). The experiment consists of two broadband HF phased-array radars, the Halley radar, which is under construction, and the Goose Bay radar, which has been operating in Labrador, Canada since 1983. These radars have very large magnetically-conjugate fields-of-view from which they are sensitive to ionospheric irregularities with wavelengths ranging from 8-17 m. The goals of the experiment are to examine the conjugate aspects of the irregularity formation, transport and dispersal processses. When it is possible, the conjugate observations of irregularity Doppler motions will also be used to examime the conjugacy of high latitude plasma motions in the ionosphere. In this presentation we will present an overview of the initial research program for the PACE radars and discuss opportunities for collaboration.

G5-5         HIGH LATITUDE HF IONOSPHERIC MODE STRUCTURE STUDY
1600

Nikhil Dave' , Naval Ocean Systems Center,
Ocean and Atmospheric Sciences Division,
Code 542
San Diego, CA 92152-5000

For specified temporal conditions, improvement of HF propagation predic-
tion for frequency management requires knowledge of which ground ranges are
accessible to which frequencies for transmissions on a given bearing from a
point on the earth's surface. Also of interest is information regarding reflecting
layers, number of hops, and path losses for all of the modes reaching a specified
ground range for these conditions. The results of such a study can be displayed
as plots of frequency versus ground range for each time and bearing. Mode
structure is highlighted in terms of 1-hop, 2-hop, and higher modes; path losses
are shown by shading. Much information which would not otherwise be obvious is
conveyed by such a display, thus simplifying the reaching of conclusions regard-
ing the best use of the ionosphere for communication.

As an example, such a study is done based on a HF propagation prediction
program (AMBCOM) for HF transmission originating in Andoya, Norway using a
representative set of frequencies in the HF spectrum. The study is performed
for a selected number of hours, months, and bearings around the transmitter so
as to gain knowledge of propagation patterns as a function of these variables.
Since Andoya is a high-latitude station, it has the property that comparison
between results for north and south bearings can indicate differences between
high-latitude and mid-latitude propagation. Another advantage of studying pro-
pagation around Andoya is that there is some published data of observed max-
imum usable frequencies for this station (Folkestad, K., in Folkestad, K., editor,
"Ionospheric Radio Communications" Finse, Norway, April 13-19, 1967, pp. 279-
288), which can be used for comparison.

Some of the more interesting mode structure diagrams resulting from this
study are presented with discussion regarding implications for usable frequen-
cies. Comparison is made with predictions of less accurate programs such as
HFBC84.

G5-6
1620

NEED FOR AN ANTARCTIC INCOHERENT SCATTER RADAR
TO EXPLOIT HEMISPHERIC DIFFERENCES TO STUDY
HIGH-LATITUDE PHENOMENA

Vincent B. Wickwar
Geoscience and Engineering Center
SRI International
Menlo Park, CA  94025

To understand the upper atmosphere, particularly the
very complex high-latitude phenomena, requires observations
made under different conditions, e.g., levels of magnetic
activity, season, and so on.  However, one important set of
differences has not been exploited sufficiently in the quest
to understand the upper atmosphere.  These are hemispheric
differences, including insolation, separation between
geographic and geomagnetic poles, magnetospheric inputs, and
the upward propagation of tides and gravity waves from the
mesosphere.  A strong network of instruments, particularly
incoherent-scatter radars, in the northern hemisphere.  To
take advantage of hemispheric differences will require sig-
nificant additional observational capability at high
latitudes in the southern hemisphere, i.e., in Antarctica.
The instrument that can add the greatest number of ap-
propriate measurements and complement the present
capabilities is an incoherent-scatter radar.

H3-1
1400

SIMULATION STUDIES OF ELECTRON BEAM
INJECTION FROM SPACECRAFT:
OPTIMUM CONDITIONS FOR BEAM PROPAGATION

R. M. Winglee
Department of Astrophysical, Planetary
  and Atmospheric Sciences,
University of Colorado,
Boulder, CO 80309-0391

P.L. Pritchett
Department of Physics,
University of California, Los Angeles
Los Angeles, CA 90024-1547

Electron beams injected from spacecraft have been used over the last ten years to probe the ionosphere and magnetosphere and to investigate beam-plasma interactions. During such beam injections, spacecraft charging can become appreciable and the properties of the beam can become significantly modified as the beam propagates away from the spacecraft. Two-dimensional (three velocity component) electrostatic simulations are used to investigate the optimum conditions for which the beam can most easily propagate away from the spacecraft and maintain a coherent structure. Important factors in determining the spacecraft charging are the ratio of the beam to background density, the beam energy, and the spacecraft size. Even with small spacecraft charging the beam can be subject to disruption due to beam-plasma interactions. Disruption can be partially suppressed if the beam injection is rapidly pulsed. The spatial extent of the plasma perturbations and induced electrostatic wave emissions is discussed.

H3-2
1420

PLASMA OBSERVATIONS IN THE VICINITY OF THE SHUTTLE
L. A. Frank and W. R. Paterson
Department of Physics and Astronomy
The University of Iowa
Iowa City, IA 52242

P. M. Banks and R. I. Bush
STAR Laboratory
Stanford University
Stanford, CA 94305

W. J. Raitt
Center for Atmospheric and Space Sciences
Utah State University
Logan, UT 84322

Outgassing by the Shuttle-Orbiter and electron beams emitted from the Orbiter's bay alter the ionospheric plasma environment. These phenomena have been observed with a plasma analyzer on board the free-flying Plasma Diagnostics Package. This instrument sampled the velocity distributions of electrons and positive ions with energy-per-unit charge between 2 V and 36 kV at distances up to 400 m from the Orbiter. Electron beams emitted from the Orbiter's bay are observed to result in a narrow sheet of energy-degraded electrons on magnetic field lines directly behind the Orbiter. This sheet is oriented parallel to the direction of motion of the spacecraft and to the direction of Earth's magnetic field. The width of the sheet perpendicular to those vectors is approximately 20 m. Outgassing of neutral molecules results in a cloud of gases that surrounds the Orbiter and moves through the ionosphere with an orbital speed of 8 km s$^{-1}$. These gases are subject to collisions with atmospheric gases and to ionization by charge exchange with ambient ionospheric ions. This latter process is responsible for distributions of hot ions, mostly $H_2O^+$, observed during the free flight. These ions are entrained in a long tail, $\gtrsim$ 10 km in length, behind the Orbiter. This population of hot ions may be a source of free energy for plasma waves, e.g., broadband electrostatic noise.

H3-3    QUASI-STATIC ELECTRIC FIELD MEASUREMENTS NEAR THE
1440    SPACE SHUTTLE AT TIMES OF SHUTTLE THRUSTER OPERATION
        John T. Steinberg, Donald A. Gurnett and
        Christoph K. Goertz
        Dept. of Physics and Astronomy
        The University of Iowa
        Iowa City, IA  52242

During the Spacelab-2 mission of the space shuttle, the ionospheric plasma surrounding the orbiter was investigated with the University of Iowa Plasma Diagnostics Package (PDP).  Quasi-static electric fields were measured using a double floating probe.  The electric field measurements reported here are all made when the PDP was over 80 meters away from the shuttle.  Generally, the measured electric field was approximately equal to the motional electric field $\vec{V} \times \vec{B}$, where $\vec{V}$ is the velocity of the spacecraft relative to the ionosphere.  However, at certain times when the shuttle's Reaction Control System (RCS) thrusters were operated, the measured field was reduced in magnitude from $\vec{V} \times \vec{B}$ by up to 20%.  The observed screening of the motional electric field can be explained in the following manner.  Charge exchange reactions between ambient $O^+$ ions and the neutral molecules from the thruster plume will produce pickup ions.  The pickup ions are displaced in the direction of the motional electric field, producing a pickup current, which screens the motional field.  The pickup current is closed by field-aligned currents which are carried by a propagating Alfven wave.

H3-4    DISTRIBUTION OF RADIATED VLF ENERGY
1520    FROM A PULSED ELECTRON BEAM IN THE
         IONOSPHERE
         D. J. Donohue, K. J. Harker, and P. M. Banks
         Space, Telecommunications and Radioscience Laboratory
         Stanford University
         Stanford, California 94305

This talk addresses one of the primary objectives of the CHARGE-3 rocket electron beam experiment, an analysis of VLF wave generation and propagation from pulsed electron beams in space plasmas. Spatial and frequency distributions of the radiated VLF energy will be discussed and a prediction of the optimal locations for ground-based receiving antennas will also be presented.

For the radiated energy calculation, two important tools have been developed. The first is a mathematical treatment of the radiation source characteristics of a coherent electron beam. The solution to a single charged particle orbiting a magnetic field line in a homogenous medium is summed coherently over all electrons in the beam to give the far-field distribution. To examine wave propagtion away from the beam, this field distribution is then treated as a radiation source in a 3-dimensional computer ray tracing program which has been developed for special application to VLF ionospheric propagation. Details of the beam wave generation theory will be presented here while the 3-D ray tracing program will be described in a separate session. Results of the research will be shown in the form of 3-D ray paths and a prediction of the VLF radiation "footprint" and corresponding distribution of electric field intensity.

H3-5
1540

# ELECTRON BEAM EMISSIONS FROM A MOTHER-DAUGHTER SOUNDING ROCKET

B.E. Gilchrist, P. M. Banks, P.R. Williamson, T. Neubert
Space,Telecommunications, and Radioscience Laboratory
Stanford University, Stanford, CA 94305
S. Noble, J. Jost
SRS International, Dickinson, TX 77539
F.T. Djuth
The Aerospace Corporation, El Segundo, CA 90245
W. J. Raitt, N.B. Myers
Center for Atmospheric and Space Sciences
Utah State University, Logan, UT 84322
S. Sasaki
Institute of Space and Astronautical Science
4-6-1 Komaba, Meguro, Tokyo, Japan

During the Charge-2 sounding rocket experiment at White Sands in December, 1985, electron beams with energies of 1 keV and currents from 1 to 40 mA were injected downwards from a mother payload. The tethered daughter payload was propelled out to a distance of 426 m perpendicular to the Earth's magnetic field using a nitrogen thruster source. In addition to electron beam emissions, sequences were performed in which the potential between the mother and the daughter were varied up to 500 V. A 50 MHz pulsed doppler radar was simultaneously operated at Presidio, TX. It viewed the expected 170 - 190 km altitude ionization region perpendicular to B. Results from simultaneous vehicle potential/charging measurements, ground radar observations, and wave-fields monitored from the daughter payload are presented.

Near the mid-point of a long DC beam emission, occurring at 250 km altitude, a 3 second thruster firing was observed to cause unusual and pronounced mother/daughter charging and tether current flow. At the same moment, a radar event was observed from the ground occurring near the range expected for ionization in the 170 - 190 km altitude regime. The sense and magnitude of the change in vehicle potential and current flow indicates that substantially higher electron current was flowing to the mother during this interval. The radar observation indicates a substantial beam escape occurred only in conjunction with thruster firing. It was also observed that the VLF waves stimulated during DC beam emissions were almost identical in spectral shape and intensity to waves observed during potential bias sweep sequences without beam emission. This points to the importance of the return current relative to an electron beam for generation of VLF wave emissions.

H3-6       MODEL OF THE INTERACTION OF A HOLLOW CATHODE
1600       WITH THE IONOSPHERE

M. Dobrowolny and L. Iess
Istituto Fisica Spazio Interplanetario
CNR
00044 Frascati, Italy

    We present self consistent calculations of the expansion of
a plasma source of the hollow cathode type into an ambient plas-
ma. The source is polarized with respect to the surrounding  me-
dium. The model considered is a fluid model with inclusion  of
anomalous friction arising from plasma instabilities. The poten-
tial profiles which are calculated show a very large extent  of
the interaction region. Correspondingly we obtain quite substan-
tial current enhancements with respect to the operation of the
plasma source in vacum.

J5-1     EXCESS IR FLUX IN THE MICROWAVE BACKGROUND: P.L. Richards, Dept.
1400     of Physics, Univ. of California, Berkeley, CA 94720

# RADIO OBSERVATIONS OF QUASAR ABSORPTION SYSTEMS

F.H. Briggs
Department of Physics and Astronomy
University of Pittsburgh
Pittsburgh, PA   15260

The light emitted by high redshift quasars often passes through intervening material that chances to lie along our lines of sight to the quasars. Distinctive patterns of absorption are created which can be discovered and classified through inspection of the quasars' optical spectrum. The absorbers are too distant to be detected photographically, but, in fact, normal galaxies at these redshifts are also undetectable.

The class of absorber that is typified by large column densities of neutral gas is suitable for study at radio wavelengths by observation of the 21cm line of neutral hydrogen (HI). Radio techniques provide unique information that complements the studies performed at optical wavelengths: Autocorrelation spectrometers can obtain high resolution of the velocity structure of the absorber. Very Long Baseline Interferometers (VLBI) can resolve the absorber spatially with fine angular resolution. Combination of radio and optical results produces a measure of the HI spin temperature, which is generally an indicator of the kinetic temperature of the absorbing gas.

The radio source PKS 0458-020 provides a good example of the capabilities of the radio techniques. The background quasar has an emission redshift z = 2.286. An intervening absorber has z = 2.04 which places the frequency of observation of the 21cm line at 467 MHz. Detailed VLBI and VLA study of the radio continuum of the background source shows structure on a wide range of scales from 10 milliarcseconds to 2 arcseconds. Therefore VLBI experiments performed in the absorption line can probe the absorber on these angular scales, which tranlate into distances of 50 pc to 10 kpc at z = 2.04. The observation finds that the absorber extends more than 5 kpc across the line of sight and that the spin temperature is less than 500 K. These properties resemble those of the spiral galaxies that are observed nearby at the present, and support the conclusion that this class of absorber contains gas-rich disk galaxies that are the progenitors of spiral galaxies.

OBSERVATIONS OF QUANTIZATION IN GALAXY REDSHIFTS

J5-3       W.G.TIFFT and W.J.COCKE
1440       Steward Observatory
           University of Arizona
           Tucson, Arizona 85721

The Hubble law, whereby galaxy redshifts are observed to increase for fainter galaxies, is central to modern cosmology. The assumption that the redshift is a Doppler shift converts the Hubble law into a velocity-distance relationship which couples with gravitational theory to provide the framework of expanding universe cosmologies. The assumption of a Doppler basis for the redshift also leads to well known problems, excess motion in clusters and in various other situations requires large amounts of invisible mass. Rarely discussed alternatives are that the redshift might not be entirely Doppler in origin or that the extrapolation of gravitational theory to the scale of galaxies is incorrect or incomplete. Basic tests of the velocity interpretation of the redshift are possible and there is clear evidence that something is indeed wrong.

Among the possible tests, one addresses the question of continuity. Velocity is a continuous variable, is the redshift? The answer to this very basic question appears to be no, the redshift appears to have quantum properties. Evidence for this conclusion comes from studies of absolute and differential redshifts in dynamical systems and globally. 21-cm radio data plays a prominent role in the work. Several studies of accurate redshift differences in isolated double galaxies indicate that the distribution of differences is quantized in steps near 72 km/s. Reproduced below is the cumulative distribution of redshift differences within the three best samples of pairs available. Conventional dynamics predicts a smooth monotonic distribution peaking at zero. Observations yield a quantized distribution and suggests that an exclusion principle could be operating which prevents identical redshifts (zero differences). Analysis of clusters also yields a characteristic 72 km/s periodic pattern. The quantization can be traced to the global level as well, suggesting that the phenomenon is not limited to individual gravitational potential domaines.

The current status of the principal tests will be reviewed. A broad introductory review of the subject is available in Sky and Telescope (January 1987).



Delta V

0       50      100      150      200      250
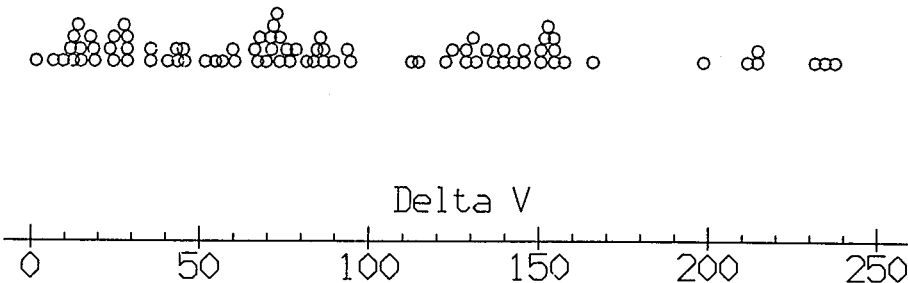
J5-4
1520

A SEARCH FOR MEDIUM-SCALE STRUCTURE
IN THE MICROWAVE BACKGROUND

Peter Meinhold and Philip Lubin
Department of Physics
University of California at Santa Barbara
Santa Barbara  CA   93106

We have built and are testing a stabilized balloon
gondola with a one meter microwave telescope to make meas-
urements of the Cosmic Background Radiation (CBR) anisotropy
on medium angular scales (1 to 10 degrees).

Our radiometer is a liquid Helium cooled Superconduc-
tor-Insulator-Superconductor mixer, operated at 90 GHz (3mm
wavelength), which could optimally give us a sensitivity
of approximately 0.03 mk for temperature fluctuations on
our scale in a 15 hour flight.

Stabilization and tracking are accomplished with an
active servo, controlled by an on-board computer.  Orien-
tation information comes from an inertial gyro system and a
magnetometer, with real time adjustment capability from
the ground.  A star camera is used for absolute reference.

Results of testing of the various systems will be pres-
ented, along with an overview of the experiment and our
flight status.



Gondola Side
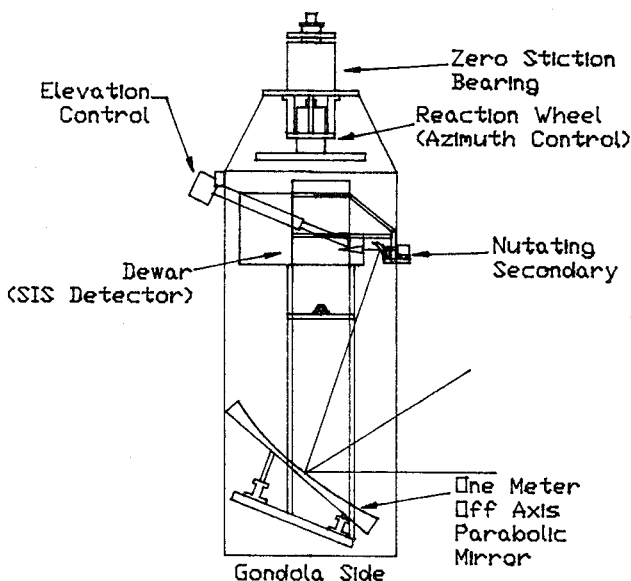
J5-5
1540
OBSERVATIONS OF THE SUNYAEV-ZEL'DOVICH EFFECT: M. Birkinshaw, Dept. of Astronomy, Harvard Univ., Cambridge, MA 02138

J5-6    MICROJANSKY RADIO SOURCE SURVEYS
1600    K. I. Kellermann
        National Radio Astronomy Observatory
        Edgemont Road
        Charlottesville, VA 22903

The VLA has been used at 5 GHz to survey small regions of the sky to determine the density of microjansky radio sources. The most sensitive survey was made in the D configuration to synthesize a 16.5 arc second beam corresponding to an effective aperture of 700 meters. After 80 hours of integration time, the rms noise level was only 5 $\mu$Jy which is close to the value expected from thermal noise fluctuations.

We detected a total of 28 sources above our completeness level of 25 $\mu$Jy corresponding to a source density of about $3 \times 10^6$ sources per sr. We have also analyzed the P(D) distribution to estimate the source density down to one microJy where we estimate that there are about $10^9$ sources per sr. This is only 0.1 percent of the number predicted from an extrapolation of the strong source count based on a uniformly filled static Euclidean model.

At the 25 $\mu$Jy limit of our survey there are about 24 sources per synthesized beam, so the data are clearly confusion limited. Further, even more sensitive surveys are planned using higher resolution to both to reduce the confusion level and to obtain better information on the angular size and structure of the microjansky radio sources.

VERY SMALL-SCALE STRUCTURE IN THE
            MICROWAVE BACKGROUND

E. B. Fomalont
National Radio Astronomy Observatory
Charlottesville, VA   22903-2475

Deviations from isotropy of the Cosmic Background Radiation provide a source of information about the early universe.  At an angular scale of an arcminute or less primeval galaxy and cluster formation may produce fluctuations which can be measured with sensitive instruments.  Even upper limits to such fluctuations can place significant constraints on models of the interaction of matter and energy at early epochs.

The sensitive VLA observations at 5 GHz, described by Kellermann in a companion paper, to determine the density of weak radio sources has been used to determine limits to the structure of the sky emission between 10" to 60" angular scales.  Because of the high density of weak sources, sophisticated modeling methods were needed to distinguish between blends of point sources and possible sky fluctuations.

We find the 2-sigma limit of fluctuations of 0.12 mK on a scale of 60" and a limit of 0.5 mK on a scale of 18".  Recently, another small region of sky has been observed with nearly the same sensitivity.  Limits to the possible sky fluctuations from the new observations are consistent with the above values.

J5-8    OBSERVATIONS OF HIGH REDSHIFT HYDROGEN
1640

Juan M. Uson, K. Anantharamaiah and Durgadas Bagri
National Radio Astronomy Observatory
Socorro, NM 87801

We have used the NRAO–VLA telescope in the P–band to search for the redshifted "21–cm" emission of proto–clusters of galaxies. At the observed frequency of $333.1 \pm 1.6$ MHz the redshift probed is $3.26 \pm 0.02$ .

If baryons are the main massive component of the Universe, the most natural path for the evolution of large–scale structures is the "Top–down" scenario proposed by Sunyaev and Zel'dovich (Astron. Astrophys., 20, 189–200, 1972). In this theory, the first structures to develop as the Universe expands will have masses of the order of $3 \cdot 10^{14}$ M$_\odot$ with an average diameter of 2 Mpc and a line–of–sight velocity dispersion of about 600 km· s$^{-1}$. At a redshift of 3.3, the predicted structures would be between 4' and 7' in diameter, depending on the value of $\Omega$, the density parameter of the Universe and emit a "21–cm" line that should have an observed width of about 500 kHz, with a peak flux between 4 mJy and 15 mJy, again depending on the value of $\Omega$.

We have used the VLA in its "D" configuration. The field of view is determined by the primary beam of the antennas (HPBW = 156') and the "D–array" gives a resolution of about 3'. We observed a "blank" field centered at R. A. = $10^h50^m$ ; Dec. = $68^o$. We used 127 channels with a channel–width of 24.414 kHz, centered at 333.125 MHz. The main source of systematic errors was interference, which determined the observing and data reduction techniques as well as the frequency and band used. We will discuss our choices in some detail.

After subtraction of the continuum (about 11 Jy from many point sources with fluxes up to 1.2 Jy) the channel images have (rms) fluctuations as low as 5.7 mJy, only about 20% above the theoretical sensitivity expected from the useful data collected in 34 hours of observation. At the writing of this *Abstract* the images are still being analyzed. The results will be presented at the meeting.

Session B-8    0835-Fri.    CR2-6
SCATTERING—II
Chairman: Professor D.P. Nyquist, Dept. of Electrical Engineering,
Michigan State Univ., East Lansing, MI


B8-1      SCATTERING FROM A CONDUCTING STRIP USING
0840      THE BIVARIATIONAL TECHNIQUE WITH PHYSICAL
OPTICS TRIAL CURRENTS

R. G. Olsen and G. Ellis
Electrical and Computer Engineering Department
Washington State University
Pullman, WA 99164-2752


E. F. Kuester
Electrical Engineering Department
University of Colorado
Boulder, CO 80302

A number of methods have been used to study
electromagnetic scattering from a perfectly
conducting strip. These include an infinite series
of Mathieu functions, numerical solutions of
integral equations, physical optics and the
geometric theory of diffraction. Until recently,
the variational method has been used almost
exclusively to develop low frequency scattering
formulas.

The purpose of this work was to determine if
the bivariational technique could be used to develop
as simple formula for the high frequency scattering
problem which is significantly more accurate than
the physical optics formula. To do this, physical
optics trial functions for the induced current were
chosen because they can be determined a priori with
a minimum amount of effort. Since these trial
functions often have components of current normal to
the boundary which are discontinuous, they lead to
non-convergent integrals in the standard
bivariational formula. Thus, a new formula was
developed in which the non-convergent term was
subtracted but the variational property was
retained.

Using this formula, a very simple expression
for the radar cross section of a strip was derived.
Numerical results were generated and compared to
numerical solutions of the exact integral equation
and the physical optics solution. It can be
concluded that the bivariational formula is no
better than physical optics and that it suffers from
innacuracies at grazing angles of incidence typical
of the physical optics solution since edge
diffraction currents are neglected in both cases.

241

# Analytic Element Method for EM Scattering from a Metallic Plate

*by A. Q. Howard, Jr.*

*and J. W. Miles*

SCHLUMBERGER WELL SERVICES
HOUSTON, TEXAS 77252-2175

## Abstract

We give a new technique for solving a class of three dimensional electromagnetic scattering problems. This technique, the analytic element method (AEM), is developed to compute the scattered electromagnetic field from a thin planar perfectly conducting plate, with an irregular perimeter and holes. General sources can be easily described, but for numerical examples, plane wave sources are used. In common with finite element methods, scatterer dimensions are required to be no more than a few wavelengths. The numerical method is based upon an **E** field integral equation, which is solved using a generalization of the volume current method where the plate surface current is expanded in raised Bessel functions defined on disc shaped subdomains, or patches. This approach produces a representation of the vector potential which is a continuous function, with continuous derivatives of the observation point coordinates. Consequently, both the integration and differentiation operations occurring in the integral equation are performed analytically. The resulting matrix equation for the plate current amplitudes is full, complex symmetric. Each matrix element $I_{nm}$ contains a monopole and quadrupole current interaction term between the $n^{th}$ and $m^{th}$ surface elements. This interaction factors into a product of radial and angular functions. The angular behavior of the patch interactions is isotropic for the monopole and varies as $\cos 2\phi_{nm}$ for the quadrupole, where $\phi_{nm}$ is the angle between the centers of the $n^{th}$ and $m^{th}$ patches. Such a representation is ideally suited for table look up. The matrix elements are Fourier Bessel numerical integrals which are evaluated on the real axis. Numerical results for the two independent components of the plate current are in agreement with established results.

# DISCRIMINATION OF CONDUCTING PLATES BY E-PULSE TECHNIQUE

W.M.Sun, K.M.Chen, D.P.Nyquist and E.Rothwell

Department of Electrical Engineering & Systems Science
Michigan State University, East Lansing, MI 48824

Rectangular conducting plates of various dimensions have been illuminated by Gaussian pulses at various aspect angles in a time-domain scattering range which was built on a ground plane. Transient responses of the plates were measured and from them the natural frequencies of the targets were extracted by using a hybrid E-pulse / least square technique recently developed at Michigan State University. Invariance of the target's natural frequencies with respect to the aspect angle was studied.

The E-pulses of the plates were synthesized on the basis of their natural resonant frequencies. These E-pulses were then used to convolve with the transient responses of the plates to discriminate among them.

A study is being conducted to study the transient behavior of a conducting plate coated by a layer of lossy material. The effects of the lossy coating on the target's natural frequencies and on the effectiveness of the E-pulse technique to discriminate such targets are investigated.

B8-4   **HIGH FREQUENCY SCATTERING BY A THIN MATERIAL**
0940   **HALF-PLANE AND STRIP**

John L. Volakis
Radiation Laboratory
Department of Electrical Engineering and
Computer Science
The University of Michigan
Ann Arbor, MI  48109-2122

Diffraction coefficients will be presented for a thin
dielectric half plane and strip having arbitrary permittivity and
permeability.  These were derived by modeling the thin material
layer with a pair of modified resistive and conductive sheets
(Senior and Volakis, Radio Sci, 22, 1987).  The resulting integral
equations were then solved via the dual integral equation approach.
Using the half plane solution up to third  order multiple diffraction
coefficients were also generated for the case of a strip.  The
latter were obtained via the extended spectral ray method (Herman
and Volakis, Radio Sci, 22, 335-349, 1987) and include the surface
wave diffraction effects in a uniform manner.  Numerical and
measured results will also be presented to validate the accuracy
of the model and that of the derived diffraction coefficients.

B8-5    COLLECTIVE RAY AND HYBRID RAY-MODE METHOD FOR
1020    SOURCE EXCITED PROPAGATION IN A MULTI-LAYERED MEDIA-
I. FORMULATION

I.T. Lu
Department of Electrical Engineering/Computer Science
Polytechnic University
Route 110, Farmingdale, NY 11735  USA

When source-excited wave phenomena in a layered medium are resolved into travelling wave (ray) constituents, wave coupling at boundaries and interfaces generates a proliferation of wavefields that makes successive tracking impractical for all but a few such encounters.  When wave processes are modelled alternatively by composite layer reflection and transmission matrices, one loses the possibility of tracking some travelling wave constituents individually, as may be desirable.  These observations apply to wave phenomena that emphasize propagation vertically across the layer boundaries as well as to those that emphasize propagation along the layers, as is the case when source and receiver are widely separated in range; in that event, the composite effects may also be presented in terms of the normal modes.  By a more flexible arrangement, one may attempt to retain some ray fields and account for the remaining ones collectively through use of modified collective layer reflection and transmission matrices or through use of some guided modes subject to a remainder field that accounts for truncation effects. Such a hybrid format can actually be constructed self-consistently by utilization of a new and very general Green's function formulation (I.T. Lu and L.B.Felsen, Geophys. J. R. astr. Soc., 84, 31-48,1986).  This formulation is structured so as to permit access to all "interesting" layers (e.g. those containing a source or receiver, or causing significant change of ray phases) but to treat the remaining "uninteresting" ones in "hidden" form.  The general theory is applied here to multilayer dielectrics, with emphasis on the physical interpretation of the various wave processes. Computational aspects are discussed as well.

B8-6    COLLECTIVE RAY AND HYBRID RAY-MODE METHOD FOR
1040    SOURCE EXCITED PROPAGATION IN MULTI-LAYERED MEDIA -
        II. APPLICATION TO GAUSSIAN BEAM INPUT

I.T. Lu and L.B. Felsen
Department of Electrical Engineering/Computer Science
Polytechnic University
Route 110, Farmingdale, NY 11735  USA

Gaussian beams, either individually or as synthesizing basis fields, provide useful models for the response due to Gaussian or more generally shaped high frequency source inputs, respectively. When propagating into a layered environment, an initially well collimated beam undergoes diffusion after successive reflections and refractions, and is converted eventually into the oscillatory pattern of one or more guided modes. Multiple layering accelerates the diffusion process. Utilizing a general matrix Green's function method (Lu, this meeting), this phenomenology is examined here for a plane parallel waveguide filled with a two-layer dielectric, and excited by a sheet beam source in one of the layers. The beam is modeled via the complex source point method whereby a Gaussian-waisted input is generated from a line current by assigning complex values to the source coordinates. This scheme avoids the need for plane wave spectral decomposition and synthesis, but the analytic continuation to complex source coordinates requires precautions which are discussed. Algorithms based on beam tracking, mode summation and a hybrid beam-mode format are presented, and their role in explaining the beam-to-mode transition is emphasized. Numerical implementation illustrates these aspects.

B8-7  COMPUTERIZED RAY-OPTICAL ANALYSIS OF RADIATION THROUGH
1100  THREE-DIMENSIONAL LAYERED RADOMES
      J. S. Bagby, Dept. of Electrical Engineering
      Univ. of Texas at Arlington, Arlington, TX   76019

      A fully-automated, ray-optical technique for calculating the
far-field produced by a phased-array aperture antenna enclosed in
an arbitrary three-dimensional layered dielectric radome is
presented.  This technique utilizes the high-frequency
Geometrical Optics Approximation, and accounts for direct and
singly-reflected rays in the far-field of the antenna system.

      The radome surface shape is described by the user-supplied,
multi-valued function $z = F(x,y)$, and the aperture antenna array
is modeled as a collection of sources with arbitrary pattern,
excitation, and location within the radome.

      Points of transmission and reflection for direct and
singly-reflected rays are determined numerically.  At these
points the fields associated with the rays are decomposed into
parallel and perpendicular polarized components, and the
appropriate planar Fresnel-type layer transmission or reflection
coefficient is applied.  The resultant fields are then summed in
the far-field of the radome to form the radiation pattern.

      This technique is applied to analysis of the far-fields of
the nose radar system of the General Dynamics F-16 aircraft, and
numerical results generated on an IBM PC-XT computer are
presented and compared to measured radiation patterns.
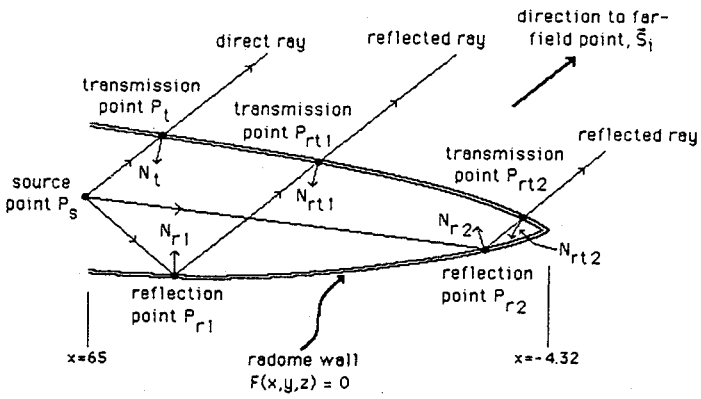
B8-8    A HYBRID METHOD FOR SOLVING TIME-DOMAIN
1120    INTEGRAL EQUATIONS IN TRANSIENT SCATTERING

Anton G. Tijhuis*
Laboratory of Electromagnetic Research
Department of Electrical Engineering
Delft University of Technology
P.O. Box 5031, 2600 GA Delft
The Netherlands

In global techniques for solving transient-scattering problems, the unknown field is to be found from space-time-domain source-type integral equations. Conventionally, two types of techniques have been employed for solving such equations. In frequency-domain techniques, the transient response of the scatterer is represented as a Laplace or Fourier inversion integral, the integrand of which is obtained by solving the corresponding frequency-domain equations. The main advantage of such techniques is that they produce stable and accurate results; their main disadvantage is that the computation time consumed in determining the frequency-domain response typically increases with some integer power of $|\omega|$. In the marching-on-in-time method, one utilizes the property in the time-domain integral equations that the scattered field at each space-time point is expressed in terms of field values at previous instants. Its principal advantage is its numerical efficiency, which is achieved by using the same discretization at all instants; its main disadvantage is that the accumulation of discretization errors may give rise to instabilities.

In this paper, we propose a hybrid method that combines the advantages of both approaches, while avoiding their disadvantages. In this method, we discretize in space only. As in the marching-on-in-time method, we use the same space discretization at all instants. This results in a finite, time-invariant, linear system of equations for the discretized field quantities. From this system, the field is resolved by transforming to the time-Laplace domain, as outlined above. Compared with the marching-on-in-time method, this approach has the advantage that instabilities are inherently avoided; compared with frequency-domain techniques, the advantage is the fixed computational effort required in determining each Fourier component.

Numerical results obtained for some simple scattering geometries will be presented and discussed.

B8-9      COMPUTATION OF A BRANCH-CUT INTEGRAL
1140      ARISING IN TRANSIENT SCATTERING BY A
          PERFECTLY CONDUCTING CYLINDER

K. Naishadham and A. Arnett
Department of Electrical Engineering
453 Anderson Hall
University of Kentucky
Lexington, KY  40506-0046

The time-domain Green's function due to a magnetic line source residing on the surface of a perfectly conducting cylinder has been presented by E. Heyman and L. B. Felsen (*I.E.E.E. Trans. Ant. and Propag.*, AP-31, 426, 1983). The Singularity Expansion Method (SEM) representation of the Green's function involves a branch-cut integral in the complex spectral plane, manifested by the infinite extent of the cylinder. In this paper we discuss an algorithm to compute this integral. The algorithm can easily be modified to compute the branch-cut integral in the SEM representation of the transient field due to a line source, located off the cylinder surface, or due to plane wave excitation.

Numerical computation of the integrand requires determination of the complex zeros of Hankel function of the second kind in the order-plane. These zeros are determined using a complex-order Bessel function subroutine (A.G. Tijhuis, private communication) and a zero-search procedure (B. K. Singaraju, et. al., AFWL Mathematics Note 42) consisting of successive numerical integration of the function along the periphery of rectangular cells into which the search area is divided. The accuracy of the zeros thus determined is checked by comparison with published results. These zeros occur frequently in electromagnetic scattering by circular cylinders, as poles of the amplitudes of creeping waves in the angular wavenumber plane.

The branch cut integral for the problem being considered is evaluated numerically by dividing the integration interval into three subintervals according to the suitability of the appropriate small and large-argument approximations of the integrand. The exponential decay of the integrand for large values of the integration variable $ka$, where $k$ is the wavenumber and $a$ is the cylinder radius, facilitates truncation of the seminfinite integration interval at $|ka| = 10$. For $|ka| \leq 0.01$, the small argument approximations of the Hankel functions and the order-plane zeros are employed to simplify the integrand. For $0.01 < |ka| \leq 2$, the integrand is computed numerically and for $|ka| > 2$, the large-argument approximations are utilized. The branch point at $ka = 0$ is a removable singularity, as can be shown by approximating the integrand over a small circle centered around the branch point, and taking the limit of the integrand as $|ka| \rightarrow 0$. The branch-cut integral is computed for several observation times for an observer location on the cylinder, and the influence of the branch-cut contribution on the early-time response is evaluated.

G6-1        Effects of Multiple Refractive Scattering on
0900            Trans-ionospheric Propagation

Richard A. Sprague
Ocean and Atmospheric Sciences Division
Naval Ocean Systems Center
San Diego, CA 92152-5000

Henry G. Booker
Department of Electrical and Computer Engineering
University of California, San Diego
LaJolla, CA 92037

When the fluctuations of relative electron density within the ionosphere become large, multiple refractive scattering by large scale (greater than the Fresnel scale) irregularities begins to dominate diffractive scattering by smaller scale (Fresnel scale) irregularities. A theory based on the deeply modulated phase changing screen which describes this transition from weak to strong scattering has been presented by Booker and MajidiAhi (Booker and MajidiAhi,J.Atmos.Terr.Phys.,43,1199,1981). Previously, it has been used to predict the effects on HF signals which are below the penetration frequency and are returned to the earth by ionospheric reflection (Booker and Tao,J.Atmos.Terr.Phys.,49,915,1987;Booker,Tao and Behroozi-Toosi,J.Atmos. Terr.Phys.,49,939,1987).

In this paper the theory of multiple refractive scattering is applied to trans-ionospheric propagation of signals from the penetration frequency up to the gigahertz range. The model currently assumes transmission from a satellite in geo-stationary orbit to an earth-bound receiver and assumes a constant representative irregularity drift velocity of 200 m/s. We also assume isotropic irregularity structure. Plots and tables illustrating the effects of scattering on system performance (correlation bandwidth, spatial scale of intensity correlation, etc.) as a function of the strength of the density fluctuations and length of line-of-sight path from receiver to satellite are presented.

G6-2      ASPECT SENSITIVITY MEASUREMENTS OF EQUATORIAL
0920      SPREAD-F IRREGULARITIES AT JICAMARCA
          Erhan Kudeki and Elaine Chapin
          Department of Electrical and Computer Engineering
          1406 W. Green Street, University of Illinois, Urbana, IL 61801
          Donald T. Farley
          School of Electrical Engineering
          Cornell University, Ithaca, NY 14853
          Ronald F. Woodman
          Jicamarca Radio Observatory, Aptd. 3747, Lima, Peru

        The first central moments of the angular spectra of 50 MHz equatorial
spread F radar returns were measured at Jicamarca with a multiple baseline
radar interferometer.  The measurements show to what extent the naturally
occurring 3 meter plasma irregularities are aligned in the ambient geomagnetic
field direction in the equatorial F region, and how the alignment strength varies
as a function of Doppler shift, irregularity lifetimes, turbulence strength, and
other background conditions.  Typical values for the angular half width of the
bottomside spread F irregularities vary between $0.1^o$ and $0.025^o$, close to the
resolution limit of the measurement technique.  The smallest angular half width
observations correspond to instances with strongest signal levels and broadest
Doppler spectra.  When broad and frequency aliased Doppler spectra are
observed, half width values are often independent of Doppler shift.

G6-3
0940

# RADAR INTERFEROMETER OBSERVATIONS OF
# MESOSPHERIC ECHOING LAYERS AT JICAMARCA

Erhan Kudeki and Gary R. Stitt
Department of Electrical and Computer Engineering
1406 W. Green Street, University of Illinois, Urbana, IL 61801

VHF radar observations at Jicamarca show that the most intense mesospheric echoes at the equator are returned from thin horizontal layers of relatively long lifetimes (tens of minutes to hours). A few such layers may be present at a time, and they are typically separated in altitude by a few kilometers. Interferometric studies of radar returns from these layers indicate that the width of Doppler spectra are usually determined by the spatial integration effect of finite size scattering volumes. Returns from lower mesospheric layers appear to be due to randomly distributed scatterers being convected through the observation volume by an essentially non-turbulent wind field. The scatterers in question may possibly be specularity points on corrugated refractive index surfaces. Higher mesospheric layer echoes, however, imply the existence of turbulent flow fields in the vertical plane, with strong eddy motions at scale sizes comparable with the scattering volume dimensions of about a kilometer.

G6-4     SIMULATION AND ANALYSIS OF THE EFFECTS OF
1020     SCINTILLATION PM TRANSIONOSPHERIC
         COMMUNICATIONS SYSTEMS

N. R. Lo, S. J. Franke, and C. H. Liu, Dept. of Electrical and
Computer Engineering, University of Illinois, Urbana, IL 61801

Simulations of transionospheric communication have been carried out.
The simulation consists of two phases.   First, transionospheric
communication channels under different propagation conditions are
generated using a phase screen model with power-law irregularities. The
second phase involves the evaluation of the performance of a phase
modulated digital system in those channels. This second phase is carried
out using COMSIM, a communication simulation software package
provided by Lockheed.  A systematic study has been carried out for
different carrier frequencies, phase variances and power-law indices.
Comparisons will be made for the performance of several types of
modulations.

G6-5
1040

PHASE AND AMPLITUDE FLUCTUATIONS OF A PROPAGATING
ELECTROMAGNETIC WAVE IN THE IONOSPHERE AS A RESULT OF
SCATTERING AND LOSS MECHANISMS
G. R. Akers
E-Systems, Greenville Division
P. O. Box 1056
Greenville, TX  75401

ectromagnetic
wave propagating in an ionospheric attenuative medium are
derived.  The classical electromagnetic wave equation is modified
to account for damping and a perturbation technique for small
ionic inhomogenieties is utilized.  The effect of these ionic
loss mechanisms is apparent in the integral solution as
illustrated in the amplitude and phase fluctuations decaying
spatially.

# A METEOR ECHO PROCESSING SYSTEM FOR ST/MST RADARS

R. L. Obert
S. K. Avery
J. P. Avery
University of Colorado
Department of Electrical and Computer Engineering and
Cooperative Institute for Research in Environmental Sciences
Campus Box 425
Boulder, Colorado        80309-0425

## ABSTRACT

MEDAC (Meteor Echo Detection And Collection) is a radar processing system designed to run in parallel with the normal operation of an ST/MST radar. While normal ST/MST radars use turbulence scatter to determine wind profiles in the lower to middle atmosphere, MEDAC uses scatter from meteor trails to determine atmospheric tidal components from the upper atmosphere.

A brief description of MEDAC's hardware and its interaction with the radar will be given. Results obtained during a campaign at the Poker Flat, Alaska MST radar installation, in which MEDAC was tested and compared with turbulence methods of tidal observations, will also be presented.

H4-1      LABORATORY STUDIES OF ION ENERGIZATION
0900      BY ELECTROSTATIC ION CYCLOTRON WAVES

R. L. Merlino
Dept. Physics & Astronomy
University of Iowa
Iowa City, IA  52242-1479

High latitude satellite observations at ~ 1 $R_E$ have indicated two kinds of energetic ion distributions:  "conics," with peak fluxes between the directions perpendicular and parallel to the geomagnetic field, and highly collimated distributions with peak fluxes along the magnetic field (e.g., Shelley et al., GRL $\underline{3}$, 654, 1976).  Both distributions provide a strong source of $0^+$ ions for the magnetotail.  The ion "conic" distributions are usually attributed to perpendicular ion heating at low altitudes and subsequent magnetic focusing as the energized ions move up the magnetic field lines.

We report here a laboratory study of ion-conic formation by electrostatic ion-cyclotron (EIC) waves.  The experiments were carried out in a single-ended cesium Q-machine with a region of non-uniform (diverging) magnetic field.  The EIC waves are excited by drawing a supercritical electron current in a small current filament along the axis of the device.  Using gridded ion-energy analyzers, we followed the evolution of the ion-velocity distribution as the ions passed through the heating region and subsequently flowed out along the diverging $\underline{B}$ field.  As expected, the ions (heated in the perpendicular direction by the EIC waves) transfer their energy from perpendicular to parallel motion as they travel along the diverging field lines while conserving their magnetic moment.

H4-2
0920

TRANSVERSE ION ENERGIZATION AND LOW FREQUENCY
PLASMA WAVES IN THE MID-ALTITUDE AURORAL ZONE
W.K. Peterson and E.G. Shelley
Lockheed Palo Alto Research Laboratory
S.A. Boardsen and D.A. Gurnett
The University of Iowa
B.G. Ledley
NASA Goddard Space Flight Center
M. Sugiura
Koyoto University
T.E. Moore and J.H. Waite, Jr.
NASA Marshall Space Flight Center

The transport of ions from the ionosphere to the
magnetosphere requires that ions acquire significant energy
in directions both transverse and parallel to the magnetic
field.  There is a considerable body of experimental
evidence that shows that transverse energization occurs over
a wide range of altitudes on auroral field lines.  Many
recent analytical and simulation studies have addressed the
micro-physics involved in transverse ion energization.
There are however remarkably few published high resolution
plasma and plasma wave observations obtained in the
mid-altitude auroral region available to compare with the
analytical and simulation studies.

Several hundred hours of high resolution plasma data
were surveyed and a wide variety of plasma environments that
are difficult to simply characterize were found.  We present
a comprehensive set of high-sensitivity, high-resolution
plasma wave, ion, and magnetometer data obtained from an
evening auroral zone crossing at r/Re ~ 2.5 by the Dynamics
Explorer -1 Satellite.  The total density, thermal
structure, and composition of the plasma in this
representative interval varied rapidly, as did the the
character (mode) of low frequency plasma waves observed.  We
did not find an unambiguous particle and wave signature of
local transverse ion energization, but we did frequently
find intervals where local transverse ion heating was
consistent with the observations.

H4-3
0940
## HEATING OF IONS ON AURORAL FIELD LINES IN THE PRESENCE OF A LARGE AMPLITUDE CYCLOTRON WAVE

K.-I. Nishikawa
Department of Physics and Astronomy
The University of Iowa
Iowa City, Iowa 5242

Heating of oxygen ions has been investigated in the presence of a large amplitude hydrogen cyclotron wave which is commonly observed on auroral field lines. A three wave decay process, in which a large amplitude pump hydrogen cyclotron wave decays into a daughter hydrogen cyclotron wave and a low frequency oxygen cyclotron wave, is studied theoretically and by means of particle simulations. Both one- and two-dimensional simulations showed a decay instability resulting in strong heating of both the oxygen ions and the hydrogen ions. In particular, the high energy tails of the oxygen ions are observed in the perpendicular distribution.

On the other hand, heating of hydrogen ions is also studied by means of simulations in the presence of an electrostatic oxygen cyclotron (EOC) wave which is commonly observed on auroral field lines at low altitudes (400-600 km). Two types of instabilities have been found which can be driven by an EOC wave. One of them is an oscillating current-driven electrostatic hydrogen cyclotron instability whose frequency is near the hydrogen cyclotron frequency. The other is an oscillating lower hybrid two-streaming instability whose frequency is near the lower hybrid frequency, $\omega \approx \omega_{pH}$. The simulations with the use of two-dimensional codes confirmed the presence of both instabilities resulting in strong heating of hydrogen ions. High energy tails of the hydrogen ions are observed in the perpendicular distribution.

H4-4
1000

GENERATION OF BROADBAND ELECTROSTATIC NOISE AND
PLASMA HEATING IN THE MAGNETOTAIL

M. Ashour-Abdalla[1,2] and D. Schriver[2]
[1]Institute of Geophysics and Planetary Physics
[2]Department of Physics
University of California
Los Angeles, CA   90024

The earth's plasma sheet boundary layer in the magne-
totail is a very active area of space and is the primary
region of plasma transport and heating in the tail. Two of
the main features of the boundary layer are its high-speed
ion beams that flow both earthward and tailward along mag-
netic field lines and the intense broadbanded electrostatic
noise found in the boundary layer.  We have used linear
theory and computer simulations to examine the various wave
modes that can be driven unstable by an ion beam free energy
source and how the wave energy is then transferred back to
the plasma.  We have done this for various intitial plasma
configurations determined from observations; for example, we
added cold ionospheric plasma to the predominantly hot
plasma to simulate lobe plasma convecting into the boundary
layer as well as the effects of counterstreaming ion beams.
Our results show that ion beams can generate broadband
electrostatic noise and that the heating resulting from
wave-particle interactions is consistent with plasma
observations in the central plasma sheet.

# REAL MODIFICATION

Suman Ganguly
Center for Remote Sensing
8200 Greensboro Drive, Suite 503
McLean, VA 22102

Controlled ground based ionospheric modification is a well established technique. However, all the experimental facilities here have fallen by at least two decades behind the current technology of high power transmitters. After briefly describing the results achieved with the present day facilities, we present a scenario for the generation of strong ionospheric modification and the impact of such a situation to the society.

H4-6
1100

ELECTROMAGNETIC TORNADOES IN SPACE
Tom Chang
Center for Theoretical Geoplasma Physics
MIT Center for Space Research
Cambridge, MA 02139

Imagine tornadoes the size of earth or larger containing whirlwinds of charged particles reaching speeds of tens of thousands of kilometers per hour. Such are the exotic phenomena recently detected by polar orbiting satellites. Space physicists have measured positive ions at altitudes from one to several earth radii at the auroral and polar cusp latitudes. These ions gyrate around the earth's magnetic field lines at extremely high speeds with energies ranging from tens of eV to several keV; and populations of these ions have been christened "ion conics".

A recent theory (Chang et al., Geophys. Res. Lett. 13, 636-639, 1986) suggests that the charged particles are merely tracers of an extended region of turbulent states of low frequency, electromagnetic waves. These turbulent waves rotate about the earth's magnetic field in a manner not very different from that of a funnel-like tornado which commonly descends upon the midwestern plains during a hot, humid, summer day.

Since charged particles also gyrate around the magnetic field, the rotating electric fields can push the ions along and energize them to very high energies and speeds. Using a mathematical tool commonly known as the "Monte Carlo" technique, we have calculated the effects of the electromagnetic turbulence on the charged particles (Retterer et al., Phys. Rev. Lett., 59, 148-151, 1987). This result is the very first successful quantitative prediction of an observed conic. For the special case considered, it was possible to determine that the conic was oxygen-dominated, a result verified recently by the EICS instrument on board the Dynamics Explorer 1 satellite. (Peterson et al., private communication).

H4-7
1120

QUASILINEAR ION HEATING BY ELECTROSTATIC ION
CYCLOTRON WAVES IN THE HIGH LATITUDE IONOSPHERE

P. Satyanarayana
Science Applications International Corporation
McLean, VA 22102

M.J. Keskinen, P.K. Chaturvedi, S.L. Ossakow
Plasma Physics Division
Naval Research Laboratory
Washington, DC 20375-5000

Recently, much attention, both theoretical and
experimental, has been given to the problem of ion
energization and conics in the terrestrial ionosphere and
magnetosphere. Some observations indicate ion conic
formation in the high latitude ionosphere as low in altitude
as 400-600 km. Various mechanisms, both AC and DC, have been
proposed to account for this energization with considerable
quantitative progress being made using wavelike sources,
e.g., ion cyclotron waves. However, the problem of ion
heating and acceleration by low frequency waves in the
collisional ionospheric environment has not been resolved.
In this study we develop a simple model of quasilinear ion
heating by current-driven electrostatic ion cyclotron waves
in the presence of ion-ion collisions including multi species
effects. We find both analytically and numerically ion-ion
collisional effects (1) reduce the absolute magnitude of
heating predicted by quasilinear theory and (2) lead to
temperature isotropization ($T_\perp \simeq T_\parallel$) on the order of several
tens of ion cyclotron periods where $T_\perp (T_\parallel)$ is the average ion
temperature perpendicular (parallel) to the ambient
geomagnetic field.

H4-8
1140

ELECTROMAGNETIC WAVES FROM ANTENNA-
PLASMA NONLINEARITIES OBSERVED IN A
BISTATIC PROPAGATION EXPERIMENT
H.G. James
Communications Research Centre,
P.O. Box 11490, Station "H",
Ottawa, Ontario K2H 8S2
Canada

On 21 Jan. 1976, the ISIS-I and ISIS-II topside sounder spacecraft participated in a recorded rendezvous during which the minimal separation was 58 km. The ISIS-II sounder was commanded to operate as a transmitter and the ISIS-I sounder as a receiver for a bistatic propagation experiment. The rendezvous occurred at high latitudes and at a height of about 1400 km. During the observations in question, the angle between the separation vector and the magnetic field varied from about 100° to about 80°.

The close encounter revealed the existence of anomalous signal enhancements at certain frequencies in the range 0.5 to 3.5 MHz, the plasma frequency being about 0.25 MHz and the gyrofrequency about 0.97 MHz. These signals propagated in the normal cold-plasma upper-branch O and X modes. Using conventional theories of transmitting and receiving antennas to define reference intensities, two types of enhancement were identified: signals near twice the gyrofrequency $2f_c$ and above the transmitter carrier frequency were 10 - 20 dB above the reference intensity, and a component at a separation of about $f_c$ below the carrier was amplified by up to 50 dB.

Cyclotron convective amplification and three-plane-wave decay nonlinearity have been examined as possible explanations. Neither postulate accounts satisfactorily for the observations. Nonlinear electron motion in the intense near field of the transmitting dipole is thought responsible for both types of spectral anomaly.

Condensed Technical Program
(Continued from inside front cover)


<u>1700-1800</u>
Commission B Business Meeting                                          CR2-6
Commission C Business Meeting                                          CR0-36
Commission E Business Meeting                                          CR1-46
Commission F Business Meeting                                          CR2-28
Commission H Business Meeting                                          CR1-9

<u>THURSDAY, 7 JANUARY</u>

<u>0835-1200</u>
B-6      EM Theory                                                     CR2-26
C-2      Spectrum Estimation Applications                             CR0-36
J-4      Low Frequency Radio Astronomy                                CR0-30

<u>0855-1200</u>
A-4      Measurements of the Properties of Materials                  CR1-40
F-2      Atmospheric Sensing                                          CR2-6
G-4      World-Wide Ionospheric Observing Campaigns and Studies       CR2-28
H-2      Electron Beam and Mass Injections in Space Plasmas - I       CR1-9

<u>1355-1700</u>
A-5      EMI Measurements and Standards                               CR1-42
B/F-1    Random Media                                                 CR2-6
G-5      High Latitude Ionospheric Phenomena                          CR2-26
H-3      Electron Beam and Mass Injections in Space Plasmas - II      CR1-9
J-5      Cosmology                                                    CR0-30

<u>1535-1700</u>
B-7      Resonances                                                   CR2-6

<u>FRIDAY, 8 JANUARY</u>

<u>0835-1200</u>
B-8      Scattering - II                                              CR2-6

<u>0855-1200</u>
G-6      Ionospheric Scatter Phenomena                                CR2-26
H-4      Space Plasma Heating by Natural and Man-Made Wave Sources CR1-9